SO(3) Yang-Mills theory on the lattice

D I S S E R T A T I O N

zur Erlangung des akademischen Grades
doctor rerum naturalium
(Dr. rer. nat.)
im Fach Physik

eingereicht an der
Mathematisch–Naturwissenschaftlichen Fakultät I
Humboldt–Universität zu Berlin

von
Dottore in Fisica Andrea Barresi
geboren am 02.09.1975 in Genova

Präsident der Humboldt-Universität zu Berlin:
Prof. Dr. Jürgen Mlynek

Dekan der Mathematisch–Naturwissenschaftlichen Fakultät I:
Prof. Dr. Michael Linscheid

Gutachter:

1. Prof. Dr. A. Di Giacomo
2. Prof. Dr. D. Ebert
3. Prof. Dr. M. Müller-Preussker

eingereicht am: 26. März 2003
Tag der mündlichen Prüfung: 03 Juli 2003

Abstract

The understanding of which degrees of freedom are relevant for the confinement of quarks is a long standing problem. Since it is widely believed that the center of the gauge group plays an important role, it is interesting to study a theory with a trivial center. The simplest model to investigate this problem is provided by a theory in an odd-dimensional representation of the gauge group $SU(2)$.

Center-blind theories were studied long time ago in two different discretizations, the adjoint Wilson and the Villain action, and they turned out to be problematic for two reasons. In both cases a bulk phase transition was shown to overshadow the physical finite temperature one. Another feature, pointed out in the Villain case, was the presence of twist sectors, which could cause difficulties in the construction of an ergodic algorithm. The lattice artifacts responsible for the bulk phase transition were identified with $\mathbb{Z}_2$ monopoles and they could be suppressed by the use of an appropriate chemical potential. A preliminary investigation of the finite temperature phase transition by other authors was done only in the Villain case and without taking care of the twist sectors.

In this thesis we perform a lattice study of the Wilson action in the adjoint representation of the gauge group $SU(2)$ with a chemical potential, which suppresses the $\mathbb{Z}_2$ monopoles at zero and non-zero temperature. We investigate the effects of the chemical potential λ on some observables. For large enough λ at vanishing temperature the observables do not show any discontinuity in the adjoint coupling. In this region we study the existence of a finite temperature phase transition restricting ourselves mainly to the trivial twist sector. In order to detect this phase transition we are able to define a new order parameter, which we successfully test also for the case of the fundamental representation of $SU(2)$. Furthermore we analyze the spatial distribution of the fundamental Polyakov loop and the Pisa disorder operator which detects the condensation of magnetic charges. These different tools provide an indication for a finite temperature phase transition or crossover decoupled from the bulk phase transition.

Keywords:
adjoint Wilson action, $\mathbb{Z}_2$ monopole suppression, order parameters, phase transitions

Zusammenfassung

Das Verständnis dafür, welche Freiheitsgrade für das Eingeschlossensein der Quarks von Bedeutung sind, ist ein altbekanntes Problem. Da weithin angenommen wird, dass das Zentrum der Eichgruppe eine bedeutende Rolle spielt, ist es interessant, eine Theorie mit einem trivialen Zentrum zu untersuchen. Das einfachste Modell, um dieses Problem zu untersuchen, ist eine Theorie mit ungeradzahliger Dimension der Darstellung der Eichgruppe $SU(2)$.

Theorien mit einem trivialen Zentrum werden schon seit langer Zeit in zwei verschiedenen Diskretisierungen untersucht: die adjungierte Wilson-Wirkung und die Villain-Wirkung. Es stellte sich heraus, dass sie aus zweierlei Gründen problematisch sind. Zunächst zeigte sich, dass in beiden Fällen ein *bulk*-Phasenübergang den physikalischen Phasenübergang bei endlicher Temperatur überschattet. Darüberhinaus erwies es sich im Falle der Villain-Theorie, dass die Anwesenheit von Twist-Sektoren für die Konstruktion eines ergodischen Algorithmus problematisch sein kann. Die Gitter-Artefakte, die den *bulk*-Phasenübergang verursachen, wurden mit $\mathbb{Z}_2$ Monopolen identifiziert. Diese Monopole können mit Hilfe eines entsprechenden chemischen Potentials unterdrückt werden. Eine erste Untersuchung des Phasenübergangs bei endlicher Temperatur durch andere Autoren wurde nur im Falle der Villain-Wirkung durchgeführt, wobei in dieser Untersuchung die Twist-Sektoren ohne Berücksichtigung blieben.

In der vorliegenden Arbeit untersuchen wir nichtstörungstheoretisch die Wilson-Wirkung in der adjungierten Darstellung der Eichgruppe $SU(2)$ mit einem chemischen Potential, welches die $\mathbb{Z}_2$-Monopole bei nicht verschwindender Temperatur und bei Temperatur Null unterdrückt. Wir untersuchen hierbei die Auswirkungen des chemischen Potentials λ auf einige Observable. Für hinreichend große λ zeigen die Observablen keine Diskontinuität in der adjungierten Kopplung. In diesem Gebiet des Phasendiagramms untersuchen wir, meist eingeschränkt auf den trivialen Twist-Sektor, die Existenz eines Phasenübergangs bei endlicher Temperatur. Um diesen Phasenübergang zu identifizieren, gelingt es uns, einen neuen Ordungsparameter zu definieren, den wir erfolgreich auch in der fundamentalen Darstellung der $SU(2)$ testen. Ferner analysieren wir die räumliche Verteilung der fundamentalen Polyakov-*loop*-Variable und des Pisaer Unordnungs-Operators, welcher die Kondensation magnetischer Ladungen beschreibt. Die Ergebnisse, die wir mit diesen Untersuchungsmethoden erhielten, lassen auf einen vom *bulk*-Phasenübergang entkoppel-

ten Phasenübergang bei endlicher Temperatur oder einen *cross-over* schließen.

Sclagwörter:
adjungierte Wilson Wirkung, $\mathbb{Z}_2$-Monopol-Unterdrückung, Ordnungsparameter, Phasenübergang

Contents

1 Introduction

Gauge theories are a key element of particle physics, since they provide a unified description of the electromagnetic, the weak and the strong interaction. The gauge symmetries originated by the gauge group dictate the form of the Lagrangian and, in this way, the dynamics. Non Abelian gauge theories were introduced in 1954 by Yang and Mills [1], but at the beginning [2] the reaction of the physical community was quite cold; it was in fact clear that gauge invariance forbids massive terms for the charged vector fields in the Lagrangian, thus implying a long range interaction in contradiction with experiments. The problem was solved in models with a scalar field via spontaneous symmetry breaking, which generates a mass for the vector bosons [3]. These ideas paved the way for the Standard Model of particle physics [4, 5, 6]; even if the Higgs boson must be still detected and possible extensions of the SM will be checked in the next generation of accelerators, nowadays, thanks to its extraordinary agreement with experimental results, it is the accepted model for the fundamental forces of nature. The Lagrangian is invariant under the group $SU(3)_c \times SU(2)_{\rm I} \times U(1)_{\rm Y}$; the $SU(2)_{\rm I} \times U(1)_{\rm Y}$ symmetry associated with the weak isospin I and the weak hypercharge Y describes the unified electroweak interactions and the color $SU(3)$ symmetry governs the strong interactions.

Several historical steps were needed in order to understand that the strong force could be described by Quantum Chromodynamics (QCD). It was soon realized that the hadrons could not be elementary particles, due to their proliferation. Gell-Mann and Zweig proposed a model able to explain the occurrence of the hadrons in multiplets [7, 8] by introducing elementary constituents called quarks, but these objects were thought more as a useful tool to classify hadrons than as really physical objects. These early expectations were disattended by the experimental data obtained in the deep inelastic electron-nucleon scattering. These data confirmed the Bjorken hypothesis of scaling of the structure functions [9] and this behavior could be well explained if the hadrons were made up of point-like particles, which were called partons [10, 11]. Later on the partons were identified with the quarks on the basis of their quantum numbers. New experiments pointed out that they should carry a new degree of freedom. In fact the existence of states like the baryon Δ^{++} and the discrepancy between the predicted and the observed ratio of total cross sections for the processes $e^+e^- \to$ hadrons and $e^+e^- \to \mu^+\mu^-$, posed some difficulties. It was soon realized that they could be easily solved if the quarks carried a further quantum number, called color. The same experimental data fixed also the color group to be $SU(N)_c$ with $N_c = 3$. All these achievements led Fritzsch, Gell-Mann and Leutwyler to propose a non Abelian $SU(3)$ gauge theory with quarks as the theory of the strong interactions [12] and nowadays it is widely believed that it is

the correct one thanks to the agreement with several experimental data.

QCD describes the behavior of quarks and gluons; the hadrons are made up of quarks and the gluons are the vector bosons which mediate the interaction. Both quarks and gluons carry the quantum number of color and as a consequence a pure non Abelian gauge theory, i.e. a theory with only gauge fields, is already interacting. This constitutes a striking difference with QED where the photons, which are $U(1)$ neutral, do not self-interact. This characteristic of QCD is at the origin of a property called asymptotic freedom [13, 14, 15]: the strength of the strong interactions decreases as the momentum exchanged in a process increases and the partons behave like free particles. In this regime a perturbative expansion in the coupling constant is feasible; the theoretical computations give a nice agreement with experimental data thus substantiating the idea that QCD is the theory of the strong interaction.

On the other hand, in the low-energy regime the strength of the coupling constant increases and the quarks are strictly bound into hadrons, which are colorless objects. This is another peculiarity of QCD with respect to QED; the Lagrangian is written in terms of the fundamental fields, quarks and gluons, which are colored particles, but in nature only colorless objects are detected. The strong experimental evidence about the absence of colored sources in nature is so impressive that confinement is believed to be a fundamental property of QCD at large distances. Moreover, the hadronic spectrum is characterized by the Regge trajectories, which suggest that the potential binding the quarks together should rise linearly at large distances. Another relevant phenomenon in the infra-red regime of QCD is the spontaneous breaking of the chiral symmetry; the vacuum is not invariant under chiral transformations and an octet of Goldstone bosons is expected, which can be identified with the octet of pseudoscalar mesons $(\pi^{\pm}, \pi^0, K^{\pm}, K^0, \bar{K}^0, \eta)$.

At high temperatures or baryon densities the theory is supposed to undergo a phase transition, with the linear potential substituted by a Debye screening one and chiral symmetry restoration; the first effect could be signalled in experiments by the J/ψ suppression [16] and the second via the enhancement in the production of strange hadrons. The picture which arises from these considerations suggests the existence of two different regimes. A low energy hadronic phase characterized by confinement and chiral symmetry breaking and a high density quark-gluon plasma phase in which deconfinement and chiral symmetry restoration take place. Unfortunately the experiments about high energy heavy ion collisions still do not give clear indications about the occurrence of the transition between the two phases. It would be also interesting to understand whether chiral symmetry restoration and confinement occur at the same temperature or not.

Since the pioneering work of 't Hooft [17, 18] and Polyakov [19], the relevance of topology and geometry in the comprehension of these problems were realized, and the importance of topological solutions like instantons, monopoles and vortices recognized. The instantons [20] are classical solutions of the equation of motions of pure Yang-Mills theory in a 4d Euclidean space; the early expectations that they could explain confinement were soon unfulfilled, but they provided a solution for the $U(1)_A$ [21, 22] problem and there are good indications that they could be useful in the chiral symmetry breaking problem [23, 24, 25, 26]. Many models of the QCD vacuum were proposed in order to explain confinement and some of them

exploited the properties of topological configurations. Two of the most famous are the dual superconductivity [27, 28, 29, 18, 30] scenario and the vortex model of the vacuum [31, 32, 33]. In the first case magnetic monopoles are considered to be the relevant degrees of freedom; their condensation in the vacuum leads to the formation of thin flux tubes of chromoelectric field between the quarks, which bind them into hadrons; this picture resembles the situation in a superconductor, but with electric and magnetic fields exchanged, hence the name dual superconductivity. In the other model the relevant degrees of freedom are thought to be vortices and their condensation should explain confinement. Topology plays a role since for a gauge group $SU(N)$ the Abelian magnetic monopoles are classified by the first homotopy group of the Abelian subgroup $U(1)^{(N-1)}$, which corresponds to $\Pi_1(U(1)^{(N-1)}) = \mathbb{Z}^{(N-1)}$, and vortices by the first homotopy group of the gauge group modulo its center, i.e $\Pi_1(SU(N)/\mathbb{Z}_N) = \mathbb{Z}_N$. Even if it is proved that in some toy-models (Georgi-Glashow model in 2+1 dimensions [19], N=2 supersymmetric Yang-Mills broken to N=1 in 3+1 dimensions [34,35]) confinement is due to the condensation of magnetic monopoles, both the dual superconductor scenario and the vortex model are unsatisfactory and an explanation is still missing.

The confinement and chiral symmetry breaking phenomena are difficult to understand also because they occur in the low-energy regime, where a perturbative expansion of the coupling constant makes no sense, and adequate non-perturbative methods must be developed. In 1974 Wilson introduced a non-perturbative approach to the problem by discretizing 4d space-time on a Euclidean lattice [36]. The matter fields live on the sites of the lattice and the gauge fields are the connections between them. The quantization of this theory is performed in the path integral formalism. In the Euclidean lattice formulation a quantum field theory looks like a classical statistical system thus allowing the use of common techniques. Wilson introduced this approach to explain confinement and indeed he proved that, in the strong coupling limit, which corresponds to a high temperature expansion in a statistical system, a pure Yang-Mills theory confines static color charges in the fundamental representation. Anyway in a non Abelian gauge theory the continuum limit is obtained in the weak coupling limit and in this region the result of Wilson does not apply. But the lattice formulation allows also the use of Monte Carlo techniques, as Creutz showed first in his seminal work about pure $SU(2)$ gauge theory [37], and many useful informations can be obtained through numerical simulations. Monte Carlo simulations showed that QCD is confining at zero temperature for all the values of the coupling constant, so also in the weak coupling limit, and the string tension [38] and other properties of the confining flux tubes were measured. Lattice simulations were essential also to study the properties of QCD at finite temperature. In pure $SU(N)$ gauge theories, through the use of appropriate order parameters, it was found evidence for a deconfinement phase transition driven by the spontaneous breaking of the global center symmetry $\mathbb{Z}_N$, as early theoretical expectations suggested [39, 40]. When the fermions are included the situation becomes more complicated and the nature of the transition from a confined to a deconfined phase strongly depends on the numbers of flavors and on the masses of the quarks [41]. In the case of 2 massless flavors there is no indication for a discontinuous phase transition, but for $N_f \geq 3$ the transition is found to be first order. With 3 light quarks the phase diagram is quite complex

and when the masses of the quarks assume values near to the physical ones, it is no more so clear whether there is still a phase transition or rather a crossover. A complete phase diagram of QCD with 3 quarks flavors can be found in [42].

Lattice simulations are however useful also to investigate the different models of confinement, like the dual superconductor and the vortex vacuum. In recent years much work has been done in order to elucidate these models. The mechanisms underlying them are of course gauge independent, but both of them were mostly studied with the help of particular gauges; on the lattice, as far as gauge invariant observables are studied, there is no need to fix the gauge, but it turned out that this procedure was useful to extract the degrees of freedom considered to be relevant for confinement. In the dual superconductor picture the effective Lagrangian is supposed to be a dual Abelian-Higgs model with a $U(1) \times U(1)$ symmetry and magnetic monopoles; the relevant degrees of freedom are extracted through the use of Abelian gauges, the most famous and used being the maximal Abelian gauge (MAG). The observables can be computed in the Abelian projected theory, i.e. in the theory first gauge fixed with MAG and then projected onto the Abelian subspace; they numerically agree very well with the observables computed in the original theory [43, 44]. This property is named Abelian dominance. The situation for the vortex model is similar. There are some gauges, like the maximal Center gauge (MCG), which are used to locate the center vortices and to reduce a non Abelian $SU(N)$ gauge theory to its center degrees of freedom by projection. The observables computed in the center-projected and in the original theory almost agree and one speaks of center dominance [45]. In both cases, anyway, there are problems with the gauge fixing procedure because of the presence of Gribov copies.

It would be interesting to have a way to understand which are the relevant degrees of freedom for confinement. As a simple toy-model one can consider the gauge group $SU(2)$ and compare it with the theory in the adjoint representation, i.e. an $SO(3)$ theory. These two different discretizations are believed to posses the same continuum limit, but this expectation is based only on perturbative arguments; since recently some doubts have been raised [46, 47], it is worth performing a non-perturbative investigation of the $SO(3)$ theory. Moreover this model is interesting because it has no center, since $SO(3) = SU(2)/\mathbb{Z}_2$; for this reason not only the projection onto $\mathbb{Z}_2$ makes no sense, but the deconfinement phase transition, if there is any, cannot be so easily associated with the breaking of the center symmetry, as it is usually done for a $SU(N)$ gauge theory in the fundamental representation. It has been shown anyway that this model has non trivial twist sectors [48,49,50]; they are not associated to the presence of a center but are defined by the first homotopy group, which for $SU(2)$ and $SO(3)$ is the same, i.e. $\Pi_1(SU(2)) = \Pi_1(SO(3)) = \mathbb{Z}_2$. A non trivial twist sector signals the presence of a center vortex and they could still play a role in the dynamics of the theory. One could go further and study a group with trivial center and trivial first homotopy group; the simplest group with these characteristics is G_2, which is anyway rather cumbersome to simulate on the lattice [51, 52]. The purpose of this thesis is to make a non perturbative study of the $SO(3)$ theory at finite temperature

and to understand whether a finite temperature phase transition occurs and which are the degrees of freedom responsible for that. A preliminary investigation was already done, but only within a particular discretization, the Villain action, and without taking care of the twist sectors [53].

In Chapter 2 we will introduce some basics notations about the discretization of a continuum theory on a lattice and explain how to get the continuum limit of the discretized theory. After having explained in more detail the problem of confinement and chiral symmetry breaking, we will describe some techniques that can be used to detect a phase transition, i.e. the study of thermodynamics and the definition of appropriate order parameters. In Chapter 3, after a general introduction about the relationship between confinement and topology, we will expose in detail the two aforementioned models of the QCD vacuum: the dual superconductor and the vortex model. We will explain how they are formulated in the continuum and how they are then studied on the lattice. We will focus our attention in particular on two order parameters which are commonly used for $SU(N)$ theories in the fundamental representation to study the deconfinement phase transition, i.e. the disorder operator and the vortex free energy. In Chapter 4 we will review some old results about theories in representations different from the fundamental one. We will show that in all these cases bulk phase transitions at zero temperature occur and that they are driven by lattice artifacts of some sort. With the help of a particular discretization, the Villain action, the lattice artifacts are identified with $\mathbb{Z}_2$ monopoles and through the introduction of twist sectors the connection with a theory in the fundamental representation is clarified. In Chapter 5 we will describe our work. We focused our attention not on the Villain discretization, but rather on the adjoint Wilson action. This allows a numerical check of the ideas developed for the Villain case. Also for the adjoint Wilson action $\mathbb{Z}_2$ monopoles and twist observables, which are slightly different from the definitions given within the Villain discretization, can be constructed. We investigated in particular the adjoint Wilson action with a λ chemical potential which suppresses the $\mathbb{Z}_2$ monopoles. We studied the effect of varying λ on various observables. We observed a change of order of the bulk phase transition and tunneling between different twist sectors. We investigated then the finite temperature phase transition in a fixed twist sector by using the distribution of the Polyakov loop in the fundamental representation and the Polyakov loop in the adjoint representation. In Chapter 6 we suggest a possible mechanism of symmetry breaking in $SO(3)$ and we define a corresponding order parameter able to detect this symmetry breaking. We tested it in the $SU(2)$ theory in the fundamental representation and we investigated then the adjoint Wilson action with the monopole suppression term in a fixed twist sector. In Chapter 7 we construct the disorder operator, used before us by the Pisa group to investigate only the finite temperature phase transition of a $SU(N)$ theory in the fundamental representation, for a center-blind theory. We studied both the case with $\lambda = 0$ and then with $\lambda \neq 0$. Finally, in Chapter 8, we draw some conclusions. We relegated some technicalities in the appendices. In Appendix A we explain some basics notions about the Monte Carlo techniques and some details about the algorithm used. In Appendix B we introduce the basics concepts and formulae for data analysis. In Appendix C we describe the MAG gauge fixing procedure. In Appendix D we develop a decomposition of the

gauge field motivated by the ideas explained in Chapter 6.

Chapter 2

Lattice QCD

The lattice formulation of QCD [36] was introduced long time ago in order to understand the confinement phenomenon and to carry out a non-perturbative analysis of the theory.

In the first chapter we will give first of all an introduction to the lattice regularization of Yang-Mills theories in the presence of matter fields [54]. We will analyze in detail the different steps essential to discretize the theory, since in our work we tried to understand what happens when a basic aspect, i.e. the representation of the gauge action, is varied. After that, we will explain how to recover the continuum limit of the theory, thus allowing the possibility of getting results which can be compared with real-world observables.

Then we will go deeper into the problem of confinement and its characterization. We will review the different tools, thermodynamics and order parameters, which were used until now to describe the finite temperature phase transition, and we will emphasize the differences between the adjoint representation, with a trivial center, and the fundamental representation, with non-trivial center. The discussion about the order parameters will be important because it will naturally bring us, in the next chapter, to the description of two models of the QCD vacuum, the dual superconductor and the vortex model.

2.1 Formulation of lattice gauge theories

The discretization of a continuum action on the lattice is not a unique procedure. It is a construction made up of different steps and each of them can be implemented in several ways. It is widely believed, anyway, that universality holds, i.e. that all the differently discretized quantum theories have the same continuum limit.

First of all a lattice must be introduced in order to discretize space-time; there are many possible choices like the hypercubic, which is the simplest and most commonly used one, the body-centered cubic [55] and the random lattices [56,57]. Complicated geometries will increase the computational effort but it is expected that the physics will be unaffected in the continuum limit, if universality holds. For this reason the hypercubic grid with lattice spacing a and size $N_S^D \times N_T$ (with D spatial dimensions) is almost uniquely used.

The next step is the introduction of matter and gauge fields on the lattice. The

matter fields, $\psi(x)$, are attached to each site and the gauge fields, $U_\mu(x)$, are associated with the links; in this way the gauge field preserves its function of parallel transporter and it is then represented as

$$U(x, x+\hat{\mu}) \equiv U_\mu(x) = e^{iagA_\mu(x)}\,, \tag{2.1}$$

where $U_\mu(x)$ are $SU(N)$ matrices and $A_\mu(x) \equiv A^a_\mu(x)\cdot T^a/2$, with the normalization $\mathrm{Tr}T_aT_b = \delta_{ab}/2$. The definition of the link variable as a discretized path ordered product implies that

$$U(x, x-\hat{\mu}) \equiv U_{-\mu}(x) = U^\dagger(x-\hat{\mu}, x)\,. \tag{2.2}$$

The lattice gauge fields live in a definite representation of the gauge group and not of the algebra like in the continuum theory. The quark fields are Grassmanian variables which live in the fundamental representation of the algebra of the gauge group. The gauge fields, in the absence of matter fields, can be chosen in any representation of the gauge group. This is a non-trivial aspect which will turn out to be very important for our work; anyway they are also commonly chosen in the fundamental representation.

The next task is the definition of an action for the fields previously introduced and the usual way is looking for the simplest object which possesses some important symmetries, i.e. it must be Poincaré and gauge invariant. The first observation is that the Poincaré symmetry group is reduced to a discrete subgroup as soon as a discrete space-time is introduced; the continuous rotation group is replaced by the discrete hypercubic group and translations must be integer multiples of the lattice spacing a. Under local gauge transformations $\Omega(x)$ the fields transform as

$$\begin{aligned}
(\psi(x))^\Omega &= \Omega(x)\psi(x)\,,\\
\left(\bar{\psi}(x)\right)^\Omega &= \bar{\psi}\Omega^\dagger(x)\,,\\
(U_\mu(x))^\Omega &= \Omega(x)U_\mu(x)\Omega^\dagger(x+\hat{\mu})\,.
\end{aligned} \tag{2.3}$$

Given the transformation laws it is easily understood that the only gauge invariant objects are obtained by taking the trace over the color indices of a product of links along a closed path (Wilson loop), or along a line which stretches across the lattice and it is closed through periodic boundary conditions (Wilson/Polyakov line), or along a path which begins with an antifermion and ends into a fermion. For $SU(N)$ with $N \geq 3$ the trace is complex and the real part is taken in order to average the loop and its charge conjugate. In a $SU(N)$ gauge theory with fermions the minimal choice to build a Lorentz scalar and color-singlet lattice action is to use for the matter fields the following naïve discretized version of the Dirac operator

$$\bar{\psi}D\psi = \frac{1}{2a}\bar{\psi}(x)\sum_\mu \gamma_\mu[U_\mu(x)\psi(x+\hat{\mu}) - U^\dagger_\mu(x-\hat{\mu})\psi(x-\hat{\mu})]\,, \tag{2.4}$$

and for the gauge variables to sum over all the possible μ,ν orientations of the real part of the trace in the fundamental representation of a 1×1 loop (plaquette)

$$\sum_{1\leq\mu<\nu\leq 4} \mathrm{Re}\ \mathrm{Tr}_F\ [U_{\mu\nu}(x)] \equiv \sum_{1\leq\mu<\nu\leq 4} \mathrm{Re}\ \mathrm{Tr}_F\ [U_\mu(x)U_\nu(x+\hat{\mu})U^\dagger_\mu(x+\hat{\nu})U^\dagger_\nu(x)]\,. \tag{2.5}$$

The action is then given by summing over all the points of the lattice and it is straightforward to show that it gives the familiar Yang-Mills continuum action with fermions in the limit $a \to 0$ up to corrections $O(a^2)$:

$$\begin{aligned} S &= \beta \sum_x \sum_{1\le\mu<\nu\le 4} \left(1 - \frac{1}{N} \text{ Re Tr}_F \left[U_{\mu\nu}(x)\right]\right) \\ &+ \frac{1}{2a}\bar{\psi}(x) \sum_\mu \gamma_\mu [U_\mu(x)\psi(x+\hat{\mu}) - U_\mu^\dagger(x-\hat{\mu})\psi(x-\hat{\mu})] + m_q \sum_x \bar{\psi}(x)\psi(x) \\ &= -a^4 \left(\frac{\beta}{4N} \sum_x \text{ Tr}_F \left[F_{\mu\nu}(x)F^{\mu\nu}(x)\right] + \bar{\psi}(x)\gamma_\mu(\partial_\mu + igA_\mu)\psi(x) \right. \\ &+ \left. m_q \sum_x \bar{\psi}(x)\psi(x) + O(a^2) \right), \qquad \beta = \frac{2N}{g^2} \ . \end{aligned} \tag{2.6}$$

This lattice action, being gauge and Lorentz invariant by construction, is also invariant under $\mathcal{P}, \mathcal{C}$ and $\mathcal{T}$ transformations.

Let us concentrate for a while on the pure gauge part of the action and emphasize some aspects which will be important in the following. The choice of taking 1×1 loops is of course arbitrary and every bigger loop gives always the same leading order in a, i.e. a^4 Tr$_F$ $[F_{\mu\nu}(x)F^{\mu\nu}(x)]$; usually bigger plaquettes, for instance 1×2, are considered besides the minimal ones in improved actions, when one wants to suppress $O(a^2)$ corrections and recover the continuum limit on coarser lattices. Moreover, as already explained, the gauge fields must not necessarily live in the fundamental representation; the choice of another representation, despite having the same naïve continuum limit, has consequences that will be analyzed in detail in Chapter 3. The key point is that all this modified (in the sense that differ from the minimal prescription) actions must give the same continuum limit, if universality holds.

The main topic of this work is confinement and its characterization; since it is believed to be a characteristic of a pure non Abelian gauge theory, in this thesis we will not deal with fermions, but for sake of completeness some further comments about the invariance of the fermionic action are worth. It possesses a global symmetry related to baryon number conservation and which leads to the conservation of a vector current

$$\begin{aligned} \psi(x) &\to e^{i\theta}\psi(x)\,, \\ \bar{\psi}(x) &\to \bar{\psi}(x)e^{-i\theta}\,, \end{aligned} \tag{2.7}$$

and in the limiting case $m_q = 0$ is also invariant under

$$\begin{aligned} \psi(x) &\to e^{i\theta\gamma_5}\psi(x)\,, \\ \bar{\psi}(x) &\to \bar{\psi}(x)e^{i\theta\gamma_5}\,. \end{aligned} \tag{2.8}$$

The consequence of having both axial and vector symmetries in a hard-cutoff regularization scheme is the violation of the Adler-Jackiw-Bell theorem; this is due to the fact that the naïve discretized Dirac action has the notorious fermion doubling problem: in the continuum limit it gives $2^d = 16$ flavors instead of 1 and the chiral

charges of these extra fermions cancel exactly the ABJ anomaly. The doubling problem leads to the Nielsen-Ninomiya no-go theorem [58]: it is not possible to define a local, translationally invariant and hermitian lattice action that preserves chiral symmetry and does not have doublers. Two remedies were usually adopted: Wilson suggested to add an additional term which goes to 0 in the naïve continuum limit and breaks explicitly chiral invariance but removes the doublers; the other approach exploited the larger symmetry group of the discretized fermion action, $U(4) \otimes U(4)$, to reduce the doubling problem from $2^d = 16 \to 16/4$ and to maintain a remnant chiral symmetry (staggered fermions). The basic step to solve the problem was the rediscovery [59] of the Ginsparg-Wilson relation [60]

$$\gamma_5 D + D\gamma_5 = aD\gamma_5 D\,, \tag{2.9}$$

and understanding that chiral symmetry can be realized in different ways [61, 62]. Eq. (2.9) implies in fact a novel continuous symmetry of the fermionic action, given in its infinitesimal form by

$$\begin{aligned} \delta\psi &= \gamma_5 \left(1 - \frac{1}{2}aD\right)\psi\,, \\ \delta\bar{\psi} &= \bar{\psi}\left(1 - \frac{1}{2}aD\right)\gamma_5\,, \end{aligned} \tag{2.10}$$

which can be interpreted as a lattice form of chiral symmetry. The Nielsen-Ninomiya theorem is thus bypassed because the anticommutation relation between γ_5 and the Dirac operator D, which was usually assumed to guarantee the invariance of the fermionic action under the old continuous chiral symmetry transformations (2.8), is substituted by eq. (2.9) and fermions of definite chirality can be safely defined on the lattice.

After having introduced the gauge and the matter fields and having defined an action, the theory must be quantized by specifying the functional integral; in particular a measure must be chosen and a good choice should respect gauge invariance. For the gauge group this is accomplished by using the Haar measure and the expectation value of an observable $O(\{U_\mu(x), \psi(x)\})$ (which depends on the gauge configuration $\{U_\mu(x)\}$ and on the matter fields $\{\psi(x)\}$) reads as

$$\begin{aligned} \langle O \rangle &= \frac{1}{Z}\int (DU)(D\bar{\psi})(D\psi) O \exp(-S(U_\mu, \bar{\psi}, \psi))\,, \\ Z &= \int (DU)(D\bar{\psi})(D\psi) \exp(-S(U_\mu, \bar{\psi}, \psi))\,, \end{aligned} \tag{2.11}$$

where $(DU) = \prod_{x,\mu} dU_\mu(x)$, $(D\psi) = \prod_{x,\alpha} d\psi_\alpha(x)$ and $(D\bar{\psi}) = \prod_{x,\alpha} d\bar{\psi}_\alpha(x)$. One can show that the partition function Z for a field theory at finite temperature [63] differs from the functional integral of the theory at zero temperature because of the compactification of the temporal variable,

$$Z = \int (DU)(D\bar{\psi})(D\psi) \exp\left(-\int d^3x \int_0^{\frac{1}{T}} dt L[U_\mu, \bar{\psi}, \psi]\right)\,, \tag{2.12}$$

and the expectation value of the observables is obtained through the modified integral. The fields must satisfy the necessary boundary conditions at $t = 0$ and $t = \frac{1}{T}$, in particular boson fields satisfy periodic boundary conditions and fermions antiperiodic boundary conditions. Since on a finite lattice also N_S is limited, to ensure that the temporal direction results compactified with respect to the others, $N_T \ll N_S$ must be chosen.

Now that the basic aspects were introduced, we can go further describing how to reach the continuum limit of lattice QCD and studying in more detail the problem of confinement.

2.2 The physical continuum limit

Since one of the fundamental purposes of lattice QCD is to give quantitative predictions about physical observables, we must be able to recover its continuum limit. The regularized theory in a finite volume has a physical temperature T and volume V which are determined by the lattice spacing a and by the number of lattices sites in the temporal and in the spatial directions in the following way:

$$T = \frac{1}{N_T a(\beta)} \quad , \quad V = (N_S a(\beta))^3 \, , \tag{2.13}$$

with the lattice spacing which depends on the bare coupling $\beta \equiv 2N/g^2$. Moreover, all the physical observables are measured on the lattice in terms of the cut-off a

$$ma = 1/\xi \, , \tag{2.14}$$

where m indicates a mass and ξ a correlation length. In order to get the continuum limit we must act on the bare parameters of the theory in such a way that we can send $a \to 0$, $N_T, N_S \to \infty$ while keeping finite the physical mass m; it means that the correlation length ξ has to diverge, such that the system is undergoing a second order phase transition and reaching a critical hypersurface in the space of the bare parameters. Any meaningful continuum limit must be taken by approaching the critical hypersurface, but to establish whether a discretized theory possesses a well defined and non-trivial continuum limit is not easy at all. The nature of the continuum limit is related to the fixed points of the $\beta-$functions of the theory

$$\beta(g_R) \equiv m_R a \frac{\partial g_R}{\partial m_R a}|_{g_0} = \frac{\partial g_R}{\partial \ln m_R a}|_{g_0} \, , \tag{2.15}$$

which describes how the renormalized coupling g_R varies with the cut-off a at fixed bare coupling g_0 and

$$\beta_{LAT}(g_0) \equiv -a \frac{\partial g_0}{\partial a}|_{g_R} = -\frac{\partial g_0}{\partial \ln m_R a}|_{g_R} \, , \tag{2.16}$$

which determines the change of g_0 with the cut-off keeping g_R fixed. If the value of g_R is such that the $\beta(g_R)$ equals zero, then it means that g_R does not change under variations of the cut-off and we have reached a fixed point. If the slope of

$\beta(g_R)$ at zero is positive, then the renormalized coupling in the continuum limit is driven towards the fixed point, called infrared fixed point; if the slope is negative, then g_R is driven away and the fixed point is called ultraviolet fixed point. For β_{LAT}, due to the minus sign, the situation is the opposite: its zeros with a positive slope, i.e. the infrared fixed points, repel the bare coupling as we move towards the continuum limit, the ultraviolet fixed points attract g_0. Combining the informations about the fixed points of the $\beta-$functions, the following picture is obtained: if one starts with bare parameters in the basin of attraction of an ultraviolet fixed point, then it is possible to reach different renormalized couplings g_R within certain bounds determined by the infrared fixed points; outside this basin, the renormalized coupling will approach the infrared fixed point.

In QCD the bare parameters are the coupling constant g and the masses of the quarks, but in the limit of infinite or zero quark masses the continuum limit is controlled only through g. The $\beta-$function can be computed in perturbation theory:

$$\beta_{LAT}(g) = -\beta_0 g^3 - \beta_1 g^5 + \dots \tag{2.17}$$

with the first two terms (for $SU(N)$ gauge group and N_f quark flavors)

$$\begin{aligned} \beta_0 &= \frac{1}{16\pi^2}\left(\frac{11N}{3} - \frac{2N_f}{3}\right), \\ \beta_1 &= \frac{1}{(16\pi^2)^2}\left(\frac{34N^2}{3} - \frac{10NN_f}{3} - \frac{(N^2-1)N_f}{N}\right), \end{aligned} \tag{2.18}$$

which are universal, i.e. gauge and regularization scheme invariant. It can be also shown that these two terms coincide for $\beta_{LAT}(g_0)$ and $\beta(g_R)$. Since $N_f < 16$, β_0 is positive and this is a manifestation of a fundamental property of QCD, asymptotic freedom: the strength of the strong interactions decreases as the momentum exchanged in a process increases; in other words $g = 0$ is an ultraviolet fixed point of the theory and the continuum limit is reached sending $g \to 0$, or equivalently $\beta = 2N/g^2 \to \infty$, by keeping the renormalized coupling g_R fixed. Asymptotic freedom implies dimensional transmutation, i.e. the fact that QCD dynamically generates a mass scale

$$\Lambda_{LAT} \equiv \lim_{g\to 0} \frac{1}{a} \exp\left(-\frac{1}{2\beta_0 g^2}\right) (\beta_0 g^2)^{\beta_1/(2\beta_0^2)}, \tag{2.19}$$

which is a constant independent of g. This 2-loop definition of Λ is not unique, but once it is known in one scheme, it can be related to the value in any other scheme. It gives explicitly the perturbative relation between the lattice spacing a and the bare coupling g. Close enough to the fixed point at $g = 0$ perturbation theory holds, the system is in a regime of asymptotic scaling and every mass in lattice units varies as a function of g according to

$$am = aC_m\Lambda_{LAT} = C_m \exp\left(-\frac{1}{2\beta_0 g^2}\right) (\beta_0 g^2)^{\beta_1/(2\beta_0^2)} \{1 + O(g^2)\}. \tag{2.20}$$

If two masses m_1 and m_2 are considered then both would scale according to (2.20) and their ratio is given by

$$\frac{m_1}{m_2} = \frac{C_{m_1}}{C_{m_2}} \{1 + O(a^2 m^2)\}. \tag{2.21}$$

Close enough to the continuum limit this ratio should be nearly constant and in this case one speaks of scaling.

In the case of quark masses different from zero, one has to take care also that the continuum limit is taken along lines of constant physics; it means that ratios of hadron masses, one for each non degenerate quark mass m_q, must be kept constant as the couplings (β, m_q) are varied.

2.3 Confinement and chiral symmetry

As already explained in the introduction, QCD is commonly believed to confine color charges into hadrons at low energies. This idea is supported by experimental facts, which put very strict bounds on the existence of free quarks.

In Millikan-like experiments, devoted to detect particles with fractional electric charge, the observed number of events is much smaller than the number expected from thermodynamical arguments applied to the evolution of the early Universe, i.e. $n_{obs}/n_{exp} \sim 10^{-15}$; an upper bound on the ratio of the cross section for quark production to the total cross section can be obtained from high energy collisions experiments, i.e. $\sigma_q/\sigma_{tot} \sim 10^{-15}$. The strong experimental evidence about the absence of free color charges in nature suggests that confinement should be a fundamental property of QCD at large distances and it could be explained more naturally in terms of a symmetry than with the fine tuning of some parameters.

Although reliable results from heavy ion collisions experiments are still lacking, in recent years lattice simulations gave an interesting picture of the QCD phase diagram, showing different behaviors by varying the temperature and the density. At zero temperature confinement takes place and quarks are bound into hadrons. The hadronic spectrum is characterized by Regge trajectories, which suggests a linear rising potential at large distances. Moreover, the light pions in the spectrum indicate the spontaneous breaking of the chiral symmetry, measured through the chiral condensate $\langle\bar{\psi}\psi\rangle$. At high temperature the picture changes and another phase is supposed to occur, in which color charges are deconfined thus forming a quark-gluon plasma. The linear confining potential is supposed to be substituted by a Debye screening one and chiral symmetry should be restored; a possible experimental signature of the change in the potential is the J/ψ suppression and the evidence for the restoration of chiral symmetry would be given by the enhancement in the production of strange hadrons.

Since there are several indications about the existence of different phases, it is then interesting to understand whether they are separated by a phase transition or rather a crossover and what kind of mechanism is responsible for that. In a pure $SU(N)$ gauge theory in the fundamental representation without matter fields lattice simulations strongly indicate the presence of a finite temperature deconfinement phase transition [64, 65]. Confinement is usually characterized by a non-vanishing string tension and it is associated with a global $\mathbb{Z}_N$ symmetry, whose spontaneous breaking, signalling the deconfinement phase transition, is monitored by the vacuum expectation value of an order parameter, the Polyakov loop [66,67]. In the vicinity of the critical point an effective theory in terms of the order parameter can be written,

with a potential which breaks the center symmetry. This conjecture leads to a correspondence between the dynamics of the phase transition in a $SU(N)$ Yang-Mills theory in (d+1)-dimensions and a $\mathbb{Z}_N$ spin system in d dimensions [39, 40]. The $SU(2)$ theory in the fundamental representation exhibits a second order phase transition and it belongs to the same universality class of the 3d Ising model, while $SU(3)$ shows a weak first order phase transition resembling the behavior of the 3-state Potts model in 3 dimensions. So in this case, thanks to the presence of the center $\mathbb{Z}_N$, the order of the phase transition and the critical exponents are obtained with simple symmetry arguments.

It is then interesting to study what happens if another representation of the gauge group without the center, like the adjoint one, is chosen and check whether it shows also a finite temperature deconfinement phase transition and if the critical exponents coincide with the exponents of the 3d Ising model, as one would naively expect from universality arguments. This case is more cumbersome since the center symmetry is always unbroken, so the Polyakov loop cannot be used as an order parameter, and the string tension between static adjoint charges can vanish also in the confining phase, since a gluon can screen an adjoint charge. We will analyze in the next chapters what happens in this case.

With dynamical fermions the situation is more complicated. The center symmetry is explicitly broken by the fermionic action and the string tension can vanish also in the confined phase due to the formation of quark-antiquark pairs. In this case the properties of the QCD phase transition depend on the number of quark flavors and their masses [42]. In the limit of vanishing quark masses, as already stressed, the classical Lagrangian possesses the chiral symmetry, a global one, monitored by the chiral condensate $\langle\bar{\psi}\psi\rangle$. Also in this case the critical dynamics is well described by an effective Lagrangian for the order parameter with the same global symmetry for the QCD Lagrangian [41]; it suggests a first order phase transition for $N_f \geq 3$ and a second order phase transition for $N_f = 2$ and indeed this pattern was observed in lattice simulations [68].

The finite temperature phase transition on the lattice can be studied by using different tools, thermodynamical quantities and suitable order parameters, which we will review in the next sections.

2.4 Thermodynamics

The importance of lattice QCD at finite temperature is evident not only because it can give a detailed analysis of the deconfinement phase transition, but also because one can obtain the equation of state of QCD at high temperature [69]. As is well known, the perturbative expansion, due to its infra-red problems [70], has a poor convergence even at high temperatures ($T \simeq 4T_c$), suggesting that non-perturbative effects are still present and relevant; lattice computations stimulated the refining of these techniques [71], through the resummation of hard thermal loops, in order to match the perturbative with the lattice results, thus assessing the key role played by the lattice investigation even at high temperatures.

It must be anyway stressed that the study of thermodynamical observables on

the lattice is a difficult task for different reasons. If the standard Wilson action is used, in fact, one must remember that at fixed temperature T, due to the presence of lattice artifacts, there are corrections to the field strength tensor from the continuum form $F_{\mu\nu}F_{\mu\nu}$ of the order $O((aT)^2 \equiv N_T^{-2})$, so N_T must be not too small in order to avoid too strong corrections; but at the same time one must keep in mind that all the physical observables are measured in units of the lattice spacing a, for instance the energy density goes like $\epsilon a^4 \sim N_T^{-4}$, such that to have constant accuracy the statistics required increases rapidly with N_T. Moreover, near the critical temperature the low momentum modes are dominant and the finite physical volume will influence the value of the physical observables; on the other side at high temperatures the high momentum modes will give the largest contribution to observables like the energy density and pressure, resulting in a strong influence of the finite cut-off a.

All the relevant thermodynamical quantities can be calculated from the partition function $Z(T, V)$. In the continuum the free energy density f is simply given by the logarithm of the partition function

$$f = -\frac{T}{V} \ln Z(T, V) \,, \tag{2.22}$$

and the energy density ϵ and the pressure p are obtained by differentiating it with respect to T and V

$$\epsilon = \frac{T^2}{V} \frac{\partial \ln Z(T, V)}{\partial T} \,, \tag{2.23}$$

$$p = T \frac{\partial \ln Z(T, V)}{\partial V} \,. \tag{2.24}$$

For large and homogeneous systems $p = -f$, so the entropy density $s = (\epsilon + p)/T$ and $\epsilon - 3p$ are given in terms of derivatives of the pressure with respect to the temperature

$$\frac{\epsilon + p}{T} = \frac{\partial p}{\partial T} \,, \tag{2.25}$$

$$\epsilon - 3p = T^5 \frac{\partial}{\partial T} (p/T^4) \,. \tag{2.26}$$

Unfortunately the partition function is very difficult to compute directly using lattice techniques, but one can measure the expectation value of the action, which is proportional to the derivative of the logarithm of the partition function with respect to β; the free energy density is then obtained, up to a normalization constant, by integrating this expectation value

$$\frac{f}{T^4}|_{\beta_0}^{\beta} = -N_\tau^4 \int_{\beta_0}^{\beta} d\beta' [S_0 - S_T] \,, \tag{2.27}$$

with $S_0 = 6P_0$ and $S_T = 3(P_\tau + P_\sigma)$, P_0 being the expectation value of the plaquette on symmetric lattices and P_τ, P_σ respectively the expectation value of the space-time and space-space plaquettes on asymmetric lattices. At zero temperature and more in general below T_c, since in gluodynamics the only excitations are glueballs, expected

to be rather heavy ($m_G \gtrsim 1$ MeV), the free energy f, which drops exponentially $\sim \exp(-m_G/T)$, is normalized to zero through P_0. At this point it is easy to obtain

$$\frac{\epsilon - 3p}{T^4} = N_\tau^4 T \frac{d\beta}{dT}[S_0 - S_T]\,, \tag{2.28}$$

and hence the energy density ϵ. The derivative of the bare coupling β with respect to T is connected to the renormalization group equation

$$\beta(g) \equiv T\frac{d\beta}{dT} = -a\frac{d\beta}{da} = -2Na\frac{dg^{-2}}{da}\,. \tag{2.29}$$

2.5 Order parameters

In a pure $SU(N)$ lattice gauge theory in the fundamental representation one can define different order parameters useful to distinguish the confined phase from the deconfined one. The first definition was given by Wilson in his seminal work [36], but after that other order parameters were introduced by Polyakov [66] and 't Hooft [17,31]. These order parameters are important in lattice computations because they can also give important indications about the order of the transition and its critical indices. They can be also related to the non-trivial topological content of the theory, thus giving some insight into the problem of confinement.

2.5.1 Wilson criterion

For large distance R the continuum potential $V(R)$ between two infinitely heavy quarks ($q\bar{q}$) is of the form

$$V(R) = \sigma R + C_0 + \alpha R^{-1} + O(R^{-2})\,, \tag{2.30}$$

where σ is the string tension and the coefficient α describes the coulombic correction. At large distances the linear term will dominate, but at short distances the coulombic term will become more important. This simple ansatz for the potential, called Cornell potential, shows simultaneously confinement and the coulombic short range behavior. String theory predicts the coefficient of the R^{-1} correction to be [72]

$$\alpha = -\frac{\pi}{12}\,. \tag{2.31}$$

On the lattice rectangular $R \times T$ Wilson loops $W(R,T)$ in the fundamental representation can be used to extract the lattice potential. One can regard the expectation value of a Wilson loop as the creation of a $q\bar{q}$ pair at a time $T = 0$ at point $R/2$, separated instantaneously to R and 0, allowed to evolve for time T and then annihilated. For T sufficiently large we have

$$V^W(R) = -\lim_{T\to\infty}\frac{1}{T}\log\langle W(R,T)\rangle\,. \tag{2.32}$$

If such large temporal Wilson loops obey an area law, then the theory is in the confined phase; otherwise, if a perimeter law shows up, the phase is the deconfined

one. An important analytical result is the proof of Seiler that the potential cannot increase more than linearly at large distances [73]. In strong coupling expansion, i.e. small β or large g, it can be proven that $SU(N)$ gauge theories confine, with a string tension given by

$$\sigma = -\log\frac{\beta}{2N^2} + O(\beta)\,. \tag{2.33}$$

As we already stressed, we are interested in the continuum limit, i.e. large β, but for the fundamental representation no discontinuity is observed in physical observables going to larger β, so the phase diagram is connected and confinement at zero temperature is supposed to hold also in the continuum limit. In lattice computations the string tension can be extracted from the slope of $V(R)$ at large R

$$\sigma_W = \lim_{R\to\infty}\frac{1}{R}V^W(R)\,, \tag{2.34}$$

or from the asymptotic behavior of Creutz ratios [37]

$$\sigma_W = -\lim_{R\to\infty}\lim_{T\to\infty}\log\left(\frac{\langle W(R,T)\rangle\langle W(R+1,T+1)\rangle}{\langle W(R+1,T)\rangle\langle W(R,T+1)\rangle}\right)\,. \tag{2.35}$$

The limitations of this order parameter are clear: the string tension can vanish also in the confined phase in presence of dynamical fermions because of the formation of $q\bar{q}$ pairs. In real world the matter fields live in the fundamental representation of the algebra of the gauge group, but if one considers the possibility of having static adjoint charges, they can be screened by a gluon and also in this case the string tension should vanish. It is then evident that one has to look for something else.

2.5.2 Polyakov criterion

Another characterization of the different phases can be given by Polyakov loops, which are Wilson loops closed by periodic boundary conditions. At finite temperature the paths along the temporal direction are particularly important

$$\langle L\rangle = \langle\frac{1}{N_s^3}|\sum_{\vec{x}}\frac{1}{N}\mathrm{Tr}\prod_{x_4=1}^{N_t}U_4(\vec{x},x_4)|\rangle\,. \tag{2.36}$$

The static quark potential can be extracted also from the correlators of the Polyakov loop

$$\langle L(\vec{x})L^\dagger(0)\rangle - \langle L(\vec{x})\rangle\langle L^\dagger(0)\rangle \propto \exp(-V^P(R)N_T)\,, \tag{2.37}$$

where $R=\sqrt{\sum_i x_i^2}$ and the Polyakov string tension is defined by

$$\sigma_P = \lim_{R\to\infty}\frac{1}{R}V^P(R)\,. \tag{2.38}$$

The Polyakov loop correlators are well defined in the continuum limit and they can be used to characterize confinement, but the string tension extracted from them suffers from the same limitations outlined above.

For large distances, thanks to cluster decomposition, one can obtain from the correlators the free energy of a single static charge

$$\lim_{|\vec{x}|\to\infty} \langle L(\vec{x})L^\dagger(0)\rangle = \langle L(\vec{x})\rangle^2 \,. \tag{2.39}$$

If the theory is in the deconfined phase, then the free energy required to put the charge in the box is finite and $\langle L(\vec{x})\rangle \neq 0$; on the other hand if the theory confines, the energy required is infinite and $\langle L(\vec{x})\rangle$ vanishes. This behavior reflects the global symmetry under $\mathbb{Z}_N$ central conjugations that pure $SU(N)$ gauge theories in the fundamental representation possesses and the expectation value of the Polyakov loop is an order parameter with respect to this symmetry. Suppose to multiply all the temporal links at a fixed time slice by a non-trivial element z of the center

$$U_4(\vec{x}, x_4) \to zU_4(\vec{x}, x_4) \,. \tag{2.40}$$

It is straightforward to see that the space-time plaquettes are left unchanged, but not the Polyakov loop, since a temporal link at a fixed time-slice occur only once. So if this $\mathbb{Z}_N$ symmetry is spontaneously broken, at the phase transition the expectation value of the Polyakov loop should jump from zero to a non-zero value and this is exactly what happens in lattice computations. This global symmetry is very important because lead Svetitsky and Jaffe to the conjecture that (d+1) dimensional $SU(N)$ gauge theories are in the same universality class of d-dimensional $\mathbb{Z}_N$ Ising models and also this prevision was accurately verified on the lattice. Despite its success, also this order parameter has some problems; the center symmetry is explicitly broken with dynamical fermions and for gauge theories in the adjoint representation is not a symmetry at all since the center is trivial. Moreover the corresponding operator creates a single fundamental static color source, which does not belong to the physical Hilbert space of the theory, and it is affected by ultra-violet divergences in the continuum limit.

2.5.3 't Hooft criterion

Also 't Hooft proposed an order parameter to distinguish the confined from the deconfined phase. The so called 't Hooft loop $\widetilde{W}(C)$ was introduced originally in the continuum and is an operator associated with a given closed contour C. Given a Wilson loop $W(C')$, associated with the closed contour C', the 't Hooft loop is defined by the following equal-time commutation relations

$$[W(C), W(C')] = [\widetilde{W}(C), \widetilde{W}(C')] = 0 \,, \tag{2.41}$$

$$\widetilde{W}^\dagger(C)W(C')\widetilde{W}(C) = e^{i\frac{2\pi}{N}n_{CC'}}W(C') \,, \tag{2.42}$$

where $n_{CC'}$ is the linking number of C and C'. The 't Hooft loop is dual to the Wilson loop in the sense that like the Wilson loop creates an elementary electric flux along C', the 't Hooft loop creates an elementary magnetic flux along the closed path C which affects the Wilson loop pierced by C. This duality implies opposite behaviors below and above the phase transition. At zero temperature this duality has been proved and the 't Hooft loop shows indeed a perimeter law. At $T > 0$

a different behavior is expected for spatial and temporal loops; temporal 't Hooft loops should exhibit a perimeter law in both phases, just like spatial Wilson loops an area law; spatial 't Hooft loops should show a perimeter law below the phase transition and an area law above, exactly dual to the Wilson loops. On the lattice the 't Hooft loop for a gauge theory in the fundamental representation is defined by introducing by hand an elementary magnetic flux along a closed contour C defined on the dual lattice; in order to do this one has to multiply by a non-trivial element of the center all the plaquettes P dual to a given surface S supported by C. This procedure is independent from the particular surface S chosen, so the simplest choice is the minimal surface spanning C. Thus, if C is an $R_x \times R_y$ rectangle in the (x,y) plane, one multiplies by a non-trivial element of the center the coupling of the (z,t) plaquettes dual to the plaquettes belonging to the rectangular area. If one indicates with $Z_C(\beta)$ the partition function modified with the introduction of a magnetic flux along C and with $Z(\beta)$ the usual partition function, then the 't Hooft loop is given by

$$\langle \widetilde{W}(C) \rangle = Z_C(\beta)/Z(\beta)\,. \tag{2.43}$$

In the deconfined phase an area law is expected and a dual string tension $\tilde{\sigma}$ can be measured

$$\langle \widetilde{W}(C) \rangle \sim \exp\{-\tilde{\sigma} RT\} \tag{2.44}$$

We will analyze the behavior of this order parameter in lattice simulations and how it can be extended to study the case of a center-blind action more in detail in the next chapters.

A relation between the different order parameters and the corresponding definitions of the string tension can be found. Rigorously it has indeed been proven that [74]

$$\sigma_W \geq \sigma_P \quad \text{and} \quad \sigma_P \geq \sigma_H\,. \tag{2.45}$$

This means that confinement in the sense of 't Hooft implies confinement in the sense of Polyakov and Wilson. Within the validity of the strong-coupling expansion Münster has shown that $\sigma_W = \sigma_H$ holds [75] and this equality is conjectured to survive all the way to the continuum limit.

In the next chapter we will describe two models, among the many that are suggested in the literature, of the QCD vacuum, which were intensively studied in recent years, and explain how these models can be investigated through suitable order parameters.

Chapter 3

Models of QCD vacuum

As we showed before, important informations about the deconfinement phase transition, like its order and the critical exponents, can be obtained in some cases through suitable order parameters. On the other hand, understanding the mechanism which confines quarks into hadrons would be of course extremely important to gain more insight into the strong interaction at low energies and could, in principle, provide important tools to write an effective theory which describes QCD in the infra-red sector. We will see in this chapter how some models of the QCD vacuum, which thus offer some possible, although still incomplete, explanation of confinement, can be investigated through order parameters.

In the following we will point out the relevance of topology for the description of the QCD vacuum. We will then introduce the two models under study, the dual superconductor and the vortex condensate, and the related order parameters, the disorder operator and the vortex free energy, which should detect the condensation of the topological excitations.

In the next chapters we will explain how these ideas and in particular the order parameters can be extended to the adjoint representation.

3.1 Confinement and topology

Since the pioneering work of 't Hooft [18] and Polyakov [19], it is widely believed that topology could play a key role for confinement and in particular some topological excitations of the theory could be related to this phenomenon. According to a well known theorem, in pure Yang-Mills theories there can be finite energy classical solutions of the equations of motion only in 4 spatial dimensions [76]. This solution was indeed explicitly found in a 4d Euclidean space by Polyakov et al. [20] and it was called instanton. Instantons are characterized by an integer, called Pontryagin index

$$P = \frac{1}{16\pi^2} \int_{T^4} \mathrm{Tr} F_{\mu\nu} \widetilde{F}_{\mu\nu} = \nu \,, \tag{3.1}$$

which is related to the non-triviality of the maps from the space-time $\mathbb{R}^4$, compactified to S^3 through appropriate boundary conditions on the fields, to the group manifold; according to a theorem due to Bott [77] any continuous mapping of S^3

into a simple Lie group G can be continuously deformed into a mapping to an $SU(2)$ subgroup of G; since the manifold of $SU(2)$ has the topology of S^3, the important and non-trivial mappings are $S^3 \to S^3$. This topological excitation was important to solve the $U_A(1)$ problem in QCD [22] and it is believed to be essential also to explain chiral symmetry breaking, but the early expectations that it could provide the mechanism which confines quarks into hadrons were unfulfilled. A way out to the theorem about the existence of solutions is to introduce matter (scalar) fields into the theory, thus dealing with toy-models which could anyway provide some insight into QCD. One of these examples is the Georgi-Glashow model. It was proven by 't Hooft and Polyakov that the static solutions of the classical equation of motion in 3+1 dimensions are magnetic monopoles [78, 79] and it was shown by Polyakov that at zero temperature in 2+1 dimensions they provide the mechanism which confines the static charges of the theory [19]. Another example is $N = 2$ supersymmetric Yang-Mills theory, explicitly broken to $N = 1$ by a mass term. Also in this case magnetic monopoles play an essential role and their condensation leads to confinement [34, 35]. Duality is another important concept which is supposed to play a prominent role in the game, since it is a property of many systems which possess topological excitations [80]. Duality is a property of many statistical systems and allows two different descriptions: in one case in terms of the canonical variables which appear in the Hamiltonian, with solitonic solutions which are the topological excitations of the theory; in the other case the elementary variables are the topological excitations, whose dynamics is described by a suitable Hamiltonian, and the elementary fields of the original theory are the topological excitations. Duality maps strong into weak coupling and vice versa, but unfortunately the transformation relating the fields and the Hamiltonian in one description to the other is explicitly known only in few systems and all of them are Abelian. There are many models of the QCD vacuum and many attempts of explaining confinement in QCD, but until now none of them turned out to be really satisfactory. In the following we will review two of them which are particularly appealing, since they can explain some features of the theory, and are widely investigated by the lattice community; they are the dual superconductor and the vortex models of the QCD vacuum.

3.2 Dual superconductivity

The idea that the vacuum of QCD could be described in terms of a dual superconductor is very old and dates to the works of Nambu [27], 't Hooft [30, 18] and Mandelstam [28, 29]. Usual superconductivity can be understood as the breaking à la Higgs of the electromagnetic symmetry. The effective Lagrangian is written in terms of Abelian gauge fields and of a scalar field, with a symmetry breaking potential

$$L = -\frac{1}{4}F^2 + |D\phi|^2 + V(|\phi|)\,. \tag{3.2}$$

A non-vanishing vacuum expectation value for the scalar field signals the spontaneous breaking of the symmetry, through the condensation of electric charges. The Meissner effect takes place: the magnetic fields are expelled from the material, which

becomes thus superconductor, apart from thin flux tubes of constant energy density which bind magnetic charges. The Nielsen-Olesen flux tubes [81] are obtained as static solutions of the classical equations of motion in 2+1 dimensions. In the dual superconductor the role of the magnetic and electric charges are exchanged. The condensation of magnetic charges would lead to the formation of the Nielsen-Olesen strings which should confine the electric charges into the hadrons.

Unfortunately in pure Yang-Mills theories the situation is more complicated. There is no scalar field which could provide a symmetry breaking potential and no finite energy solutions of the classical equations of motion are known in 3+1 dimensions. A possible way out was indicated by 't Hooft, who suggested how to identify the magnetic monopoles in a non-Abelian gauge theory and which are the non-Abelian degrees of freedom which play the role of electromagnetism. His prescription reads as follows:

- choose an operator X which transforms in the adjoint representation of the gauge group, i.e. $X^\Omega = \Omega X \Omega^\dagger$, like the plaquette or the Polyakov loop;
- choose a gauge fixing in which the operator X is diagonal, thus reducing the gauge symmetry from the full non-Abelian gauge group to its Cartan subalgebra, i.e. $SU(N) \to U(1)^{N-1}$;
- the procedure of gauge fixing can have some ambiguities and precisely at the space-time point x_0 where two eigenvalues λ_i and λ_{i+1} of the operator X coincide; in the vicinity of the singular point the operator X can be rewritten as

$$X = \left(\begin{array}{c|cc|c} D_1 & \multicolumn{2}{c|}{0} & 0 \\ \hline & \lambda+\epsilon_3 & \epsilon_1-i\epsilon_2 & \\ 0 & & & 0 \\ & \epsilon_1+i\epsilon_2 & \lambda-\epsilon_3 & \\ \hline 0 & \multicolumn{2}{c|}{0} & D_2 \end{array}\right)$$

  where D_1 and D_2 indicate the diagonal part of the operator and ϵ_1 is the infinitesimal distance $(x - x_0)_i$ from the singularity in the i direction. The field around the point x_0 has an hedgehog form, so a Wu-Yang monopole [82] is present at x_0 and there the gauge symmetry is enhanced $U(1)^{N-1} \to U(1)^{N-3} \times U(2)$;
- in this way one obtains a theory with magnetic monopoles and with fields which transform like photons and charged matter fields. The diagonal components of the original non-Abelian gauge field play the role of the electromagnetic field

$$(A_\mu)^\Omega_{ii} = (A_\mu)_{ii} - \frac{1}{g}\partial_\mu \Lambda_{ii}\,, \tag{3.3}$$

  and the off-diagonal components behave like the matter fields

$$(A_\mu)^\Omega_{ij} = \exp(i(\Lambda_i - \Lambda_j))(A_\mu)_{ij}\,. \tag{3.4}$$

Since the original work of 't Hooft, there was no much analytical progress in understanding confinement in QCD, but this scenario was checked in many ways and

for a long time in lattice simulations. It involves, like in the continuum case, a gauge fixing procedure. In principle on the lattice gauge fixing, as far as one is involved in the calculation of gauge invariant observables, is not mandatory like in the continuum. Since on the lattice the domain of integration is compact, the functional integral is well defined without gauge fixing. But in this case this procedure is intended as necessary to extract the relevant degrees of freedom in the infra-red sector. There are many different ways of fixing the gauge but the most important for this scenario are of course the Abelian ones. Each Abelian gauge defines a proper magnetic charge; it turns out that, even if the detailed properties of the monopoles, like the position and density, strongly depend on the Abelian projection used, in every Abelian gauge monopoles condense below a certain critical temperature and are not condensed in the deconfined phase. We will clarify the procedure by taking the maximal Abelian gauge [83] (MAG) as an example, since is very commonly used and it will be important for our work. The basic steps are usually the following:

- for thermalized $SU(2)$ gauge configurations maximize the functional

$$\sum_x \sum_\mu \mathrm{Tr}[(U_\mu(x))^\Omega \sigma_3 (U_\mu^\dagger(x))^\Omega \sigma_3] \,, \tag{3.5}$$

  with respect to the gauge transformations Ω;

- project the complete links into their Abelian part

$$U_\mu(x) \to U_\mu^{AP}(x) \equiv (b_0 \mathbb{I}_2 + i b_3 \sigma_3)/\sqrt{b_0^2 + b_3^2} \,; \tag{3.6}$$

- identify the Abelian monopoles by computing the flux through 3d elementary cubes;

Some further details about the maximal Abelian gauge fixing procedure can be found in Appendix C. An important result is Abelian dominance [43, 44]; the numerical value of observables, like the string tension, computed in the original theory and in the gauge fixed and then projected theory almost agree, thus substantiating the idea that the relevant degrees of freedom have been selected. Anyway it must be mentioned that fixing the gauge on the lattice is a non-trivial procedure, which suffers from the problem of Gribov copies. Fixing the gauge corresponds, as we have seen, to the extremization of a functional; it usually happens that the system doesn't find the absolute extremum but gets stuck into a local one. As a consequence, the value of the observable can strongly depend on the particular gauge copy used to compute it. The problem can be overcome in some ways.

In order to check the dual superconductor picture one needs to define an operator which detects the condensation of magnetic charges and this will done below.

3.3 The Pisa disorder operator

In order to understand which symmetry must be associated with the dual superconductor scenario, let us go deeper into the ideas of 't Hooft. Take a field $\vec{\Phi}(x)$ in

the adjoint representation and call $\hat{\Phi}(x) \equiv \vec{\Phi}(x)/|\vec{\Phi}(x)|$ its direction in color space, which is well defined except at the zeros of $\vec{\Phi}(x)$. Define then a gauge invariant field strength $F_{\mu\nu}(x)$

$$F_{\mu\nu} = \hat{\Phi} \cdot \vec{G}_{\mu\nu} - \frac{1}{g}\left(D_\mu \hat{\Phi} \wedge D_\nu \hat{\Phi}\right) \cdot \hat{\Phi}\,, \tag{3.7}$$

where $\vec{G}_{\mu\nu} = \partial_\mu \vec{A}_\nu - \partial_\nu \vec{A}_\mu + g\vec{A}_\mu \wedge \vec{A}_\mu$ is the gauge field strength and $D_\mu \hat{\Phi} = (\partial_\mu + g\vec{A}_\mu \wedge)\hat{\Phi}$ is the covariant derivative of $\hat{\Phi}$. After some algebra one can show that

$$F_{\mu\nu} = \hat{\Phi} \cdot (\partial_\mu \vec{A}_\nu - \partial_\nu \vec{A}_\mu) - \frac{1}{g}(\partial_\mu \hat{\Phi} \wedge \partial_\nu \hat{\Phi}) \cdot \hat{\Phi}\,. \tag{3.8}$$

If we transform to a gauge such that $\hat{\Phi}$ has a fixed color direction for each space-time point, then $F_{\mu\nu} = \partial_\mu(\hat{\Phi} \cdot \vec{A}_\nu) - \partial_\nu(\hat{\Phi} \cdot \vec{A}_\mu)$, i.e. it becomes Abelian; it must be stressed that it is usually a singular gauge transformation which exposes monopoles at the sites where $\vec{\Phi}(x) = 0$. If $F^*_{\mu\nu} = \frac{1}{2}\epsilon_{\mu\nu\rho\sigma}F^{\rho\sigma}$ is the dual to $F_{\mu\nu}$, one can define a magnetic current

$$j_\mu = \partial^\nu F^*_{\mu\nu}\,, \tag{3.9}$$

which can be non-zero in the lattice formulation. It follows from the antisymmetry of $F^*_{\mu\nu}$ that

$$\partial^\mu j_\mu = 0\,. \tag{3.10}$$

In the dual superconductor scenario the symmetry (3.10) is expected to be realized à la Wigner in the deconfined phase and to be broken à la Higgs in the confined phase.

An operator μ gauge invariant and magnetic charged can characterize the different phases. It was introduced and studied by Di Giacomo and his collaborators [84, 85, 86] for $SU(N)$ gauge theories in the fundamental representation. The operator μ is called disorder operator and is constructed in the following way. First of all a time-independent external field must be introduced

$$\Phi_i(\vec{n}, \vec{y}) = \Omega e^{iTb_i(\vec{n}-\hat{i},\vec{y})}\Omega^\dagger\,, \quad i = 1, 2, 3\,, \tag{3.11}$$

where Ω is the gauge transformation which diagonalizes the operator X, T is a generator of the Cartan subalgebra and $\vec{b}$ is the discretized transverse field generated at the lattice spatial point $\vec{n}$ by a magnetic monopole sitting at $\vec{y}$. The next step is to modify the Wilson space-time plaquettes $U_{i4}(\vec{n}, 0)$ at a fixed time-slice $t = 0$ introducing a shift given by the insertion of the external field

$$U_{i4}(\vec{n}, 0) \to \widetilde{U}_{i4}(\vec{n}, 0) = U_i(\vec{n}, 0)\Phi_i(\vec{n} + \hat{i}, \vec{y})(U_i(\vec{n}, 1))^\dagger (U_4(\vec{n}, 0))^\dagger\,. \tag{3.12}$$

The disorder operator is then defined as

$$\langle \mu(0) \rangle \;=\; \frac{\int (DU) e^{-S_M(0)}}{\int (DU) e^{-S}}\,, \tag{3.13}$$

$$S_M(0) \;=\; \beta \sum_{\mu,\nu,x} \left(1 - \frac{1}{N}\left(\widetilde{U}_{\mu\nu}(x) + (\widetilde{U}_{\mu\nu}(x))^\dagger\right)\right) , \tag{3.14}$$

where $\widetilde{U}_{\mu\nu}(x)$ is the modified plaquette (Eq. (3.12)) at $t = 0$ and the standard Wilson plaquette elsewhere. It can be shown in fact, with a change of variables, that a monopole is created at $t+1$; this procedure can be iterated until the monopole is annihilated by an antimonopole at $t+T$ and the correlation function

$$D(T) = \langle \bar{\mu}(\vec{y}, t+T)\mu(\vec{y}, t)\rangle \tag{3.15}$$

describes indeed the creation of a monopole at $\vec{y}$ at time t and its propagation from t to $t+T$. At large T, by cluster property

$$D(T) \simeq A\exp(-MT) + \langle\mu\rangle^2 . \tag{3.16}$$

$\langle\mu\rangle \neq 0$ indicates spontaneous breaking of the $U(1)$ magnetic symmetry and hence dual superconductivity. In the thermodynamic limit one expects

$$\langle\mu\rangle \begin{cases} \neq 0 & T < T_c \\ = 0 & T > T_c \end{cases} \tag{3.17}$$

At finite temperature the functional integral of e^{-S} is taken with periodic boundary conditions and the integral of e^{-S_M} with C^*-periodic boundary conditions [87], [88]

$$U_i(\vec{n}, t = N_T) = U_i^*(\vec{n}, t = 0) , \tag{3.18}$$

where U_i^* means complex conjugate of U_i. At finite temperature, in fact, there is no way of putting a monopole and an antimonopole at large distance along the t axis as it is done at $T = 0$, since at $T \sim T_c$ $N_T a$ is comparable to the correlation length. C^*-periodic boundary conditions change the sign of the term proportional to σ_3 in the links, so they create a dislocation with magnetic charge -1 at the boundary which annihilates the positive magnetic charge created by $\langle\mu\rangle$. As a consequence the magnetic charge is conserved and everything is consistent. Since $\langle\mu\rangle$ is the exponential of a sum over the physical volume it has large fluctuations and for this reason it is very difficult to measure using lattice simulations. A way out is to measure a different quantity, the derivative of the logarithm of $\langle\mu\rangle$ with respect to the coupling β

$$\rho = \frac{d}{d\beta}\log\langle\mu\rangle = \langle S\rangle_S - \langle S_M\rangle_{S_M} , \tag{3.19}$$

which yields all the relevant informations on μ. It is the difference between the Wilson action averaged with the usual measure and the modified action S_M averaged with the measure $((DU)e^{-S_M})/(\int(DU)e^{-S_M})$. The inverse relation is given by

$$\langle\mu\rangle = \exp\left(\int_0^\beta \rho(\beta')d\beta'\right) . \tag{3.20}$$

A sharp negative peak for ρ should signal a phase transition driven by the breaking of a dual magnetic symmetry (see Fig. 3.1). The result should be of course independent

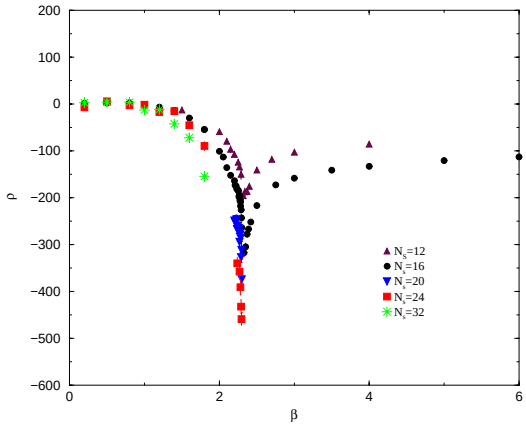

Figure 3.1: ρ as a function of β for different spatial sizes at fixed $N_T = 4$ for $SU(2)$ [84].

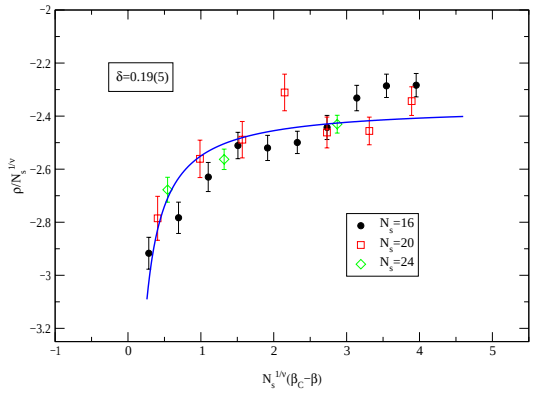

Figure 3.2: Quality of scaling at fixed $N_T = 4$ for $SU(2)$ [86].

from the Abelian projection used and, in the case of $SU(N)$ with $N \geq 3$, from the generator of the Cartan subalgebra used in the Abelian projection. To determine the order of the phase transition and its critical exponents a finite size scaling study must be performed. As a consequence of scaling arguments (for a pedagogical introduction see [89]), the order parameter and its derivative obey

$$\begin{aligned} \langle \mu \rangle &= N_S^{-\tilde{\beta}/\nu} \Phi'(N_S^{1/\nu}(\beta_c - \beta)) \,, \\ \rho / N_S^{1/\nu} &= g(N_S^{1/\nu}(\beta_c - \beta)) \,, \end{aligned} \tag{3.21}$$

where $\tilde{\beta}$ and ν are critical exponents and β_c is the coupling corresponding to the critical temperature. For $N_T = 4$ lattices, the above analysis shows that the scaling of the data is consistent for $SU(2)$ with a second order phase transition at $\beta_c = 2.2986$ with $\nu = 0.63$ (see Fig. 3.2), i.e.in the same universality class of the 3d Ising model, and for $SU(3)$ with a first order phase transition at $\beta_c = 5.6925$.

In the last chapter we will try to extend the definition of this order parameter to the case of interest for us, i.e. a theory in the adjoint representation with a monopole term.

3.4 Vortex condensate scenario

The vortex model of QCD vacuum was initially proposed by 't Hooft [31], Mack [32], Nielsen and Olesen [33] to explain confinement. After some initial work it was quite forgotten for many years until it was resurrected by the lattice community. This model assumes that center vortices, i.e. vortices whose flux is quantized according to the first homotopy group of the gauge group $\Pi_1(SU(N)/\mathbb{Z}_N)$, are the relevant degrees of freedom which eventually condense in the vacuum and cause confinement. These ideas were formalized by 't Hooft [31], who observed that for a gauge theory on a 4-dimensional torus T^4 new topological sectors, called twist sectors, arise. In fact on T^4 the gauge potentials $A_\mu(x)$ of a gauge group $SU(N)$ need to be periodic at the boundary up to gauge transformations

$$A_\mu(x+\hat{\nu}) = [\Omega_\nu(x)]A_\mu(x) = \Omega_\nu(x)A_\mu(x)\Omega_\nu^\dagger(x) + \Omega_\nu(x)\partial_\mu\Omega_\nu^\dagger(x)\,, \tag{3.22}$$

where $\Omega_\nu(x)$ are elements of $SU(N)$ which depends only on the transverse coordinate $\nu \neq \mu$ and are called twist eaters. Commutativity of displacements on the torus demands that

$$A_\mu(x+\hat{\nu}+\hat{\rho}) = [\Omega_\nu(x+\hat{\rho})\Omega_\rho(x)]A_\mu(x) = [\Omega_\rho(x+\hat{\nu})\Omega_\nu(x)]A_\mu(x)\,, \tag{3.23}$$

which implies

$$\Omega_\rho(x+\hat{\nu})\Omega_\nu(x) = z_{\rho\nu}\Omega_\nu(x+\hat{\rho})\Omega_\rho(x)\,. \tag{3.24}$$

The phases $z_{\rho\nu}$, since the twist eaters belong to $SU(N)$, are elements of $\mathbb{Z}_N$ and they can be expressed as

$$z_{\mu\nu} = \exp\left(2\pi i\frac{n_{\mu\nu}}{N}\right)\,, \tag{3.25}$$

where $n_{\mu\nu}$ is an antisymmetric tensor modulo N. This tensor has 6 independent components, which can be expressed in terms of two independent 3-vectors

$$n_{ij} \equiv \epsilon_{ijk}m_k \tag{3.26}$$

$$n_{4i} \equiv k_i\,. \tag{3.27}$$

If $n_{\mu\nu}$ is different from zero, then one deals with the so-called twisted boundary conditions; $n_{\mu\nu}$ is called twist tensor and n_{4i} determines the temporal twist, n_{ij} the spatial twist. As a consequence on the torus T^4 the bundles are classified not only by the winding number, but also by the twist, thus allowing the possibility that the Pontryagin index assumes non-integer values for non-orthogonal twists [90], i.e. $\vec{k}\cdot\vec{m} \neq 0$

$$P = \frac{1}{16\pi^2}\int_{T^4}\mathrm{Tr}F_{\mu\nu}\tilde{F}_{\mu\nu} = \nu + \frac{\vec{k}\cdot\vec{m}}{N}\,. \tag{3.28}$$

As an example for the creation of a center vortex through twisted boundary conditions consider the following 2-dimensional slice of a static $SU(2)$ lattice configuration. Set all the links to $\mathbb{I}_2$, apart from those on two orthogonal directions, for instance

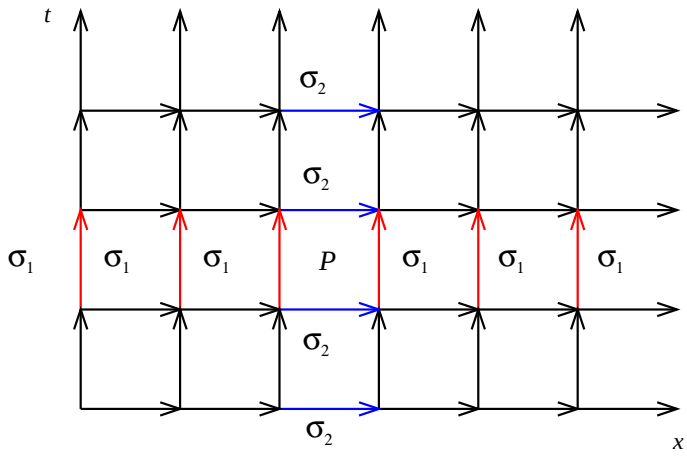

Figure 3.3: Static $SU(2)$ configuration with twisted boundary conditions.

the x and t directions; fix then the links along the x direction to σ_1 and the ones along the t direction to σ_2 [91,92]. In this case the twist eaters are σ_1 and σ_2, which satisfy the relation (3.24), i.e. $\sigma_1\sigma_2 = -\sigma_1\sigma_2$, and it is straightforward to see that each Wilson loop around the plaquette P has non-trivial value $\mathrm{Tr}_F W = -1$. A center vortex has been created on the torus in the directions perpendicular to x and t. The operator $\widetilde{W}(C)$ which creates a magnetic flux along the path C was formally introduced by 't Hooft and it is defined through the commutation relation with a Wilson loop $W(C')$ at fixed time. The Wilson loop picks up a non-trivial phase factor $\exp(2i\pi n/N)$ for each center vortex which pierces it.

A simple argument shows that these topological excitations, if they condense, can provide a mechanism of confinement for fundamental static charges. Take $SU(2)$ as a toy model and suppose that center vortices are randomly distributed in the vacuum. Put the system in a box and consider a 2-dimensional $L \times L$ slice with a Wilson loop of area A on it; if n of the total number N of vortices pierce the Wilson loop, then it will acquire a phase -1 for each intersection; assuming a binomial probability the vacuum expectation value of the Wilson loop will be given by

$$\langle W \rangle = \sum_{n=0}^{N} (-1)^n \binom{N}{n} \left(\frac{A}{L^2}\right)^n \left(1 - \frac{A}{L^2}\right)^{N-n} = \left(1 - \frac{2\rho A}{N}\right)^N . \tag{3.29}$$

In the limit $N, L \to \infty$, such that $\rho = n/L^2$ is kept constant, the Wilson loop exhibits an area law with string tension $\sigma = 2\rho$

$$\langle W \rangle = e^{-2\rho A} . \tag{3.30}$$

Even if the original ideas about center vortices were formulated without any reference to a gauge, these topological excitations can be detected on the lattice through a gauge fixing procedure. Even if there are also in this case, like in the Abelian projection for the Abelian degrees of freedom, several different possibilities of fixing the gauge degrees of freedom to the center, we will consider as a well defined example the maximal center gauge [45] (MCG), whose basics steps are the following:

- for $SU(2)$ lattice configurations maximize the expression

$$\sum_x \sum_\mu |\mathrm{Tr}[(U_\mu(x))^\Omega]|^2 \,, \tag{3.31}$$

  with respect to the gauge transformations Ω;

- project the links into their center degrees of freedom

$$U_\mu(x) \to U_\mu^{CP}(x) \equiv \mathrm{signTr}[U_\mu(x)] \,; \tag{3.32}$$

- a P-vortex is located where the plaquette of the $\mathbb{Z}_2$ configuration takes value -1;

An important result, which reminds Abelian dominance found after Abelian projection, is center dominance [45]; the observables, like the string tension, computed in the full theory and in the center-projected one agree numerically quite well and one can again think that the selected degrees of freedom are the relevant ones. Anyway there are problems with the Gribov copies also in this case and one has to refine, in some sense, the gauge fixing procedure.

As one can imagine, Abelian monopoles and center vortices are not completely uncorrelated and at least in some gauges their relation is more evident. This is realized, for instance, with the Laplacian gauge fixing [93, 94, 95].

In the following we will see in more detail the construction, already sketched previously, of the 't Hooft order parameter on the lattice [96, 97, 98, 99] and show its behavior at finite temperature [100].

3.5 Vortex free energy

In order to create a twist in the (μ, ν)-directions in a $SU(2)$ lattice configuration in the fundamental representation, one has to multiply one plaquette in every (μ, ν)-plane for a non-trivial element of the center [101, 102], which in this case is -1. This procedure, besides enforcing twisted boundary conditions, creates a 't Hooft loop of maximal size in the plane orthogonal to μ and ν. One can thus define a plaquette-dependent coupling $\beta(P)$

$$\beta(P) = \begin{cases} -\beta, & P \in P(n_{\mu\nu}) \\ \beta, & P \notin P(n_{\mu\nu}) \end{cases} \tag{3.33}$$

with reversed sign for the coclosed stacks of plaquettes dual to the planes of the maximal 't Hooft loops, called $P(n_{\mu\nu})$. In this way one can define and measure on the lattice the partition functions of the twist sectors relative to the untwisted Z_β (such that $Z_\beta(\vec{0}, \vec{0}) = 1$)

$$Z_\beta(\vec{k}, \vec{m}) = Z_\beta^{-1} \int [dU] \exp(-S(\beta, \vec{k}, \vec{m})) \,. \tag{3.34}$$

At finite temperature the temporal twists are the relevant ones; in fact the corresponding partition function is related to the maximal spatial 't Hooft loop, which

behaves, as we have already stressed, like a good order parameter. So one can concentrate on the quantity $Z_k(\vec{k}) \equiv Z_\beta(\vec{k}, 0)$, with $\vec{m} = 0$. From this quantity, which is just the expectation value of maximal size 't Hooft loops, one can compute the free energies of electric vortices. In fact, while the magnetic flux m_k through the box in the k direction is directly related to the spatial twists n_{ij}, to obtain the electric flux sectors one has to perform a $\mathbb{Z}_N$ Fourier transform with respect to the temporal twist, which is the generalization of the construction of θ-vacua as Bloch waves from ν-vacua. The general expression for the free energy $F(\vec{e}, \vec{m}, \theta)$ in a sector of given electric flux $\vec{e}$, magnetic flux $\vec{m}$ and vacuum angle θ is

$$e^{-\frac{1}{T}F(\vec{e},\vec{m},\theta)} = \frac{1}{N^3}\sum_{k_i=0}^{N-1}\sum_{\nu=-\infty}^{\infty} e^{-2\pi i\vec{e}\cdot\vec{k}/N} e^{i\theta(\nu+\vec{k}\cdot\vec{m}/N)} Z(\vec{k}, \vec{m}, \nu)\,, \tag{3.35}$$

where $Z(\vec{k}, \vec{m}, \nu)$ is the partition function for fixed twists and winding number. In the particular case $\vec{m} = 0$ and $\theta = 0$, the free energies of the electric fluxes through the L^3 box at temperature T, $F_e(\vec{e}; L, T) \equiv F(\vec{e}, \vec{m} = 0, \theta = 0) - F(\vec{e} = 0, \vec{m} = 0, \theta = 0)$ are

$$Z_e(\vec{e}) \equiv e^{-\frac{1}{T}F(\vec{e};L,T)} = \frac{\sum_{k_i=0}^{N-1} e^{-2\pi i\vec{e}\cdot\vec{k}/N} Z_k(\vec{k})}{\sum_{k_i=0}^{N-1} Z_k(\vec{k})}\,, \tag{3.36}$$

with $Z_e(\vec{0}) = Z_k(\vec{0}) = 1$.

A relation between the electric-flux partition function and the Polyakov loops can be found. In fact the partition function of the twisted sector is just the expectation value of a maximal 't Hooft loop, which is dual to a maximal Wilson loop; a maximal temporal Wilson loop is nothing else than the correlator between Polyakov loops and the remark that the partition functions in the electric-flux sector and in the twisted sector are dual to each other by a $\mathbb{Z}_2$ Fourier transform complete the linking between the different observables. This can be more formally proven starting from the gauge invariant definition of the Polyakov loop in presence of temporal twist

$$P(\vec{x}) = \frac{1}{N}\mathrm{Tr}\left(Pe^{ig\int_0^{1/T} A_0(\vec{x},t)dt}\Omega_t(\vec{x})\right)\,, \tag{3.37}$$

where $\Omega_t(\vec{x})$ is the twist matrix for twists in the temporal direction. Using the relations (3.22) ,(3.24) one can prove

$$P(\vec{x})P^\dagger(\vec{x} + L\vec{e}) = e^{-2\pi i\vec{e}\cdot\vec{k}/N}\mathbb{I}\,. \tag{3.38}$$

This shows that the expectation values of Polyakov loop correlators in the ensemble average over all the temporal twists with the enlarged partition function $Z = \sum_{k_i=0}^{N-1} Z_k(\vec{k})$ correspond to the partition functions in the electric-flux sectors,

$$Z_e(\vec{e}) = e^{-\frac{1}{T}F_e(\vec{e};L,T)} = \langle P(\vec{x})P^\dagger(\vec{x} + L\vec{e})\rangle_{L,T}\,. \tag{3.39}$$

Thus a dual relation between Polyakov loop correlators and electric-flux partition functions exists

$$\langle P(\vec{x})P^\dagger(\vec{x} + L\vec{e})\rangle \to \begin{cases} 0, & \text{for } Z_k(\vec{k}) \to 1, \quad T < T_c \\ 1, & \text{for } Z_k(\vec{k}) \to 0, \quad T > T_c \end{cases} \tag{3.40}$$

This relation was proven recently via lattice simulations for different volumes (see Fig. 3.4). A finite size scaling can be performed also in this case; by assuming

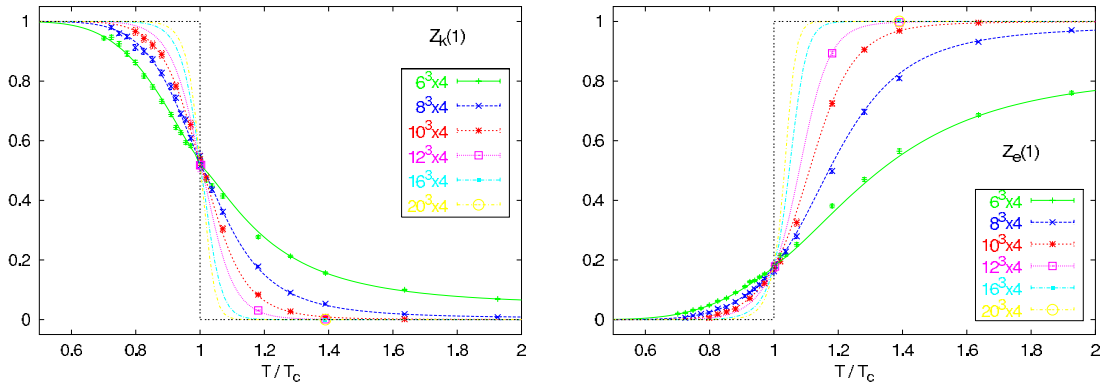

(a) temporal twist **(b)** electric flux

Figure 3.4: The partitions functions of one temporal twist (a) and one electric flux (b) over T for various lattices in the $SU(2)$ case [100].

$$Z_k(i) = f_{\pm}^{(i)}(x) \ , \ i = 1, 2, 3 \tag{3.41}$$

where the finite size scaling variable

$$x = \pm N_S T_c |t|^{\nu} \propto N_S / \xi_{\pm}(t) \ , \tag{3.42}$$

is given in terms of the reduced temperature $t = T/T_c - 1$ and of the reduced correlation length $\xi_{\pm}(t) = \xi_{\pm}^0(t)|t|^{\nu}$. As can be seen from the plots, points coming

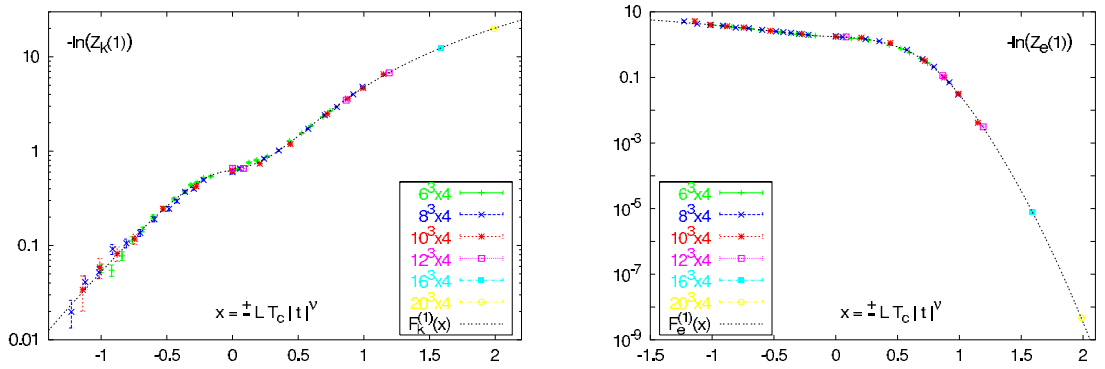

(a) temporal twist **(b)** electric flux

Figure 3.5: The free energies of one temporal twist (a) and one electric flux (b) over the finite size scaling variable x (with $x < 0$ for $T < T_c$) in the $SU(2)$ case [100].

from different volumes collapse on the same curve if for the critical exponent the

value of the 3d Ising model $\nu = 0.63$ is used (see Fig. 3.5). A dual string tension can be extracted above T_c, according to

$$\tilde{\sigma}(T) = R/\xi_+^2(t)\,, \tag{3.43}$$

where the universal ratio $R \simeq 0.104$ is known from the 3d Ising model. The universality conjecture relates also the correlation lengths of the spins in the Ising model with the correlation lengths of the Polyakov loop in $SU(2)$

$$\xi_-^{SU(2)}/\xi_+^{SU(2)} = \xi_-^{Ising}/\xi_+^{Ising} \simeq 1.96\,. \tag{3.44}$$

In this way a relation between the string tension below T_c and its dual above T_c can be obtained, i.e.

$$\frac{\sigma(T)}{T} = \frac{1}{\xi_-(t)} = T_c|t|^\nu\sqrt{\tilde{\sigma}_0^1/R_+}\ , \tag{3.45}$$

where $R_+ = \xi_-^2/\xi_+^2 R \simeq 0.4$.

In the next chapter we will introduce actions in different representations of the gauge group, stressing the differences with respect to the fundamental representation. We will see also how the definitions of the order parameters introduced in this chapter can be non-trivially extended in order to study a center-blind representation, i.e. the Villain action and the adjoint Wilson actions.

Chapter 4

Mixed actions

As already emphasized in the second chapter, the lattice discretization of a Yang-Mills theory is far from being unique, since many aspects can be varied, like the form of the action, the representation of the gauge group or the type of the lattice. An essential point of the lattice formulation is to show that in the continuum limit, when the lattice spacing a is sent to zero, all the different discretizations lead to the same (continuum) theory.

In this chapter we will review some old and more recent results about representations of the gauge action different from the fundamental one. We will concentrate on the adjoint, center-blind, representation, which was studied mainly in two different lattice discretizations, the adjoint Wilson and the Villain action. As was already shown, actions in different representations possess the same naïve continuum limit, so it is interesting to see what happens with the quantum theory via Monte Carlo simulations.

First of all we will discuss some old results about $SU(N)$ theories, with $N \geq 2$, in representations different from the fundamental; it was shown long time ago that in the $SU(2)$ case for such representations first order bulk phase transitions are present and for $SU(N)$, with $N \geq 4$ this happens also in the fundamental representation. The situation becomes more complicate at finite temperature; the deconfinement phase transition, according to universality, is expected to be second order for $SU(2)$ and first order for $SU(3)$, independently from the chosen representation; but for representations different from the fundamental the finite temperature phase transition is not observed, being overshadowed by the bulk one. As we will see these bulk transitions are due to the presence of lattice artifacts.

We will then describe in more detail the Villain action, since it offers some insight into the nature of the lattice artifacts which cause the bulk phase transition. Within this discretization it is also possible to shed some light into the relationship between different representations of the gauge action and into the topological content of the theory, i.e. the presence of twist sectors. We will review also a qualitative study about the deconfinement finite temperature phase transition done with the Villain action improved with some terms in order to suppress the lattice artifacts. We will explain in the next chapter how this ideas are mapped into the adjoint Wilson discretization and why it is worth studying also this case.

4.1 $SU(2)$ fundamental-adjoint action

Two different discretizations of an $SO(3)$ theory are commonly used. The first and more direct one was introduced by Bhanot and Creutz [103] and Greensite and Lautrup [104]; instead of dealing with $SO(3)$ matrices, computationally more expensive, they used the links in the fundamental representation and exploited the well known properties of the group characters to simulate an adjoint theory

$$S = \beta_A \sum_P \left(1 - \frac{1}{3}\Big(\big(\mathrm{Tr_F} U_P\big)^2 - 1 \Big) \right), \tag{4.1}$$

where U_P stands for the plaquette previously indicated with $U_{\mu\nu}$. The second form was used by Halliday and Schwimmer [105,106], who first recognized the importance of the non-trivial topological properties of the group manifold, which presents an additional $\mathbb{Z}_2$ compactification with respect to $SU(2)$ since $SO(3) = SU(2)/\mathbb{Z}_2$; they exploited the analogies with the Abelian case of a mixture of compact and non-compact $U(1)$ and simulated a so called Villain action (which was used also in the $U(N)$ case [102])

$$S = \beta_V \sum_P \left(1 - \frac{1}{2}\sigma_P \mathrm{Tr}_F U_P \right), \tag{4.2}$$

with the help of a $\mathbb{Z}_2$-valued auxiliary variable σ_P living on the plaquettes. It turned out that in both cases there is a striking difference with the Wilson action in the fundamental representation, i.e. the presence of a first order phase transition at $\beta_A \simeq 2.5$ in the adjoint discretization and $\beta_V \simeq 4.3$ in the Villain formulation. The weak coupling regime is well separated by the strong coupling regime, but this problem can be overcome in different ways. Bhanot and Creutz circumvented this difficulty by adding a coupling in the fundamental representation and studying this mixed action in the extended coupling space $\beta_A - \beta_F$:

$$S = \beta_A \sum_P \left(1 - \frac{1}{3}\Big(\big(\mathrm{Tr_F} U_P\big)^2 - 1 \Big) \right) + \beta_F \sum_P \left(1 - \frac{1}{2}\mathrm{Tr}_F U_P \right), \tag{4.3}$$

$$\frac{1}{g^2} = \frac{\beta_F}{4} + 2\frac{\beta_A}{3}\,.$$

The same analysis can be done with the Villain formulation in the $\beta_V - \beta_F$ plane. In both cases the phase diagram is highly non-trivial and, although quantitative different, it looks qualitative the same. In the limit $\beta_A \to \infty$ the (normalized) adjoint trace of the plaquette is restricted to the value $+1$, so the fundamental trace takes values ± 1 and one obtains a $\mathbb{Z}_2$ gauge theory, which shows a first order phase transition at $\beta_F = \frac{1}{2}\ln(1+\sqrt{2}) \approx 0.44$ [107]. The bulk phase transition along the adjoint axis enters the $\beta_A - \beta_F$ plane and merges with the previous one, thus ending at the tricritical point $\beta_A = 1.25, \beta_F = 1.22$ [108], as Fig. 4.1 indicates.

Another coupling θ can be defined as $\tan\theta = \beta_A/\beta_F$ and the corresponding scaling relation for the mixed action reads then [109]

$$\Lambda(\theta) a = \exp\left(-\frac{1}{2\beta_0 g^2} \right) (\beta_0 g^2)^{\beta_1/(2\beta_0^2)}\,, \tag{4.4}$$

with

$$\log \frac{\Lambda(0)}{\Lambda(\theta)} = \frac{5\pi^2}{11} \frac{6 \tan\theta}{(3 + 8 \tan\theta)} \,. \tag{4.5}$$

This relation implies that the intrinsic scale parameter Λ can be varied with the introduction of the adjoint coupling; it was found perturbatively that $\Lambda_F/\Lambda_A \simeq 28.9$. The phase diagram of the mixed action turns out to be analytically disconnected, with the top-left part of the diagram separated from the rest, but the continuum limit can be reached also along the path $\beta_A(\beta_V) \to \infty$.

The signal given by these first order phase transition lines is quite strong and can be detected in different ways; the easiest way is starting the simulations with different initial conditions and observing that on top of the transitions the same observable will thermalize on different values for different starts. One can also construct observables which besides showing an abrupt change at the phase transition can give some insight into its nature and elucidate the link with the topology of the system: interesting observables in this sense are $\mathbb{Z}_2$ monopoles and charges, which will be defined later, and the adjoint Polyakov loop L_A, which below the $SO(3)$ phase transition stays zero and above can take two different values, one positive, indicated in the following with L_A^+, which for large β_A is approximately 1, and the other, L_A^-, negative, which is asymptotically $-\frac{1}{3}$ [110, 53]. It is important to stress

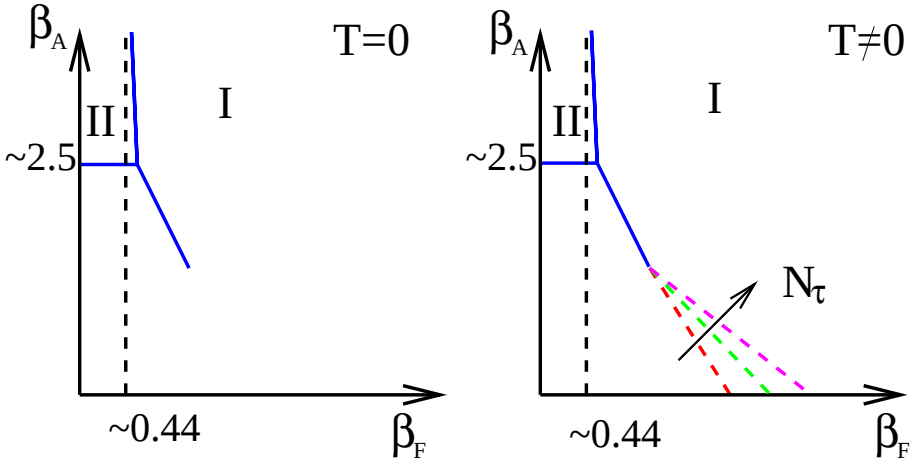

Figure 4.1: Qualitative phase diagram of the Bhanot-Creutz action at zero temperature (left) and finite temperature (right).

that all the transitions appeared to be of bulk nature, that is independent of the size of the lattice.

At finite temperature the situation, as already explained in the introduction of this chapter, becomes more involved because the lines of the second order finite temperature phase transition of the fundamental representation enter the $\beta_A(\beta_V) - \beta_F$ plane and merge together at the end-point of the first order phase transitions (see Fig. 4.1); this lead some people [111] to speculate that the phase transition could change order, thus violating universality; as we will show this is wrong and to see the decoupling of the two phase transitions one has either to increase the lattice size ($N_\tau \geq 8$) [112] or to use an improved action.

4.2 $SU(2)$ action in higher representations

For the gauge group $SU(2)$ other higher representations can be chosen, labelled by the eigenvalue $j = \frac{3}{2}, 2, \ldots$ of the Casimir operator and whose dimension is given by $d_R = 2j + 1$ [113, 114, 115, 116]; one can study a more complicated phase diagram in which each axis represent the coupling of a different representation of the Wilson action. In particular the $j = \frac{3}{2}$ and $j = 2$ representations of $SU(2)$ were studied, both with Monte Carlo simulations and analytical computations. It was found evidence, also in these cases, of a first order phase transition. In particular for a theory in the $\beta_{\frac{1}{2}} - \beta_{\frac{3}{2}}$ plane

$$S = \beta_{\frac{3}{2}} \sum_P \left(1 - \frac{1}{4}\left[(\mathrm{Tr_F} U_P)^3 - 2\mathrm{Tr_F} U_P\right]\right) + \beta_{\frac{1}{2}} \sum_P \left(1 - \frac{1}{2}\mathrm{Tr}_F U_P\right) \tag{4.6}$$

there is a line of first order phase transition starting from $\beta_{\frac{1}{2}} = 0.00, \beta_{\frac{3}{2}} = 3.90 \pm 0.10$ and ending at $\beta_{\frac{1}{2}} = 1.70 \pm 0.05, \beta_{\frac{3}{2}} = 1.09 \pm 0.09$. The phase diagram, as can be seen in Fig. 4.2, is different from the fundamental-adjoint since there is no vertical bulk phase transition; in the limit of large $\beta_{\frac{3}{2}}$, in fact, the plaquette is constrained to be $+1$ and no more ± 1, like in the adjoint case, so in that limit the theory is no more $\mathbb{Z}_2$ and the first order phase transition is absent. The theories in different representations

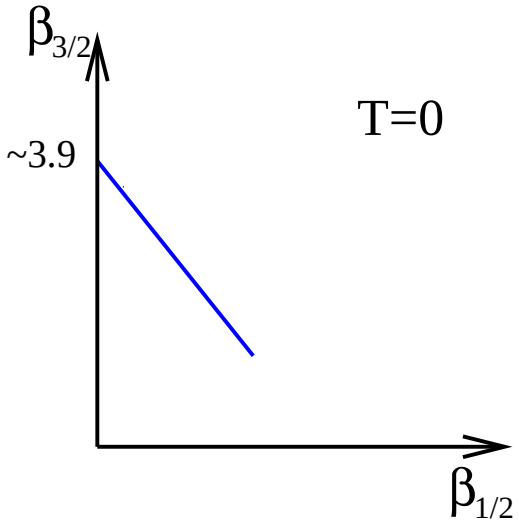

Figure 4.2: Qualitative phase diagram of a mixed action with couplings in the $j = \frac{1}{2}$ and $j = \frac{3}{2}$ representations of $SU(2)$ at zero temperature.

were studied also in different dimensionalities, with the help of analytical tools based on strong coupling expansion and Padé approximants. This analysis showed that the first order phase transition occurs for lower space-time dimensionalities by increasing the spin, as one can see from the following pattern:

	3d	4d	5d	6d
j=1/2	no	no	yes	yes
j=1	no	yes	yes	yes
j=3/2	yes	yes	yes	yes
j=2	yes	yes	yes	yes

Monte Carlo simulations and analytical studies show that the presence of a first order bulk phase transition for d=4 dimensions is the rule for all the representation of the Wilson action, with the only exception of the fundamental one.

4.3 $SU(N)$ fundamental-adjoint action

The $\beta_A - \beta_F$ phase diagram was studied also for $SU(N)$ theories, $3 \leq N \leq 6$. First order phase transitions were found along the adjoint axis $\forall N = 3, \ldots, 6$ [117]:

$$\begin{array}{ll} \beta_A = 6.40(10) & SU(3)/Z_3 \\ \beta_A = 12.00(35) & SU(4)/Z_4 \\ \beta_A = 19.5(1.1) & SU(5)/Z_5 \\ \beta_A = 32.00(1.0) & SU(6)/Z_6 \end{array}$$

However bulk phase transitions were found also along the fundamental axis for $SU(4)$ [118, 119], $SU(5)$ [118, 120], $SU(6)$ [121]:

$$\begin{array}{ll} \beta_F = 10.4 & SU(4) \\ \beta_F = 24.0(1.0) & SU(6) \end{array}$$

Indeed, it must be mentioned that a recent work raised doubts about the presence of a first order phase transition for the fundamental representation of $SU(4)$ [122].

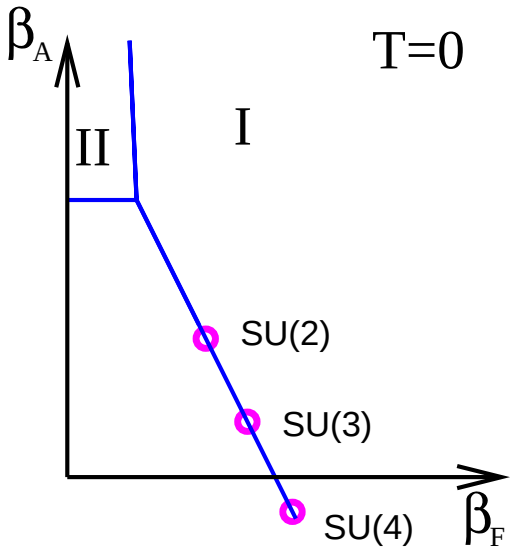

Figure 4.3: Qualitative phase diagram of an action with couplings in the adjoint and in the fundamental representations of different gauge groups at zero temperature.

The conclusion is anyway that the phase diagram is similar to the $SU(2)$ case, as Fig. 4.3 shows, with the only difference that the end point of the bulk phase transitions moves closer to the fundamental axis for $N = 3$ and eventually it crosses the fundamental axis for $N = 4$ (with the above remark about recent results).

Estimates of the location of the end-point are [123, 119, 124, 125]:

$$\begin{array}{lll} \beta_F = 4.00(7) & \beta_A = 2.06(8) & SU(3) \\ \beta_F \sim 12 - 15 & \beta_A \sim (-1) - (-5) & SU(4) \end{array}$$

When the bulk transition meets the fundamental axis, a good strategy to reach the continuum limit, if no particular improvement of the Wilson action is used, is to circumvent it by going to negative β_A.

4.4 Villain action

The formulation of a center-blind theory by using the Villain action is believed to be more convenient from a theoretical point of view because it gives some insight into the degrees of freedom involved into the bulk phase transition, but it does not correspond to an irreducible representation of the $SU(2)$ gauge theory. This fact can be easily proved by summing over the σ_P variables

$$\begin{aligned} Z &= \sum_{\sigma_P = \pm 1} \int (DU) e^{-\frac{\beta_V}{2} \sum_P \sigma_P \mathrm{Tr}_F U_P} \\ &= \int (DU) \prod_p 2\cosh[\beta_V \mathrm{Tr}_F U_P] \\ &= \int (DU) \prod_p \Big(\sum_{j=integer} 2(2j+1) \frac{I_{2j+1}(\beta_V)}{\beta_V} \chi_j(U_P) \Big) . \end{aligned} \tag{4.7}$$

From the last expression it is evident that it includes contributions from all the integer representations and hence also this discretization is center-blind.

4.4.1 $\mathbb{Z}_2$ degrees of freedom and topology

The phase diagram obtained simulating this new action does not change qualitatively but the scale along the β_V axis changes quantitatively; the $SO(3)$ phase transition now occurs at $\beta_V = 4.3$ instead of $\beta_A = 2.5$. The nature of the bulk transition lines is explained by introducing two kinds of $\mathbb{Z}_2$ objects, monopoles M and charges E, defined by

$$M = 1 - \langle \frac{1}{N_c} \sum_c \sigma_c \rangle , \qquad \sigma_c = \prod_{P \epsilon \partial c} \sigma_P , \tag{4.8}$$

$$E = 1 - \langle \frac{1}{N_l} \sum_l \sigma_l \rangle , \qquad \sigma_l = \prod_{P \epsilon \hat{\partial} l} \sigma_P , \tag{4.9}$$

where the monopole is given by the product of the σ_P variables over a three-dimensional cube c and a charge by the product over all the plaquettes with the link l in common; since a monopole (charge) is present if $\sigma_c = -1$ ($\sigma_l = -1$), a phase in which a condensation of monopoles (charges) occurs is characterized by $M = 1$ ($E = 1$), while the absence of them is signaled by $M = 0$ ($E = 0$).

An intuitive picture, supported by perturbative analytical computations and non-perturbative Monte Carlo simulations, in terms of monopoles and charges can help to understand what happens in the phase diagram. Along the β_V axis ($\beta_F = 0$) the gauge fields and the monopoles are the only relevant dynamical degrees of freedom because the charges plays no role since they are trivially zero in a center-blind theory. These $\mathbb{Z}_2$ monopoles are believed to be related in some sense to the topology of the manifold of the gauge group $SO(3)$; its first homotopy group, contrary to $SU(2)$, is non trivial, i.e. $\Pi_1(\mathbb{RP}^3) = \mathbb{Z}_2$: opposite points on the S^3 sphere are identified on $\mathbb{RP}^3$ and hence paths connecting them cannot be shrunk to zero. A deeper discussion about the topology of the group and space manifolds and their relevance for physics will be done afterwards; here we must anyway stress that despite their appealing and intuitive topological meaning, these $\mathbb{Z}_2$ monopoles and charges are in no-way physical objects since they live on the scale of the lattice spacing and are believed to be irrelevant in the continuum limit. At small β_V entropy effects dominate, monopoles are present and then these non-trivial loops are contributing to the path integral; increasing β_V entropy looses out to minimize the action and the gauge degrees of freedom (in the fundamental representation) become closer to $\pm\mathbb{I}$; paths connecting points nearby $+\mathbb{I}$ to $-\mathbb{I}$ would produce a large action so they are not present and monopoles are suppressed, thus leading the first order phase transition. In this phase, characterized by $M = 0$, the Villain action becomes $\beta_V \sum_P (1 - \frac{1}{2}\mathrm{Tr}_F U_P)$, i.e. it is just a theory in the fundamental representation, so the continuum limit of $SO(3)$ without monopoles is expected to be the same as that of $SU(2)$. At finite but small β_F the $\mathbb{Z}_2$ symmetry between states around $+\mathbb{I}$ and $-\mathbb{I}$ is still at work but for larger β_F it breaks, the system choose one of the two states and the charges drive the occurring of the bulk phase transition indicated by the vertical line in the phase diagram.

The observables M and E can be analytically computed in the corners of the $\beta_V - \beta_F$ plane. For β_V, β_F small:

$$\begin{aligned} M &= 1 - 4\left(\frac{1}{4}\beta_V\right)^6 + \mathrm{O}(\beta_V^6 \beta_F^6), \\ E &= 1 - \left(\frac{1}{4}\beta_V \beta_F\right)^6 + \mathrm{O}(\beta_V^8 \beta_F^6). \end{aligned}$$

For $\beta_V \to \infty$,β_F small:

$$\begin{aligned} M &= 0, \quad \text{(exponential corrections)}, \\ E &= 1 - \beta_F^6 + \mathrm{O}(\beta_F^8). \end{aligned}$$

For $\beta_V \to \infty$,$\beta_F \to \infty$:

$$\begin{aligned} M &= 0, \quad \text{(exponential corrections)}, \\ E &= 0. \end{aligned}$$

The intuitive picture and the analytical computations can be further supported by Monte Carlo simulations, which show the expected behavior for monopoles and charges; the observables M and E are both equal to one for small β_V and β_F; by

increasing β_V the monopole density M decreases and goes rapidly to zero around the phase transition; for large β_F also the charge density E shows an abrupt change at the phase transition collapsing to zero (see Fig. 4.4).

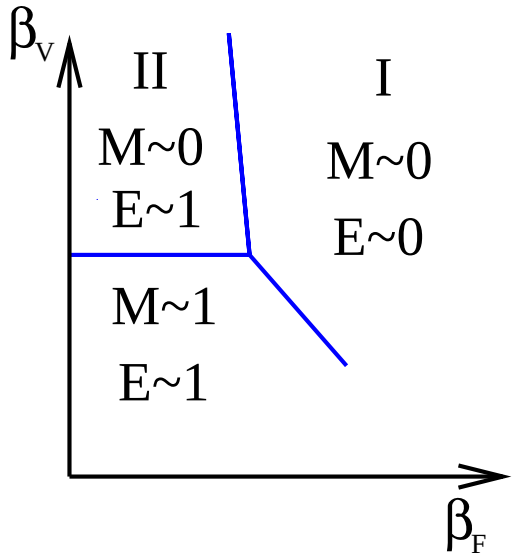

Figure 4.4: Qualitative phase diagram of the mixed Villain-fundamental action at zero temperature.

In an analogous way other $\mathbb{Z}_2$ objects can be defined

$$\widetilde{M} = 1 - \langle \frac{1}{N_c} \sum_c \sigma_c \rangle \,, \qquad \sigma_c = \prod_{P \epsilon \partial c} \eta_P \,, \tag{4.10}$$

$$\widetilde{E} = 1 - \langle \frac{1}{N_l} \sum_l \sigma_l \rangle \,, \qquad \sigma_l = \prod_{P \epsilon \hat{\partial} l} \eta_P \,, \tag{4.11}$$

where $\eta_P \equiv \mathrm{sign}\mathrm{Tr}_F U_P$. They are more general in the sense that can be measured in every representation of the theory, for instance along the β_F or the β_A axis; moreover, despite being defined in terms of variables in the fundamental representation, they are truly $SO(3)$ observables because each link appears twice in each cube and its sign drops:

$$U_\mu(x) \to -U_\mu(x) \Rightarrow \sigma_c \to \sigma_c \,.$$

The same is obviously not true for σ_l, which is a real $SU(2)$ observable. The behavior of the observables $\widetilde{M}$ and $\widetilde{E}$ is expected to be the same as M and E in regions where they can be both measured and indeed this is observed in lattice simulations, so both can be used as order parameters for the phase transitions.

4.4.2 $SU(2) - SO(3)$ connection

The problem of relating an $SO(3)$ configuration to an $SU(2)$ one was first addressed by Halliday and Schwimmer, who added a chemical potential controlling the density

of monopoles in order to study it more quantitatively [126]:

$$Z = \sum_{\sigma_P=\pm 1} \int (DU) \exp\Big(\frac{\beta_V}{2} \sum_P \sigma_P \mathrm{Tr}_F U_P + \lambda \sum_c \sigma_c \Big) . \tag{4.12}$$

In the limit $\lambda = 0$ one obtains a Villain action, but for $\lambda \to \infty$, i.e. complete suppression of monopoles, they suggested that one obtains an $SU(2)$ theory. In the case $\beta_V = 0$ a $\mathbb{Z}_2$ gauge theory is recovered, dual to a 4-dimensional Ising model [127]; it means that it possesses a second order phase transition at $\lambda \simeq 0.953$ [126]; it is also interesting to note that this theory defined in terms of 3-simplexes possesses a gauge symmetry of a higher kind respect to a $\mathbb{Z}_2$ gauge theory defined in terms of 2-simplexes, which closely relates it to a Kalb-Ramond theory [128]. The phase diagram of this extended theory was studied by Halliday and Schwimmer and it shows a line of first order phase transition terminating on a second order point.

It is worth noting that in the limit $\lambda \to \infty$ the extended action

$$Z = \sum_{\sigma_P=\pm 1} \int (DU) \exp\Big(\frac{\beta_V}{2} \sum_P \sigma_P \mathrm{Tr}_F U_P + \frac{\beta_F}{2} \sum_P \mathrm{Tr}_F U_P + \lambda \sum_c \sigma_c \Big) . \tag{4.13}$$

is self-dual [129]; in this limit σ_c is constrained to be 1, which can be solved as $\sigma_P = \prod_{l \in P} \sigma_l$, where σ_l are $\mathbb{Z}_2$ variables defined on links; a transformation $U_l \to U_l \sigma_l$ interchanges the role of the fundamental and of the adjoint terms, leaving the action invariant; this self-duality is already manifest for rather small values of λ, i.e $\lambda \geq 1$.

Kovacs and Tomboulis [130, 131], in a different context, rediscovered and made more precise what Halliday and Schwimmer and Mack and Petkova [132] already suggested,

$$Z_{SU(2)} = A \sum_{\sigma_P=\pm 1} \int (DU) e^{\beta_V \sum_P \sigma_P \mathrm{Tr}_F U_P} \prod_c \delta(\sigma_c - 1) \tag{4.14}$$

or, in other words, the partition function of an $SU(2)$ theory in the fundamental representation can be exactly rewritten à la Villain plus an additional constraint for the suppression of the monopoles constructed by using the additional $\mathbb{Z}_2$ plaquette variables. This statement, correct in the infinite volume limit ($\mathbb{R}^4$), needs a refinement on the torus ($\mathbb{T}^4$), as Alexandru and Haymaker [133] showed,

$$N_{\mu\nu} \equiv \prod_{P \in \text{ plane } \mu\nu} \sigma_P = +1 . \tag{4.15}$$

At this point the mapping between the theories in the two different representations is complete: an $SO(3)$ configuration generated with the action in the Villain form and by imposing the two above constraints, one on the 3-dimensional cubes and the other on 2-dimensional sheets, is equivalent to an $SU(2)$ configuration with periodic boundary conditions.

4.4.3 Twist sectors

A step further to understand the topology of an $SO(3)$ theory on the torus was done by Jahn and de Forcrand [48, 49, 50]. The absence of monopoles enforces

$\prod_{P \in \text{ plane } \mu\nu} \sigma_P$ to be the same in every parallel plane $\mu\nu$, so Eq. (4.15) defines only 6 constraints. They noticed that if one imposes $N_{\mu\nu} = -1$ for some $\mu\nu$ orientation, an $SO(3)$ configuration is always mapped into an $SU(2)$ one, but with twisted boundary conditions; one can then remove the global constraint by summing over all 2^6 $N_{\mu\nu}$ possibilities obtaining

$$\sum_{\text{t.s.}} Z_{SU(2)} = A \sum_{\sigma_P = \pm 1} \int (DU) e^{\beta_V \sum_P \sigma_P \text{Tr}_F U_P} \prod_c \delta(\sigma_c - 1)\,. \tag{4.16}$$

A striking difference with the $SU(2)$ case emerges: in the fundamental representation the different twist sectors are taken into account by imposing "by hand" appropriate boundary conditions, the so-called twisted boundary conditions:

$$\Omega_\mu \Omega_\nu = -\Omega_\nu \Omega_\mu$$

with Ω_μ, Ω_ν transition functions. On the other hand the $SO(3)$ theory without monopoles, which is center-blind and so it would be insensible to the previous boundary conditions, takes into account automatically the different twist sectors from the beginning. These considerations show how one can introduce a twist observable in the theory

$$z_{\mu\nu} \equiv \frac{1}{L_\rho L_\sigma} \sum_{\rho\sigma} \prod_{P \in \text{ plane } \mu\nu} \text{sign} \text{Tr}_F U_P\,, \quad (\epsilon_{\rho\sigma\mu\nu} = 1)\,, \tag{4.17}$$

which is again a truly $SO(3)$ observable since the signs of the links in the fundamental representation drops out in the product.

This observation about the twist sectors paves the way to understand how center vortices come into play in a theory without the center and the appearance of the value of the Polyakov loop $L_A = -\frac{1}{3}$. For clarity consider again the 2-dimensional slice (for instance a $x - t$ plane) of a lattice configuration in which all the links are set to $\mathbb{I}_2$, apart from these on two orthogonal directions, x and t, which are fixed to be σ_1 and σ_2 respectively [91, 92]. It is straightforward to see that it corresponds to an $SU(2)$ configuration with twisted boundary conditions and it has the following properties:

- zero action;
- non-trivial trace of every Wilson loop, i.e. $\text{Tr}_F W = -1$;
- non-trivial twist, i.e. $z_{xt} = -1$;
- trace of a Polyakov loop in the fundamental representation equal 0, hence $L_A = -\frac{1}{3}$.

In other words the presence of a center vortex, detected by $\text{Tr}_F W = -1$, is related to a non-trivial twist sector and to the negative value of the Polyakov loop in the adjoint representation. Even if the example above is just a static configuration and there is no idea on how this kind of configurations are realized dynamically, de Forcrand and Jahn guessed that a negative Polyakov loop state is a state with non-trivial twist

and motivated this idea with plots of Monte Carlo runs showing this connection (see Fig. 4.5).

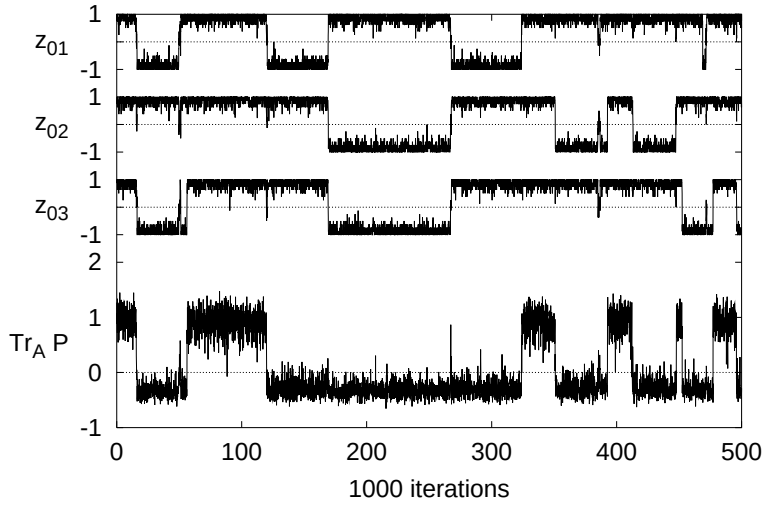

Figure 4.5: Monte Carlo history of the adjoint Polyakov loop (bottom) and of the 3 electric twist variables (top). The trace of the adjoint Polyakov loop is negative whenever twist is present (4^4 lattice, $\beta = 4.5$) [49].

They also realized that very huge barriers separate the different twist sectors, thus explaining why tunneling between them occurs so seldom and emphasizing the difficulty to have a real ergodic simulation; they suggested to use a multicanonical algorithm [134], but also in this way they could not simulate in volumes bigger than 4×8^3.

They were anyway able to measure the vortex free energy, believed to be a good order parameter for the deconfining phase transition, in this center-blind theory, thus showing that the presence of a center and its breaking are not relevant for this phase transition and suggested instead the relevance of a non-trivial first homotopy group. They also showed that in this theory the inverse lattice spacing is around 200 GeV, so the presence of lattice artifacts obliges to simulate the confined SO(3) Villain theory on enormously big lattices, 700^4. In the next section we will see how one can avoid these lattice artifacts.

4.4.4 Suppression of lattice artifacts

An investigation of the $\beta_V - \beta_F$ phase diagram avoiding the presence of lattice artifacts was realized by Gavai an Datta [135]; they explicitly took into account the suggestion of Halliday and Schwimmer of controlling the presence of monopoles and charges, the lattice artifacts, by using chemical potentials. The first step was the suppression of the monopoles by adding the chemical potential λ,

$$S = \beta_V \sum_P \left(1 - \frac{1}{2}\sigma_P \mathrm{Tr}_F U_P\right) + \beta_F \sum_P \left(1 - \frac{1}{2}\mathrm{Tr}_F U_P\right) + \lambda \sum_c (1 - \sigma_c)\,. \quad (4.18)$$

In this way they succeeded to suppress the bulk phase transition on the β_V axis but the phase diagram changed its structure; a line of first order bulk phase transitions was found extending from $\beta_V \to \infty$ to $\beta_F \to \infty$, as one expects from the duality arguments previously outlined. The lines of second order phase transition of the fundamental representation are still present and they merge again into the bulk one (see Fig. 4.6).

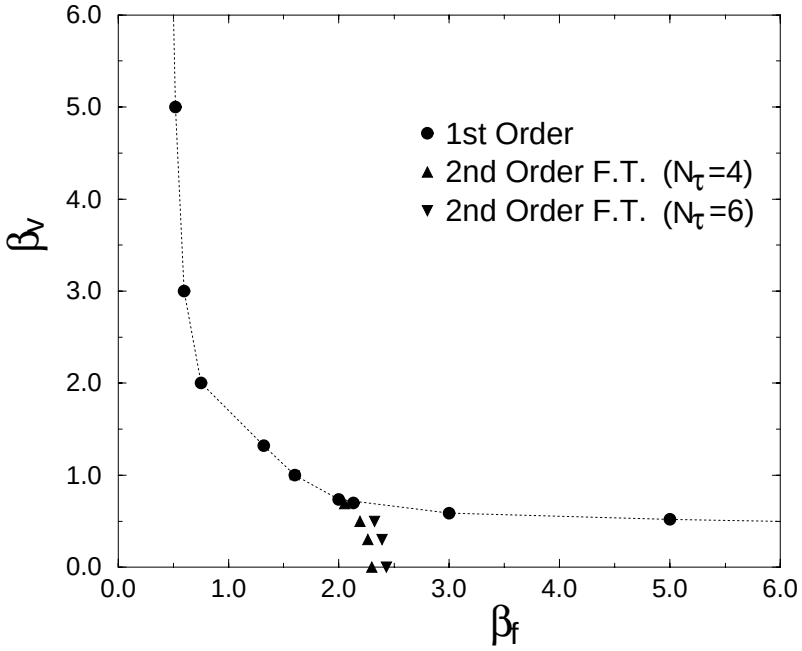

Figure 4.6: The phase diagram of the mixed action with $\lambda = 1$ on a 4×8^3 lattice. The filled circles show first order transition points. The triangles in the low β_v region show the locations of Ising-like second order deconfinement phase transitions on $N_T = 4$ and 6 lattices respectively [135].

To get rid also of this unwanted bulk transition they added γ, a chemical potential controlling the density of charges and simulated the following action:

$$S = \beta_V \sum_P \left(1 - \frac{1}{2}\sigma_P \mathrm{Tr}_F U_P\right) + \beta_F \sum_P \left(1 - \frac{1}{2}\mathrm{Tr}_F U_P\right) + \lambda \sum_c (1 - \sigma_c) + \gamma \sum_l (1 - \sigma_l) \quad (4.19)$$

They indeed found for $\lambda \geq 1$ and $\gamma \geq 5$ that the bulk phase transitions disappeared from the phase diagram and the lines of second order finite temperature crossed the β_V and β_F axis. It must be stressed that the theory in this extended space of four bare couplings is not at all center-blind and the second order phase transition line, thanks to this property, was investigated with the help of the Polyakov line in the fundamental representation.

In the particular case $\beta_F = 0, \gamma = 0$ instead a thermodynamical approach was used to understand the occurring of a deconfinement finite temperature phase transition [136]: it was found a steep rise in the energy density for asymmetric lattices with $N_T = 2, 4$ and a peak in the specific heat density only for $N_T = 2$, since for

$N_T = 4$ the data were too noisy, showing all the difficulties of a thermodynamical analysis.

It must be anyway stressed that the Villain action with the monopole suppression term constructed with the auxiliary $\mathbb{Z}_2$ plaquette fields does not yield, in the limit $\lambda_V \to \infty$, a really center-blind theory, but rather an $SU(2)$ theory in the fundamental representation. Thus, such an action is not well suited to study a center-blind theory. Moreover, in their analysis the twist sectors are not studied at all and it is not completely clear their behavior in the presence of a chemical potential for the suppression of the $\mathbb{Z}_2$ monopoles.

So it is clear that a deeper analysis is needed in order to shed some light into the problem of a finite temperature phase transition for a center-blind action. We will focus our attention, in the next chapter, not on the Villain formulation, but on the adjoint action introduced by Bhanot and Creutz, and Greensite and Lautrup. In this case, in fact, one can construct an extended action with a monopole suppression term which ensures a center-blind formulation in the entire coupling-space $\beta_A - \lambda$.

Chapter 5

Phase structure of a modified $SO(3)$ theory

We learned in the last chapter, within the Villain discretization, the role played by the lattice artifacts in the bulk phase transition and the importance of the twist sectors. We will concentrate instead our attention on the adjoint Wilson action and we will investigate how the ideas previously developed are extended to this case.

We are interested in the investigation of this theory for different reasons. In fact, even if it is still a toy-model since the group involved is $SU(2)$, it is the simplest example of action which presents a first order bulk phase transition and understanding it would pave the way to the study of larger groups, among which the physical $SU(3)$. Moreover this theory is center-blind, contrary to the fundamental representation; since a deconfinement phase transition is usually associated with the breaking of the center $\mathbb{Z}_N$ for $SU(N)$ gauge theories, is interesting to study what happens in a discretization where the center is absent and which degrees of freedom play a leading role for confinement [46, 47].

First of all we will study the effects of the lattice artifacts in this theory. A non-perturbative study is particularly important here because for this action duality arguments do not hold anymore and it can be handled less easily with respect to the Villain formulation. In order to do this, we will use a definition of the $\mathbb{Z}_2$ monopoles and of the twist observable which can be easily measured in every representation and not only in the Villain discretization. We will then control the presence of these artifacts through the use of a chemical potential, which can suppress or enhance them. With this formulation we can study a theory which is center-blind in all the coupling-space $\beta_A - \lambda$, contrary to the discretization given by Gavai et al. In the phase without $\mathbb{Z}_2$ monopoles we will study if a finite temperature phase transition occurs or not. We will study in this chapter the spatial distribution of the Polyakov loop in the fundamental representation; in the next chapters we will elaborate more sophisticated tools to detect the phase transition.

5.1 Adjoint action with chemical potential

We study the $SU(2)$ mixed adjoint-fundamental representation Wilson action which is modified by a chemical potential suppressing or enhancing the influence of $\mathbb{Z}_2$

monopoles

$$S = \sum_P \left[\frac{4}{3}\beta_A \left(1 - \frac{\mathrm{Tr}_F^2 U_P}{4} \right) + \beta_F \left(1 - \frac{\mathrm{Tr}_F U_P}{2} \right) \right] + \lambda \sum_c (1 - \sigma_c) \,. \qquad (5.1)$$

Here we have $\sigma_c = \prod_{P \epsilon \partial c} \mathrm{sign}(\mathrm{Tr}_F U_P)$. Although σ_c is constructed in terms of fundamental representation quantities, it is a *natural* $SO(3)$ quantity. In fact, for every given $SO(3)$ link variable, the corresponding $SU(2)$ representative is always determined up to a sign. But the latter is cancelled in the product over plaquettes P, since each link occurs twice for two faces of the 3-cube. In other words

$$U_\mu(x) \to -U_\mu(x) \quad \Rightarrow \quad \sigma_c \to \sigma_c \,, \qquad \forall \mu, x, c \,.$$

Although the suppression term in Eq. (5.1) looks formally identical with the one used in connection with the Villain-type action, its realization is different and leads to a different phase structure, as our data in Fig. 5.1 and the plots of Datta and Gavai in Fig. 4.6 show. The phase transition line is found by observing that on

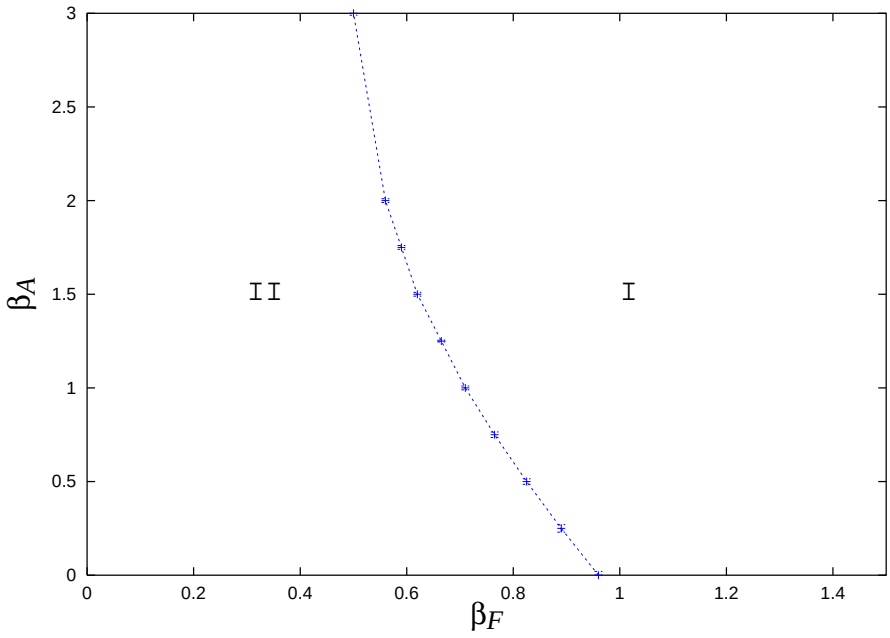

Figure 5.1: Phase diagram of the mixed fundamental-adjoint action with monopole suppression term at $\lambda = 1.0$ and $T = 0$.

top of it some simple observables, like the plaquette, thermalize on different values for different starts. The $\mathbb{Z}_2$ monopoles are suppressed in both phases but the $\mathbb{Z}_2$ charges undergo a phase transition, changing from one, in phase I, to zero, in phase II (for comparison see the Fig. 4.4). In this case the bulk phase transition, at $\lambda = 1.0$, intersects the fundamental axis, thus creating two disconnected regions in the $\beta_A - \beta_F$ plane. In the Villain discretization used by Datta and Gavai, instead, in the limit $\lambda_V \to \infty$, the theory in the fundamental and in the adjoint representation are dual to each other and in the phase diagram the β_A and β_F axis are connected;

in other words in such a limit a theory in the adjoint representation is equivalent to the fundamental one and a real center-blind theory cannot be studied. In our case such a duality is not evident and in fact we get a disconnected phase diagram. This is why we should not identify the chemical potential λ_V with λ. Moreover this kind of suppression term can be used with every representation of the gauge group $SU(2)$ and not only with the Villain discretization, so in this sense it is more general. We can also define a twist observable z_{xt} like in Eq. (4.17), which is again a truly $SO(3)$ observable, since $z_{xt} \to z_{xt}$ if $U_\mu(x) \to -U_\mu(x)$, and can be measured in every representation.

Mostly we shall be interested in the pure adjoint case $\beta_F = 0$. In this special case we have analyzed the model with the link variables represented both by $SO(3)$ matrices and by the fundamental representation 2×2 matrices, exploiting the property $\mathrm{Tr}_A = \mathrm{Tr}_F^2 - 1$. Nothing changes in the phase diagram but in the latter case simulations become much simpler and faster. This is the reason why we favored the 2-dimensional representation. A standard Metropolis algorithm has been used to update the links (for details see Appendix A).

5.2 The bulk transition

In this section we investigated the effect of a varying chemical potential ($0.0 \leq \lambda \leq 1.0$) on some simple observables, like the adjoint plaquette $\mathcal{P}$, the adjoint Polyakov loop L_A and the density of cubes $\mathcal{M} = (\sum_c \sigma_c)/N_c$. We used rather small volumes ($V = 4 \times 12^3$) in order to understand what happens by varying λ from zero to one. The volume is chosen asymmetric for convenience but the bulk effects are present also in symmetric volumes.

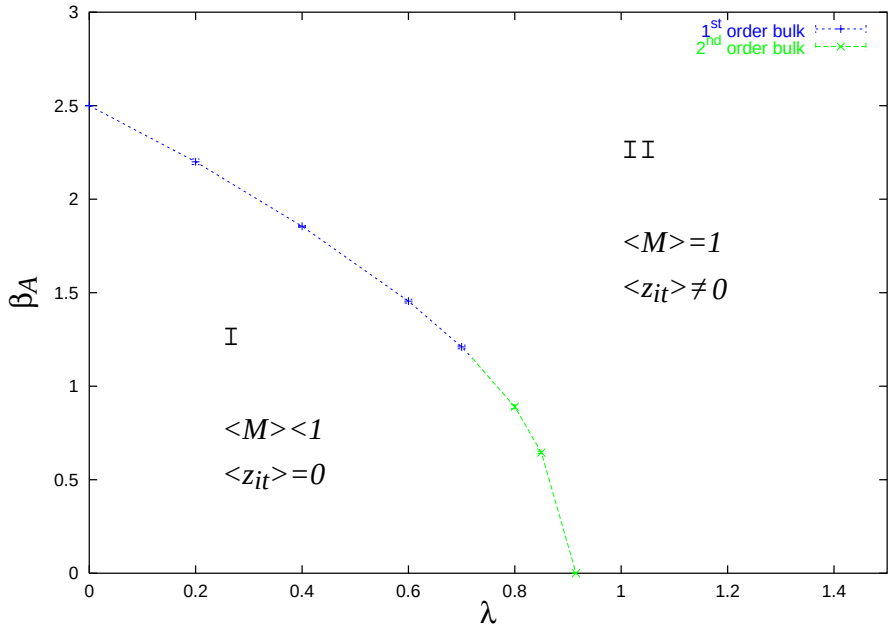

Figure 5.2: Phase diagram in the $\beta_A - \lambda$ plane at zero temperature.

As we will show more in detail in the next section, in the region of the phase diagram called I in Fig. 5.2, the twist is not well defined since there are fluctuations between the different twist sectors and it averages to zero. In region II the energy barriers between the different twist sectors become higher and tunneling is strongly suppressed. The system will stay in a fixed twist sector that can be chosen with appropriate initial conditions, and in this section, for large enough λ and β_A, we will study the trivial twist sector.

The plaquette shows a clear gap, signalling the presence of a first order phase transition, for $\lambda \leq 0.7$. For $\lambda > 0.7$ such a signal is strongly suppressed. This is indeed what we wanted and what we expected, since the chemical potential should suppress the lattice artifacts which produce the bulk phase transition and as a consequence the transition, by varying smoothly λ, should slowly become weaker and for large enough λ eventually disappear. For such values of the chemical potential ($\lambda > 0.7$) the observables seem quite smooth, but a second order bulk phase transition could still be present, as the analysis of the twist in the next section seems to suggest. At $\beta_A = 0.0$ and $\lambda = 0.953$ it is in fact expected a second order phase transition, being the theory dual to Ising 4d; this transition could eventually enter the $\beta_A - \lambda$ plane and join the first order one. A more detailed analysis must be performed to understand if the bulk phase transition is always there and in the positive case its order. At $\lambda = 1.0$ the bulk phase transition seems instead to be completely absent for $\beta_A \geq 0.0$, thus suggesting that the bulk phase transition crosses the λ axis around $\lambda = 0.953$.

The $\mathbb{Z}_2$ cube density shows a behavior similar to the plaquette, with a jump for $0.0 \leq \lambda \leq 0.7$, clear signal of a first order phase transition. Above $\lambda = 0.7$ it goes to 1, thus signalling the absence of $\mathbb{Z}_2$ monopoles, but in a smooth way, without any discontinuity. It is worth saying that the region in the $\beta_A - \lambda$ plane where the cube density goes to one coincide with the region where the twist becomes non-zero and eventually reaches one. At $\lambda = 1.0$ for each value of β_A the cube density is fixed to one and there is no presence of any bulk phase transition.

The Polyakov loop shows again an abrupt jump for $0.0 \leq \lambda \leq 0.7$. In such a range the Polyakov loop averages to zero below the bulk transition and becomes different from zero above it. The non-zero value of the Polyakov loop is always positive since we are fixed in the trivial twist sector; in the non-trivial twist sector the jump would be again present, but then the Polyakov loop would be negative. It is essential to note its behavior for $\lambda > 0.7$. At $\lambda = 0.8, 0.85, 1.0$ it takes a non-zero value no more above the bulk phase transition, but in a different region in the $\beta_A - \lambda$ plane. It means that above a certain λ its behavior is completely decoupled from the dynamics of the lattice artifacts. If we can interpret $\langle L_A \rangle$ as the free energy of a static adjoint source, then $\langle L_A \rangle = 0$ should be interpreted as a signal for confinement. It is of course true, in principle, that an adjoint static charge could always be screened by a gluon, but this effect of string breaking is expected to occur, in practice, only for for very large volumes [137, 138], so we can safely take the Polyakov loop as a signature of the presence of two phases, characterized respectively by $\langle L_A \rangle = 0$ and $\langle L_A \rangle \neq 0$. Whether these two phases are separated by a real phase transition or rather a cross-over is not easy to understand and we will address the question later on.

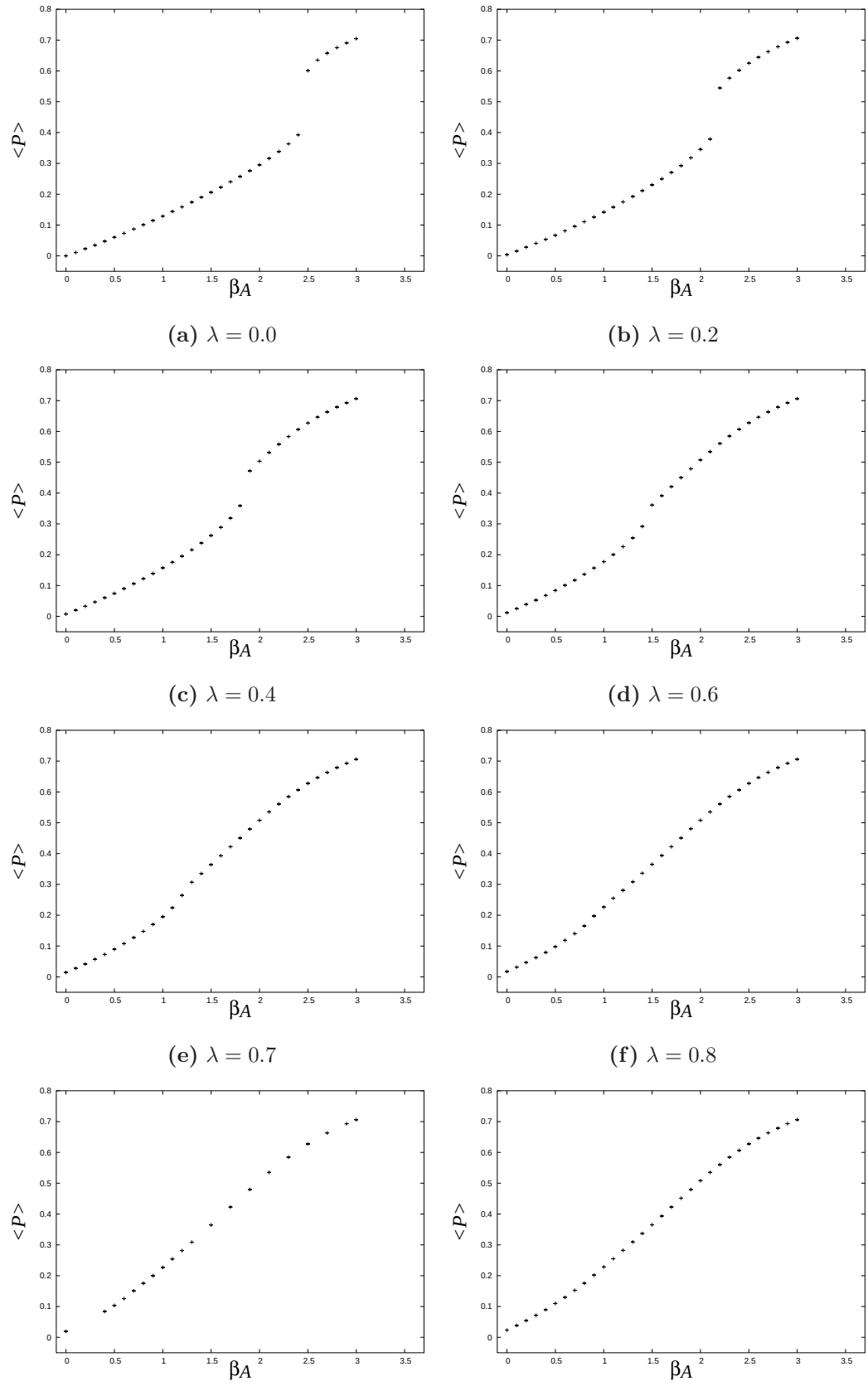

(a) $\lambda = 0.0$ **(b)** $\lambda = 0.2$

(c) $\lambda = 0.4$ **(d)** $\lambda = 0.6$

(e) $\lambda = 0.7$ **(f)** $\lambda = 0.8$

(g) $\lambda = 0.85$ **(h)** $\lambda = 1.0$

Figure 5.3: Plaquette as a function of β_A for different values of λ ($V = 4 \times 12^3$).

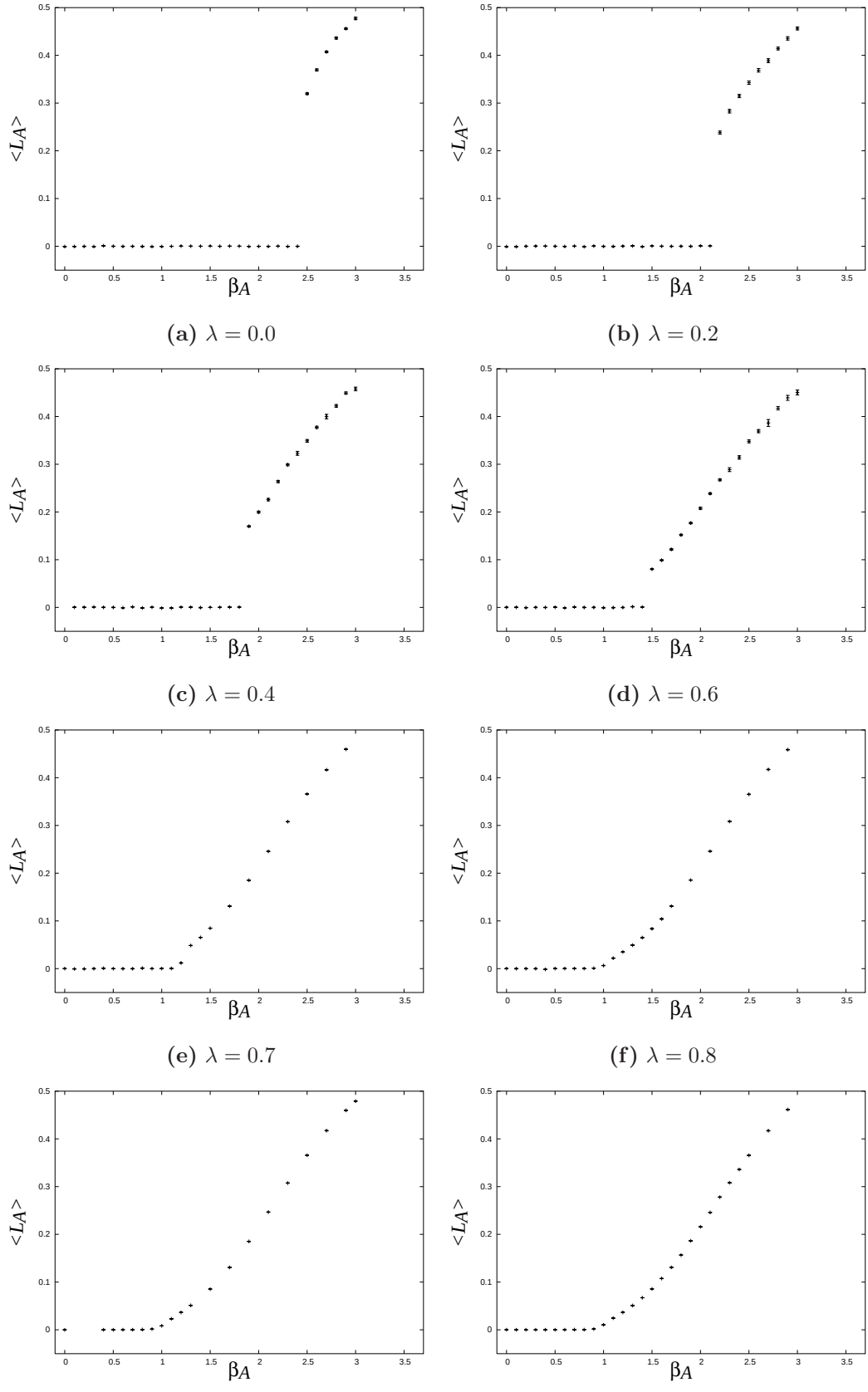

(a) $\lambda = 0.0$ **(b)** $\lambda = 0.2$

(c) $\lambda = 0.4$ **(d)** $\lambda = 0.6$

(e) $\lambda = 0.7$ **(f)** $\lambda = 0.8$

(g) $\lambda = 0.85$ **(h)** $\lambda = 1.0$

Figure 5.4: Adjoint Polyakov loop as a function of β_A for different values of λ ($V = 4 \times 12^3$).

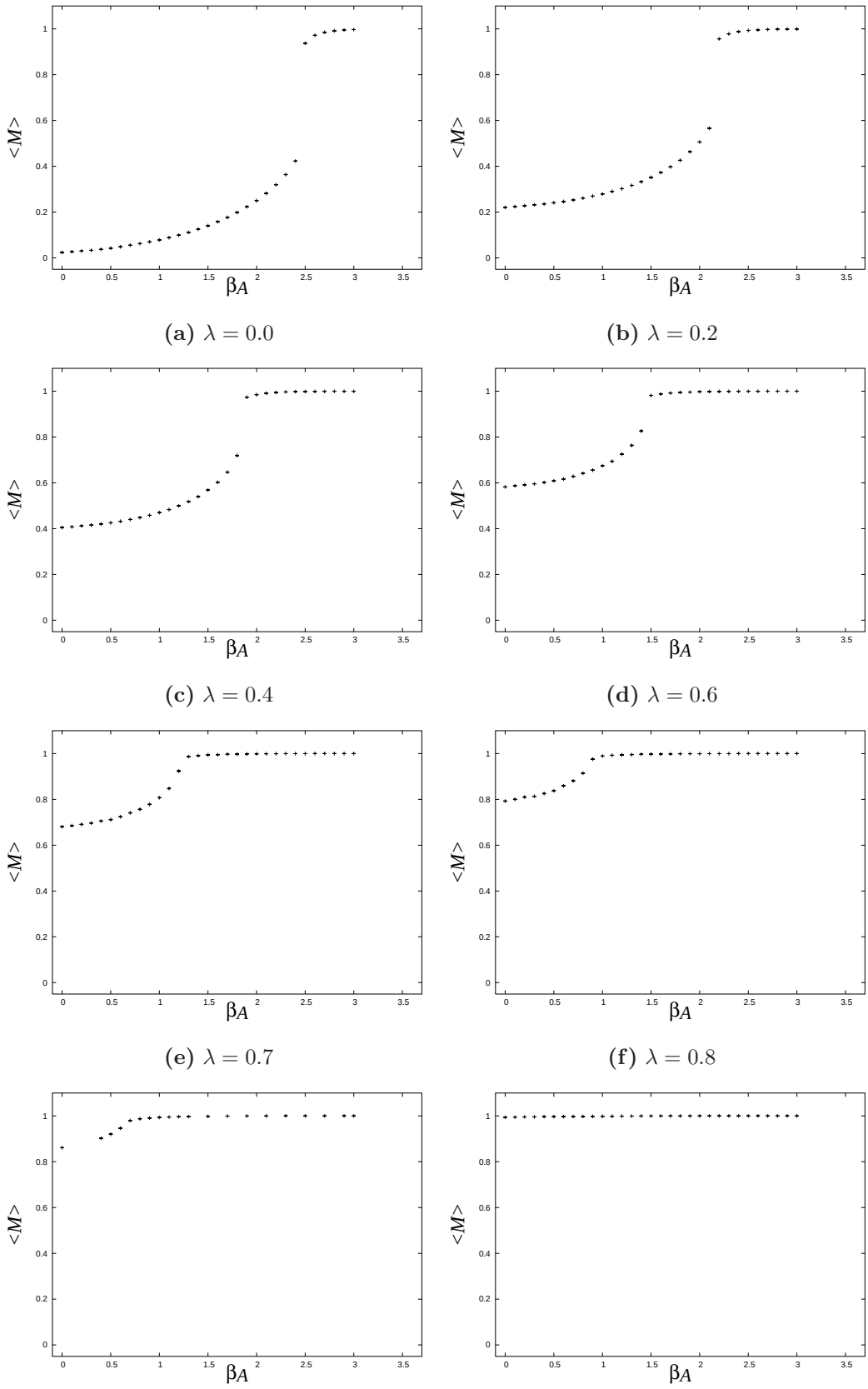

(a) $\lambda = 0.0$ **(b)** $\lambda = 0.2$

(c) $\lambda = 0.4$ **(d)** $\lambda = 0.6$

(e) $\lambda = 0.7$ **(f)** $\lambda = 0.8$

(g) $\lambda = 0.85$ **(h)** $\lambda = 1.0$

Figure 5.5: Cube density as a function of β_A for different values of λ ($V = 4 \times 12^3$).

5.3 Twist sectors and tunneling

We checked whether also in the theory we studied we can find the same behavior of the twist sectors and of the Polyakov loop that de Forcrand and Jahn found in the Villain case. We indeed observed for small volumes ($V = 4^4$) and on top of the bulk phase transition ($\lambda = 0.0$) tunneling between different twist sectors, as can be seen from Fig. 5.6. The same plot indicates the dynamical relation between the Polyakov loop and the twist observable, whose non-trivial value signals also in this case the presence of the negative state $L_A^- = -\frac{1}{3}$. For larger volumes it is difficult to see the

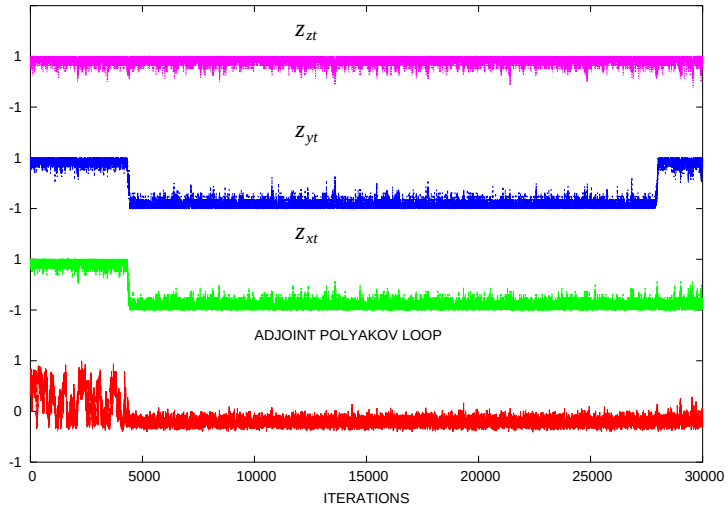

Figure 5.6: Monte Carlo history of the adjoint Polyakov loop and of the 3 electric twist variables ($V = 4^4$, $\beta_A = 2.519$, $\lambda = 0.0$)

occurrence of tunneling on top of the bulk phase transition at $\lambda = 0$ and for small λ ($\lambda \leq 0.7$), but as soon as the chemical potential is increased the situation changes.

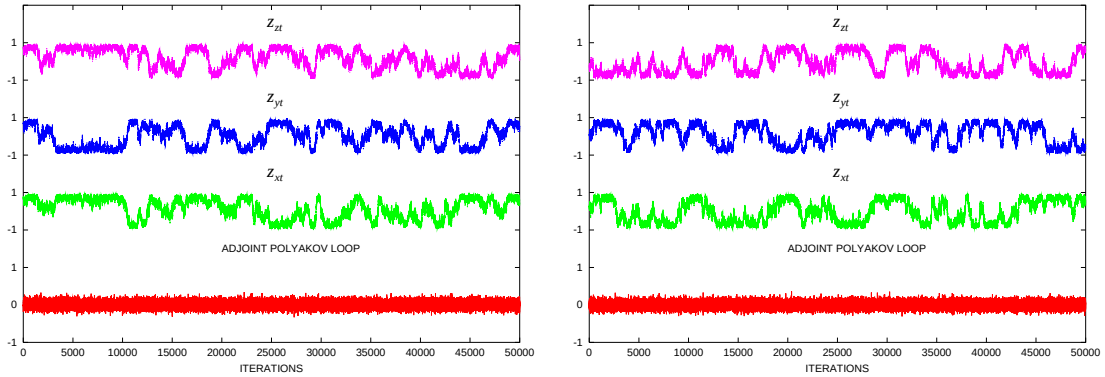

(a) $\lambda = 0.80, \beta_A = 0.90$ **(b)** $\lambda = 0.85, \beta_A = 0.65$

Figure 5.7: Monte Carlo history of the adjoint Polyakov loop and of the 3 electric twist variables ($V = 4 \times 12^3$) at $\lambda = 0.80, \beta_A = 0.90$ (a) and $\lambda = 0.85, \beta_A = 0.65$ (b).

For $\lambda > 0.7$ there are still strong fluctuations between the different twist sectors below the bulk phase transition (region I in Fig. 5.2), but on top of the phase transition tunneling becomes more evident, as Fig. 5.7 shows, and the twists begin to oscillate between -1 and +1. The value of the Polyakov loop is probably too small to observe tunneling between L_A^+ and L_A^-, although the data are more compatible with 0. The behavior of the twists, which reminds closely the behavior of the fundamental Polyakov loop in the $SU(2)$ theory in the fundamental representation, suggests the definition of an order parameter $\tilde{z}$, such that

$$\tilde{z} \equiv \frac{1}{3}(|z_{xt}| + |z_{yt}| + |z_{zt}|)\,. \tag{5.2}$$

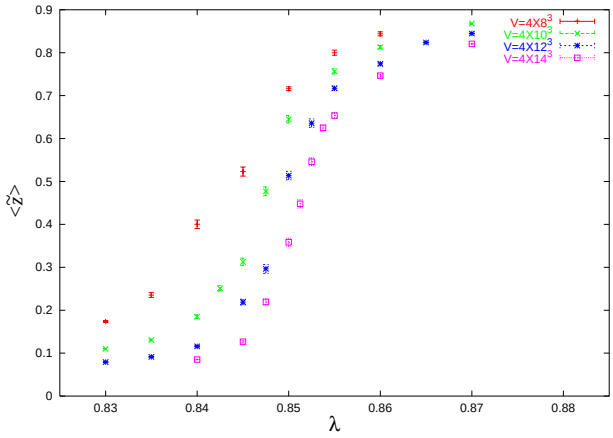

Figure 5.8: Ensemble average of the order parameter $\tilde{z}$ for different values of λ and volumes at $\beta_A = 0.65$.

In this way the new observable $\tilde{z}$ and its susceptibility, defined as

$$\chi = N_S^3 \cdot (\langle \tilde{z}^2 \rangle - \langle \tilde{z} \rangle^2) \tag{5.3}$$

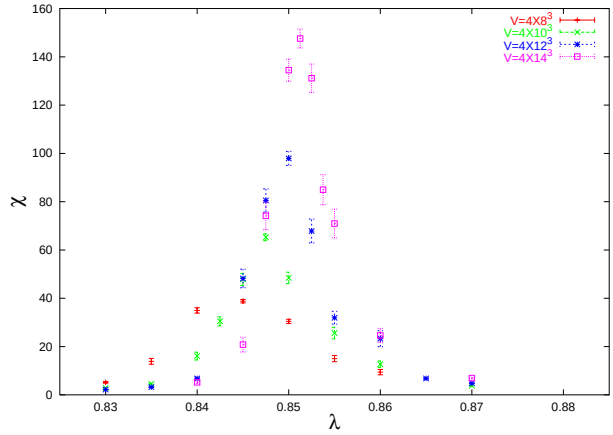

Figure 5.9: Susceptibility of the order parameter $\tilde{z}$ for different values of λ and volumes at $\beta_A = 0.65$.

can be monitored at fixed λ by varying β_A and for different volumes, as Fig. 5.8 and Fig. 5.9 show. A preliminary finite size scaling analysis shows that the peaks of the susceptibility do not increase with the lattice size according to a first order transition, but rather with the exponents of the same universality class of Ising 4d. For larger chemical potential ($\lambda \geq 1.0$) and positive β_A tunneling is no more observed, away from the bulk transition (phase II).

The occurrence of tunneling below and on top of the bulk phase transition is a clear signal of ergodicity, but only in a subspace of the phase diagram. One should construct an improved code that implements tunneling in the entire $\beta_A - \lambda$ plane and investigate the theory with this new algorithm. An attempt in this direction was done by de Forcrand and Jahn by using a multicanonical algorithm [134] and another possibility would be parallel tempering [139]. On the other hand, without such an algorithm, we have the opportunity to study the theory in a sector with the suppression of center vortices and it is then interesting to study what happens in this trivial twist sector.

The simplest thing one can do is to study the theory in a fixed twist sector for large enuogh λ and β_A, i.e. in phase II; we performed this analysis in Section 5.4, with the distribution of the Polyakov loop in the fundamental representation, and in Chapter 7, with the Pisa disorder operator. The other way, i.e. the construction of an algorithm which implements tunneling is highly non trivial. We will discuss an attempt in this direction in Chapter 6. It is worth anyway saying that we found a way to map the trivial into the non-trivial twist sectors, but unfortunately it cannot be used to build an ergodic algorithm. It can be realized by multiplying all the temporal links at a fixed time-slice $t = t_1$ with $i\sigma_3$. In this case, after a reasonable transient, the negative state becomes stable (Fig. 5.10) since a non-trivial twist has been created. In the following example we used a rather small volume, $V = 4 \times 10^3$, and the values of the couplings are $\beta_A = 2.5$ and $\lambda = 1.0$. In this case a twist has been created in the $x - t$ plane, as Fig. 5.10 shows. This

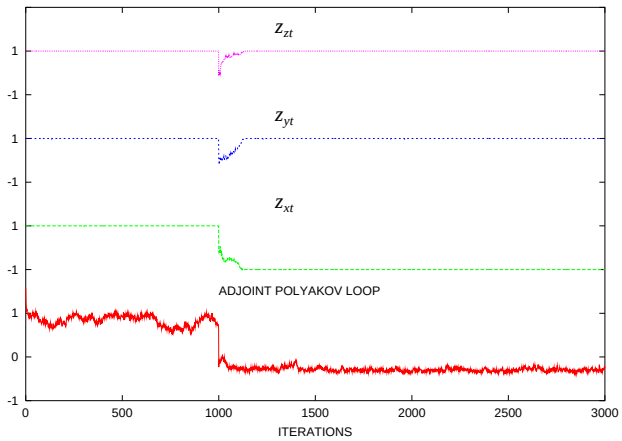

Figure 5.10: Monte Carlo history of the adjoint Polyakov loop and of the twist in the x-t, y-t, z-t planes transformed at iteration 1000 by $i\sigma_3$ ($V = 4 \times 10^3$, $\beta_A = 2.5$,$\lambda = 1.0$).

transformation does not correspond, anyway, to a symmetry of the action, since it

produces a peak in the plaquette and for this reason it cannot be used to construct an ergodic algorithm. In Fig.5.11 $\mathcal{P}_1$ indicates the average plaquette, $\mathcal{P}_2$ the average of the temporal plaquettes and $\mathcal{P}_3$ the average of the temporal plaquettes living at $t = t_1$, i.e. the ones and only those involved in the transformation.

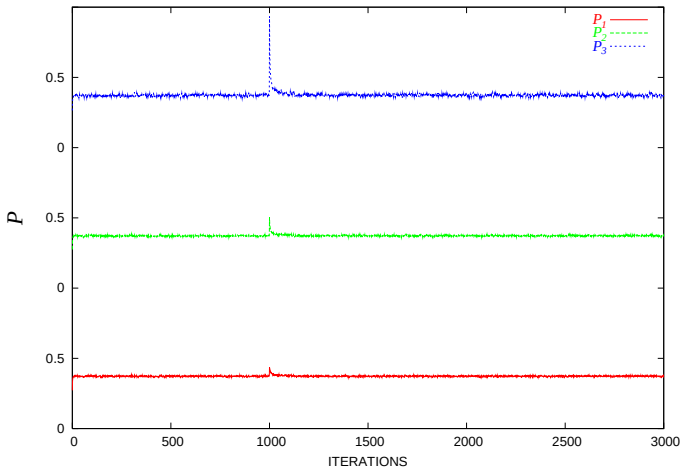

Figure 5.11: Effect of the transformation by $i\sigma_3$ on the Monte Carlo history of the average plaquette (bottom), of the average temporal plaquette (middle), of the average temporal plaquette at $N_T = 1$ (top) ($V = 4 \times 10^3$, $\beta_A = 2.5$,$\lambda = 1.0$).

The change of the action is rather high and thus the transformed configuration would be always rejected in a Metropolis accept-reject step.

5.4 Indication for a finite temperature phase transition

In the following we will study the theory at finite temperature in fixed twist-sectors, both trivial and non-trivial, with particular emphasis for the trivial one. In order to start the simulations in the desired twist sector, we used particular initial conditions and we checked during the runs that the system did not move to twist sectors different from the initial one. We used as initial condition a normal cold start, with all the links along the identity, to perform simulations in the trivial twist sector. We used instead the configurations already introduced to explain the relation between Polyakov loop and twist sectors as initial conditions for a non-trivial twist sector. In particular for the 1-twist sector we put all the links to the identity, except the ones at a fixed value of the temporal direction and at a fixed value of a spatial direction, which were fixed to two different Pauli matrices; for instance we aligned the links at $t = t_n$ along $i\sigma_1$ and the links at $x = x_m$ along $i\sigma_2$; we of course checked that the results are independent from the Pauli matrices and the spatial direction chosen to implement the 1-twist sector. For the other twist sectors we imposed similar initial conditions, taking care that we do not create any spatial twist, since at finite temperature we are interested only into the temporal ones. In fact a 2-twist sector can be generated by aligning the links along Pauli matrices at fixed time and at

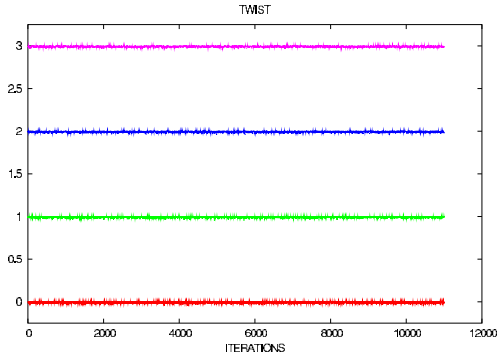

(a) Twist observable

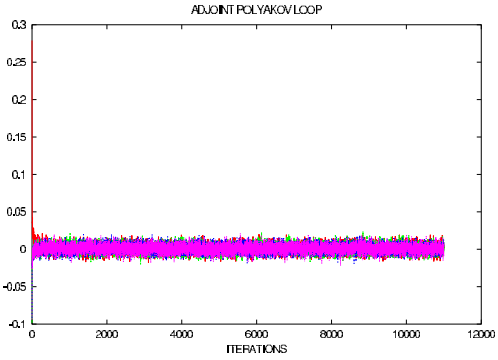

(b) Adjoint Polyakov loop

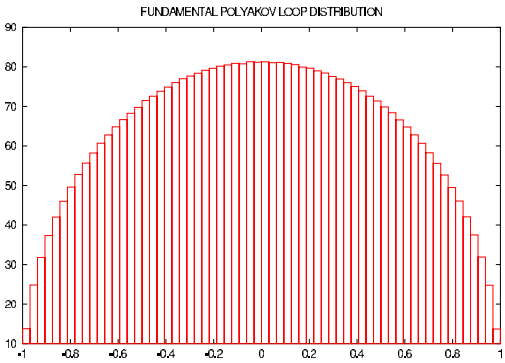

(c) 0-twists sector

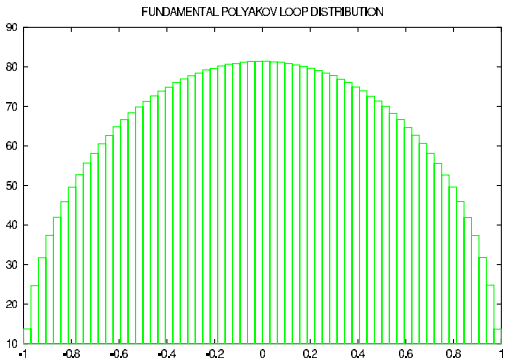

(d) 1-twist sector

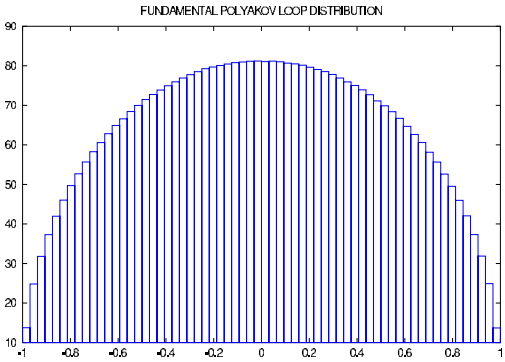

(e) 2-twists sector

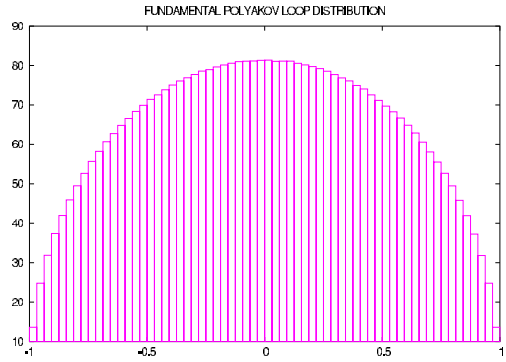

(f) 3-twists sector

Figure 5.12: Monte Carlo history of the twist observable (a) and of the adjoint Polyakov loop (b); spatial distribution of the fundamental Polyakov loop in the 0 (c), 1 (d), 2 (e), 3 (f) twist sectors ($V = 4 \times 16^3$,$\lambda = 1.0$,$\beta_A = 0.9$).

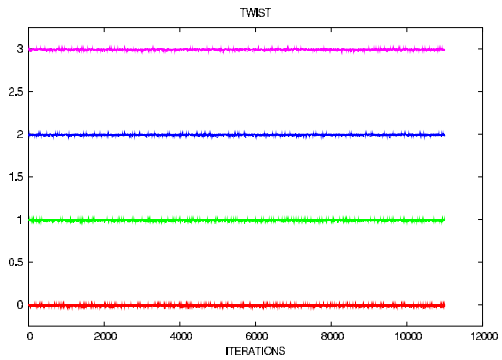

(a) Twist observable

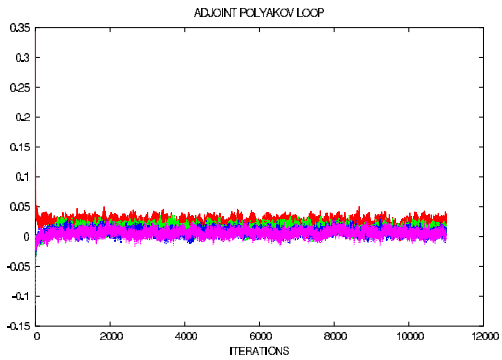

(b) Adjoint Polyakov loop

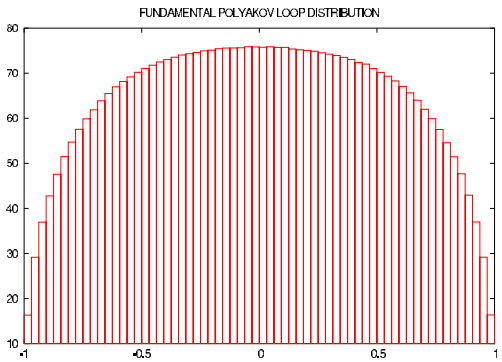

(c) 0-twists sector

(d) 1-twist sector

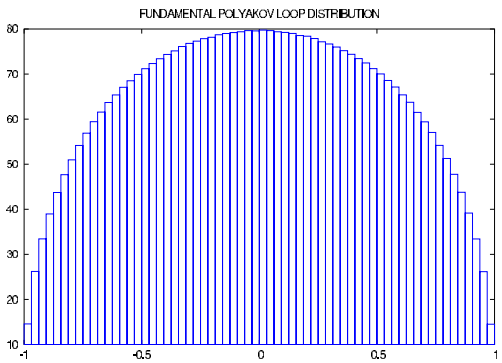

(e) 2-twists sector

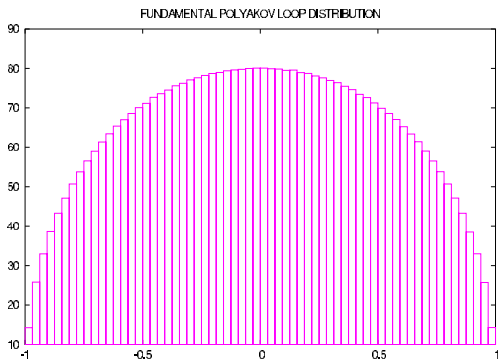

(f) 3-twists sector

Figure 5.13: Monte Carlo history of the twist observable (a) and of the adjoint Polyakov loop (b); spatial distribution of the fundamental Polyakov loop in the 0 (c), 1 (d), 2 (e), 3 (f) twist sectors ($V = 4 \times 16^3$,$\lambda = 1.0$,$\beta_A = 1.1$).

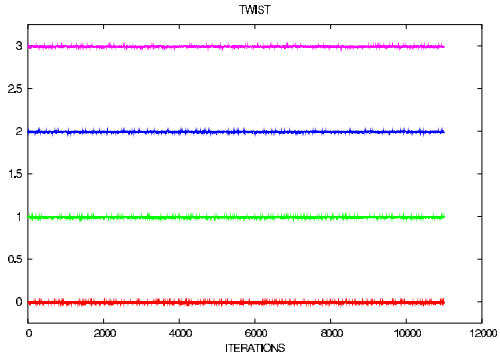

(a) Twist observable

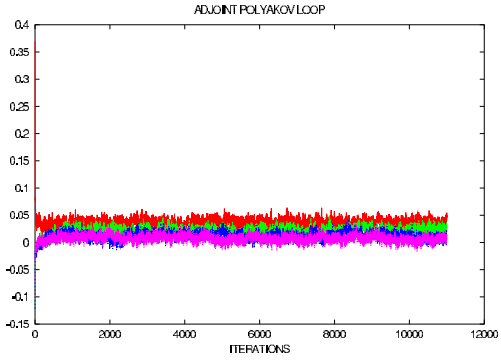

(b) Adjoint Polyakov loop

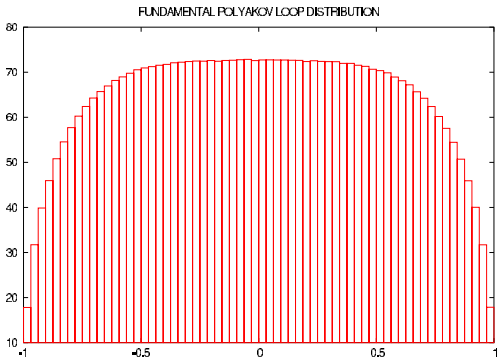

(c) 0-twists sector

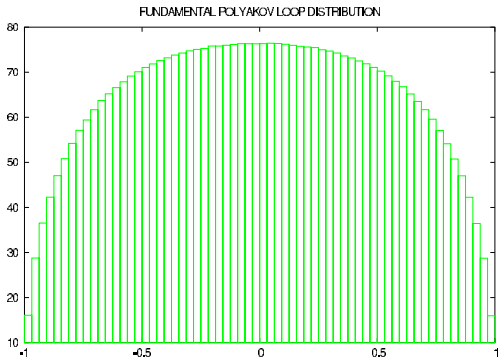

(d) 1-twist sector

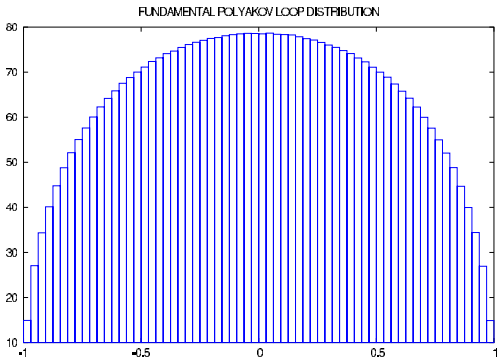

(e) 2-twists sector

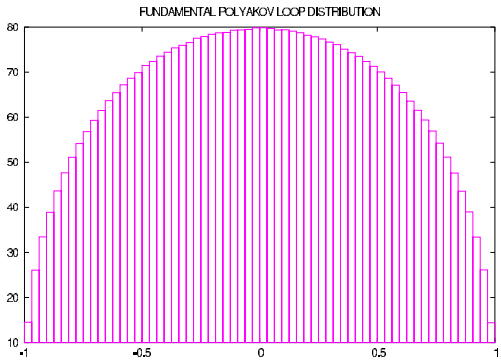

(f) 3-twists sector

Figure 5.14: Monte Carlo history of the twist observable (a) and of the adjoint Polyakov loop (b); spatial distribution of the fundamental Polyakov loop in the 0 (c), 1 (d), 2 (e), 3 (f) twist sectors ($V = 4 \times 16^3$,$\lambda = 1.0$,$\beta_A = 1.2$).

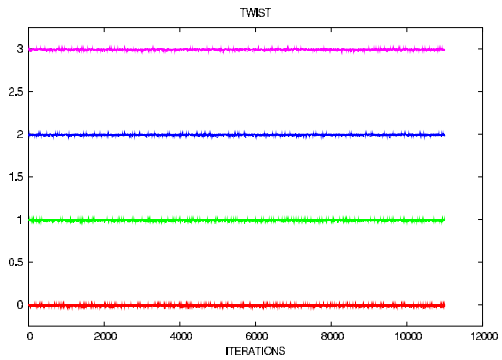

(a) Twist observable

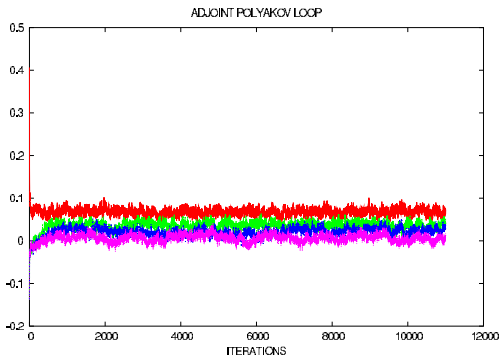

(b) Adjoint Polyakov loop

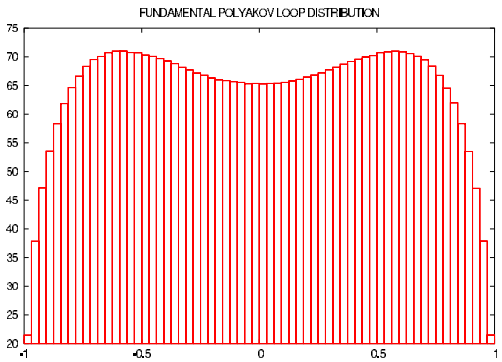

(c) 0-twists sector

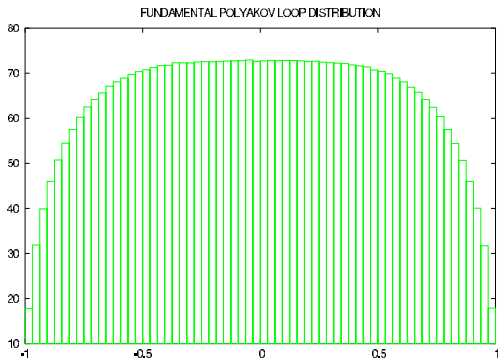

(d) 1-twist sector

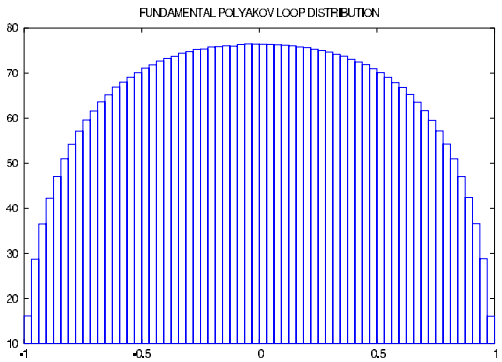

(e) 2-twists sector

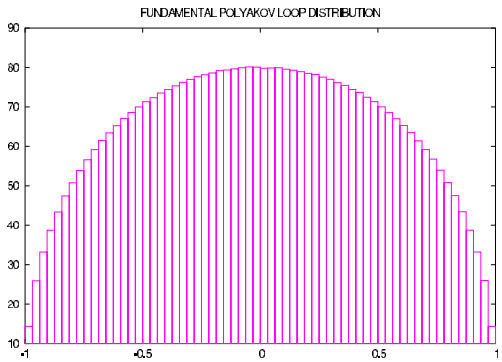

(f) 3-twists sector

Figure 5.15: Monte Carlo history of the twist observable (a) and of the adjoint Polyakov loop (b); spatial distribution of the fundamental Polyakov loop in the 0 (c), 1 (d), 2 (e), 3 (f) twist sectors ($V = 4 \times 16^3$,$\lambda = 1.0$,$\beta_A = 1.4$).

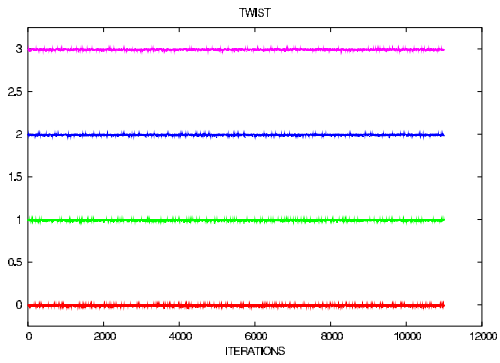

(a) Twist observable

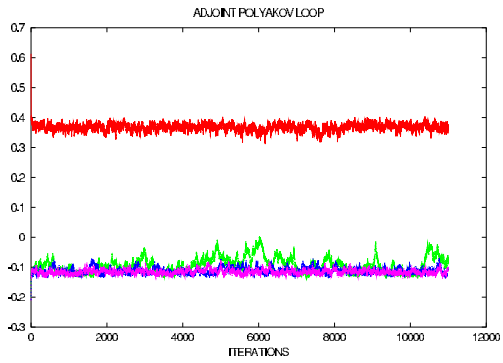

(b) Adjoint Polyakov loop

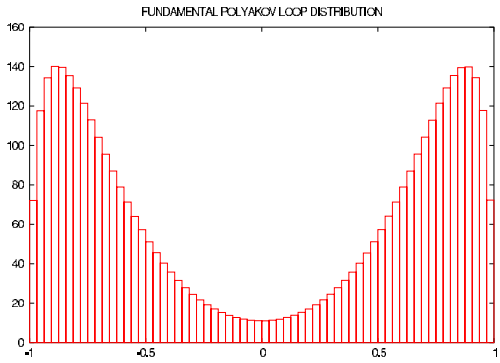

(c) 0-twists sector

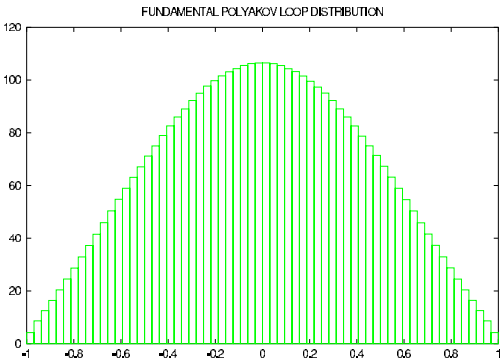

(d) 1-twist sector

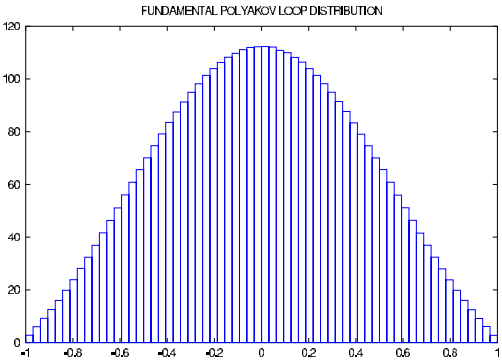

(e) 2-twists sector

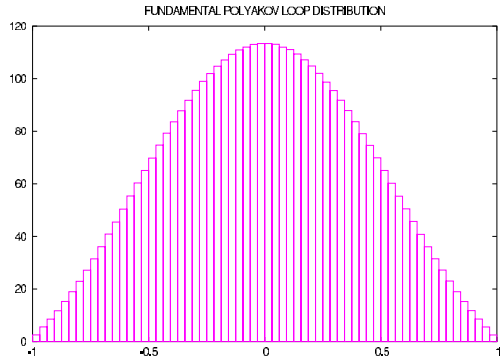

(f) 3-twists sector

Figure 5.16: Monte Carlo history of the twist observable (a) and of the adjoint Polyakov loop (b); spatial distribution of the fundamental Polyakov loop in the 0 (c), 1 (d), 2 (e), 3 (f) twist sectors ($V = 4 \times 16^3$,$\lambda = 1.0$,$\beta_A = 2.5$).

two fixed spatial directions, for instance $x = x_m$ and $y = y_r$. But if at x_m and y_r the Pauli matrices are different, a spatial twist is created in the $x - y$ plane; so the recipe is to use always the same Pauli matrix at x_m and y_r, but different from the one used at fixed time. For the 3-twist sector it is exactly the same, with the same Pauli matrix at x_m,y_r and z_s and another at t_n.

In order to check whether we can find some signal of a finite temperature phase transition, we monitored also other observables, besides the Polyakov loop L_A, like the spatial distribution of the Polyakov loop both in the fundamental and in the adjoint representation. In particular the spatial distribution of L_F turned out to be very interesting. The average of $L_F(\vec{x})$ over the spatial volume must be zero, like the other fundamental observables, due to the fact that the action is center-blind, but its spatial distribution need only to be symmetric, just to ensure that $L_F = 0$. We monitored, for different values of β_A ranging from 0.9 to 2.5 and at fixed $\lambda = 1.0$, L_A and the spatial distribution of L_F, in the trivial and in the various non-trivial twist sectors (with 1,2 and 3 temporal twists). The volume in these runs is $V = 4 \times 16^3$. As can be seen from the following plots, there is a sharp change of the spatial distribution of L_F around $\beta_A \sim 1.2$ in all the twist sectors, but it is particularly evident in the trivial twist sector. At $\beta_A = 0.9$ and $\beta_A = 1.1$ the spatial distribution is peaked at 0, as one expects for the distribution of an observable whose volume average must vanish, and quite broad; at the same couplings $L_A \sim 0$. At $\beta_A = 1.2$ the distribution shows a change that could have begun also for smaller couplings: it seems to be flat, mainly in the trivial twist sector. Above this coupling, at $\beta_A = 1.4$ it is now evident that something happened. In the 0 twist sector L_A oscillates around a positive value and the spatial distribution of L_F, being always symmetric around 0, shows now a well defined two peak structure. In the non-trivial twist sectors, where L_A fluctuates around negative values, the distribution has instead a one peak structure centered on 0, but narrower with respect to lower β_A. At $\beta_A = 2.5$ the picture is even more clear, with a two peak structure in one case and a narrow one peak distribution in the other 3 cases. This behavior is indeed expected, because

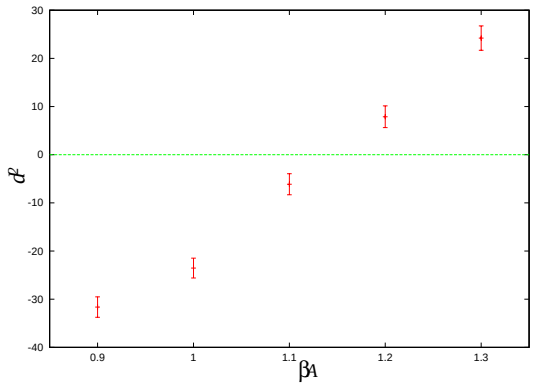

Figure 5.17: Second derivative of the fitting polynomial for the fundamental Polyakov loop distributions at various β_A in the trivial twist sector ($V = 4 \times 16^3, \lambda = 1.0$).

for large β_A the Polyakov loop $L_A \sim -\frac{1}{3}$ corresponds to $L_F \sim 0$ and $L_A \sim 1$ to

$L_F \sim \pm 1$. A more quantitative analysis of these distributions could give some useful informations about the searched finite temperature phase transition, like the critical coupling for instance. One could in fact try to measure the derivatives at $L_F = 0$ and conclude that a phase transition really takes place when the second derivative is zero, within the statistical errors (the odd derivatives being zero by definition since it is a symmetric distribution). As a first attempt, we tried to fit such distributions with some high order polynomials (up to 12th order) with a statistics of $O(10^5)$ configurations. We verified that the odd derivatives are all zero within the errors and the sign of the second derivative, important to distinguish if we are below or above the phase transition, changes from negative to positive going from $\beta_A = 1.1$ to $\beta_A = 1.2$ (see Fig. 5.17).

Putting aside for the moment a more quantitative determination of the critical coupling, we checked whether this picture is coherent. We increased the temporal direction from $N_T = 4$ to $N_T = 6$ and we monitored if the "critical" β_A increases correspondently. We indeed observed that the value around which the distribution is flat and above which shows a two peak structure in the trivial twist sectors goes to larger β_A by increasing the length of the lattice in the temporal direction. This is indeed what we expect for a finite temperature phase transition. The data collected suggest that at least for $\lambda = 1.0$ we were able to completely suppress the effects of the bulk phase transition. There is moreover the evidence of a finite temperature phase transition around $\beta_A \sim 1.15$. A more precise determination of the critical coupling and of the order of the transition was difficult by looking at the spatial density of the Polyakov loop in the fundamental representation.

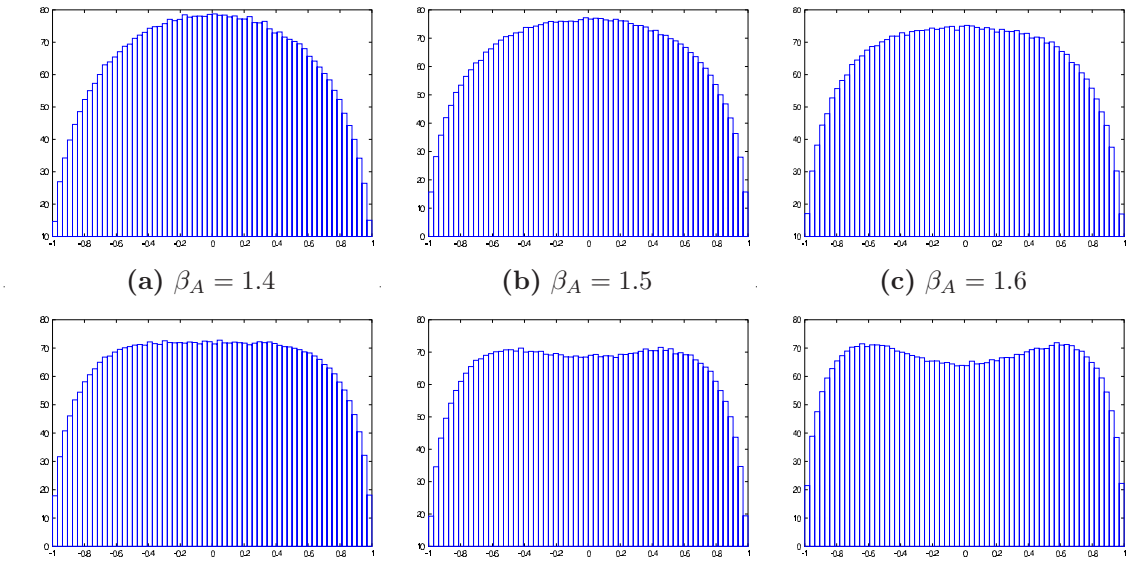

(a) $\beta_A = 1.4$ **(b)** $\beta_A = 1.5$ **(c)** $\beta_A = 1.6$

(d) $\beta_A = 1.7$ **(e)** $\beta_A = 1.8$ **(f)** $\beta_A = 1.9$

Figure 5.18: Spatial distribution of L_F for different values of β_A in the trivial twist sector ($V = 6 \times 16^3$, $\lambda = 1.0$).

From this first analysis of the phase diagram in the $\beta_A - \lambda$ plane, we can conclude that it is characterized by the bulk phase transition which connects the β_A with the

λ axis, changing presumably order around $\lambda = 0.7 - 0.8$. The finite temperature phase transition joins the bulk line and then extends for larger λ. We will try in the next chapters a further investigation of the phase diagram in Fig. 5.19 by using different tools.

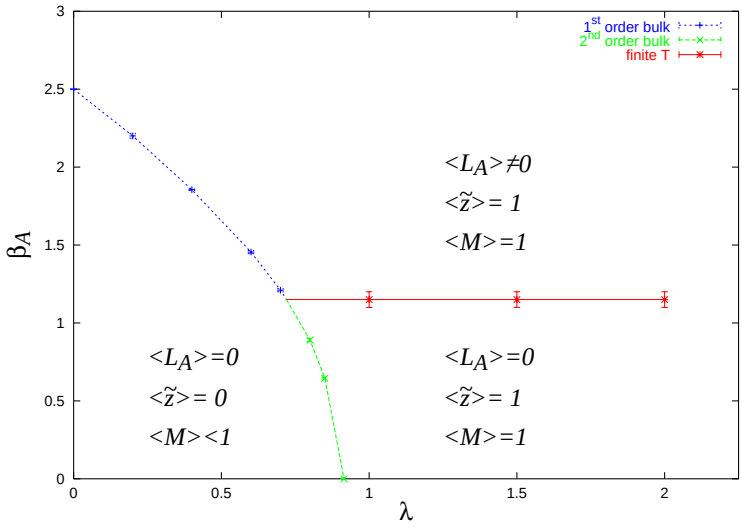

Figure 5.19: Phase diagram in the $\beta_A - \lambda$ plane at $N_T = 4$ with the bulk and the finite T transitions.

Chapter 6

A new order parameter

As we have stressed in the previous chapters, in a pure $SU(N)$ gauge theory in the fundamental representation, the deconfinement phase transition is usually associated with the breaking of a global $\mathbb{Z}_N$ symmetry. This characterization is peculiar of the lattice formulation and it is possible since the fundamental representation of $SU(N)$ possesses a non-trivial $\mathbb{Z}_N$ center. But confinement should be independent of the lattice representation chosen and a characterization of this basic property should be possible also in representations different from the fundamental. In particular it could be interesting to understand how this symmetry and its breaking are realized in a representation with a trivial center.

After some initial topological considerations, we will suggest, under precise assumptions, a possible symmetry breaking mechanism and a related order parameter in $SO(3)$. The original idea was to find a "symmetry" operator P which connects the positive Polyakov loop state, L_A^+, with the negative one, L_A^-. In this way one could define a suitable order parameter and also a way to switch from the trivial to the non-trivial twist sectors. We will show some indications that this mapping is indeed possible but still some problems must be solved. We will then elucidate these ideas in the cases of interest, $SU(2)$ in the fundamental representation, $SO(3)$ with chemical potential and Abelian projected $SO(3)$.

6.1 Symmetry breaking in $SO(3)$

It is well known that the adjoint representation of $SU(2)$, even if it has trivial center, possesses other global topological properties, which could play a very important role for the comprehension of the problem. As we already discussed in Chapter 4, topology offers indeed an interesting insight into the confinement problem. It is well known, in fact, that the $SU(2)$ group elements u live on the 3-sphere S^3 and they can be parametrized as

$$u(\theta, \phi, \psi) = \cos\theta \, \mathbb{I}_2 + i \sin\theta \, \hat{n}(\phi, \psi) \cdot \vec{\sigma} \, ,$$

where $\vec{\sigma}$ are the Pauli matrices and $0 \leq \theta \leq \pi, 0 \leq \phi \leq 2\pi, 0 \leq \psi \leq \pi$. A theorem of homotopy theory says that

$$\Pi_n(S^m) = \begin{cases} = 0 & n < m \\ = \mathbb{Z} & n = m \end{cases} \tag{6.1}$$

In our case one obtains that $\Pi_1(S^3) = 0$ and $\Pi_3(S^3) = \mathbb{Z}$. The non-triviality of the third homotopy group of S^3 suggests the idea that the elements of the $SU(2)$ group can be collected in different homotopy classes, each labelled by an integer. This is true, in the continuum formulation, for the gauge transformations, which are elements of the group. This topological argument leads to a classification of the gauge transformations into "large", $u_n(x)$, and "small", $u_0(x)$. Also the gauge fields can be classified through these integers and in particular at spatial infinity a gauge configuration can be written as

$$A_\mu \sim \frac{1}{g} u_n(x) \partial_\mu u_n(x)^\dagger \,.$$

The small gauge transformations are topologically trivial and they connect gauge fields which live in the same homotopy class; on the other side the large ones are topologically non-trivial and they bring from one homotopy class to another. The first homotopy group, which is usually related to $U(1)$ monopoles, is instead trivial in this case and it means that each closed line on S^3 can be contracted to a point and thus a topological classification is not possible. In the dual superconductor scenario the relevant gauge group of the effective theory is $U(1)$, so a topological classification in homotopy classes is again possible since $\Pi_1(S^1) = \mathbb{Z}$, showing the importance of topological configurations, i.e. Abelian magnetic monopoles.

For the adjoint representation the situation is different, since the manifold of the group $SO(3) = SU(2)/\mathbb{Z}_2$ is $\mathbb{RP}^3$. A generic $SO(3)$ element can be written as

$$\mathbb{I}_3 + \sin 2\theta (\hat{n}(\phi,\psi) \cdot \vec{T}) + (1 - \cos 2\theta)(\hat{n}(\phi,\psi) \cdot \vec{T})^2 \,, \tag{6.2}$$

where $0 \leq \theta \leq \pi, 0 \leq \phi \leq 2\pi, 0 \leq \psi \leq \pi$ and $\vec{T}$ are the 3×3 generators

$$T_1 = \begin{pmatrix} 0 & 0 & 0 \\ 0 & 0 & 1 \\ 0 & -1 & 0 \end{pmatrix} \quad T_2 = \begin{pmatrix} 0 & 0 & -1 \\ 0 & 0 & 0 \\ 1 & 0 & 0 \end{pmatrix} \quad T_3 = \begin{pmatrix} 0 & 1 & 0 \\ -1 & 0 & 0 \\ 0 & 0 & 0 \end{pmatrix} .$$

In this case both its first and its third homotopy group are non-trivial, in fact

$$\Pi_1(\mathbb{RP}^3) = \mathbb{Z}_2 \quad , \quad \Pi_3(\mathbb{RP}^3) = \mathbb{Z} \,. \tag{6.3}$$

The non-triviality of the first homotopy group can be understood heuristically from the definition of $\mathbb{RP}^3$, which corresponds to S^3 with opposite points identified. It means that not all the closed paths on $\mathbb{RP}^3$ are contractible. The loops which are closed also on S^3 are trivial; instead the loops which connect opposite points on S^3 are closed in $\mathbb{RP}^3$ but not in S^3, so they are not contractible to a point. The closed paths in $\mathbb{RP}^3$ can then be classified in two different homotopy classes, or $\Pi_1(SO(3)) = \mathbb{Z}_2$. In such a theory then $\mathbb{Z}_2$ monopoles and vortices can exist ab initio, without the need of any gauge fixing or of any dynamical symmetry breaking. Moreover, also in this case, thanks to the above topological arguments, one could classify the gauge transformations into trivial $u_0(x)$, and non-trivial,$u_1(x)$, and write at spatial infinity

$$A_\mu \sim \frac{1}{g} u_1(x) \partial_\mu u_1(x)^\dagger \,.$$

This is completely analog to the characterization of center vortices within the fundamental representation of $SU(2)$, by which the gauge field of a center vortex at spatial infinity can be written as

$$A_\mu(\theta) \sim \frac{1}{g} u(\theta) \partial_\mu u(\theta)^\dagger \,,$$

with $u(0) = -u(2\pi)$, i.e. the gauge transformations, wrapping around the vortex, pick up a phase. The counterpart of these gauge transformations in $SO(3)$, where the center is trivial, are just the non-trivial elements of $\Pi_1(SO(3))$. The only difference with respect to $\Pi_3(S^3)$ is that here there is only one non-trivial class. It would be then interesting to find how these two states can be related and we will address this question in the next section.

6.2 Order parameter

Consider again the well known result that above a certain coupling the Polyakov loop in the adjoint representation, L_A, can take two values, one positive, indicated via L_A^+, and the other negative, L_A^-, such that approximately $L_A^+ \simeq -3 \cdot L_A^-$ holds. In the limiting case $\beta_A \to \infty$ the Polyakov loop can assume two values, $L_A^+ = 1$ and $L_A^- = -1/3$; if we call $W^\pm$ the 3×3 matrices whose normalized trace gives the above values of $L_A^\pm$, it is straightforward to see that they are

$$W^+ = \begin{pmatrix} 1 & 0 & 0 \\ 0 & 1 & 0 \\ 0 & 0 & 1 \end{pmatrix} \quad W^- = \begin{pmatrix} -1 & 0 & 0 \\ 0 & -1 & 0 \\ 0 & 0 & 1 \end{pmatrix} , \tag{6.4}$$

with the possibility of making cyclic permutations of the eigenvalues for W^-. If we are looking for a $SO(3)$ element which transforms $L_A^+ = 1$ into $L_A^- = -1/3$ and vice versa, the solution is trivially given by $\mathbb{I}_3 + 2T_3^2$, which is just W^- itself. These considerations can be further generalized [140].

We are looking in general for a symmetry operator $P(\vec{x}) \in SO(3)$ such that it acts on the temporal links at a fixed time-slice t_1

$$\widetilde{U}_4(\vec{x}, t_1) = P(\vec{x}) U_4(\vec{x}, t_1) \qquad \forall \vec{x} \tag{6.5}$$

and leave the action invariant, but not the Polyakov loop: a state with positive Polyakov loop L_A^+ must be mapped into the corresponding negative state L_A^-. However, a simple calculation shows that for the most general choice of the link variables $U_\mu(\vec{x}, x_4) \in SO(3)$ only $P \equiv \mathbb{I}_3$ is consistent with the invariance of the adjoint plaquette action.

But, if one can restrict the form of the $SO(3)$ links to a suitable subset, e.g. generated by the Cartan subalgebra, then one can find other solutions, as we shall demonstrate below. Such a restriction is really suggested in the context of the dual superconductor picture of confinement, where at least the long-distance behavior of the theory should be dominated by the Abelian degrees of freedom. On the lattice this picture has been realized through Abelian projection after fixing the gauge of

the link variables to the maximally Abelian one. The restriction to the projected Abelian variables then allows to approximate many physical observables very well, in particular the string tension [141]. The approximation seems even to improve in the continuum limit [142].

The requirement that the symmetry operator to be found maps a negative into a positive state and vice versa implies that it behaves like a "parity" operator, i.e. $P^2(\vec{x}) = \mathbb{I}_3$; the only solutions of this equation are

$$P(\vec{x}) = \begin{cases} \mathbb{I}_3, & \mathbb{I}_3 + 2(\hat{n}(\vec{x}) \cdot \vec{T})^2 \quad \text{in } SO(3), \\ \pm\mathbb{I}_2, & \pm i\hat{n}(\vec{x}) \cdot \vec{\sigma} \quad \text{in } SU(2). \end{cases} \tag{6.6}$$

In the following we will express our results both in the fundamental and in the adjoint representation for a twofold reason; first of all working with Pauli matrices is easier from an analytical point of view and an element in the fundamental representation can be always uniquely mapped into an element in the adjoint representation (the opposite is not true due to a sign ambiguity); the second reason is that we will check our ideas and our order parameter also in the fundamental representation of $SU(2)$.

The operator $P(\vec{x}) = \mathbb{I}_3 + 2(\hat{n}(\vec{x}) \cdot \vec{T})^2$ is a realization of the $\mathbb{Z}_2$ center of $SU(2)$ in the subgroup generated by the Cartan subalgebra $\hat{n}(\vec{x}) \cdot \vec{\tau}$ in the *adjoint* representation. It does not commute with the general element of $SO(3)$ but it obviously commutes with all the elements generated by the same Cartan subalgebra. This observation is straightforwardly extended to $SU(3)$, where one can take, for example, the subgroup generated by the Cartan subalgebra generated by λ_3 and λ_8 in the adjoint representation, usually denoted as $\mathcal{H}^3$ and $\mathcal{H}^8$,

$$\alpha\mathcal{H}^3 + \beta/\sqrt{3}\mathcal{H}^8, \qquad \mathcal{H}^j_{ab} = -if^{ajb}$$

and construct an explicit realization of the $\mathbb{Z}_3$ center of the group with the choice $\alpha = (2/3)\pi$, $\beta = (2/3)\pi + (4/3)k\pi$, with k integer.

When $P(\vec{x})$ is non-trivial, i.e. $P(\vec{x}) = \mathbb{I}_3 + 2(\hat{n}(\vec{x}) \cdot \vec{T})^2$ in $SO(3)$ and $P(\vec{x}) = \pm i\hat{n}(\vec{x}) \cdot \vec{\sigma}$ in $SU(2)$, it can always be decomposed as follows

$$P(\vec{x}) = \begin{cases} \Omega^\dagger(\vec{x}) \cdot (\mathbb{I}_3 + 2T_3^2) \cdot \Omega(\vec{x}) & \text{in } SO(3), \\ \Omega^\dagger(\vec{x}) \cdot i\sigma_3 \cdot \Omega(\vec{x}) & \text{in } SU(2). \end{cases} \tag{6.7}$$

The requirement that the $P(\vec{x})$ given in Eq. (6.6) generates a symmetry for the action reads as follows (the lattice spacing is put $a = 1$ for simplicity and R indicates the representation):

$$\begin{aligned} &\mathrm{Tr}_R\left[U_i(\vec{x},t_1)\, U_4(\vec{x}+\hat{i},t_1)\, U_i^\dagger(\vec{x}+\hat{4},t_2)\, U_4^\dagger(\vec{x},t_1)\right] \equiv \\ &\mathrm{Tr}_R\left[U_i(\vec{x},t_1)\, P(\vec{x}+\hat{i})\, U_4(\vec{x}+\hat{i},t_1)\, U_i^\dagger(\vec{x}+\hat{4},t_2)\, U_4^\dagger(\vec{x},t_1) P^\dagger(\vec{x})\right] \\ &\forall\ \vec{x}\,,\ i=1,2,3\,,\ t_1\ \text{ fixed}\,,\ t_2 = t_1+1\,. \end{aligned} \tag{6.8}$$

A sufficient condition for (6.8) to hold is

$$P^\dagger(\vec{x})\, U_i(\vec{x},t)\, P(\vec{x}+\hat{i}) = U_i(\vec{x},t)\,, \qquad \forall\vec{x}\,,\ i\,, \tag{6.9}$$

or

$$P(\vec{x}) = U_i(\vec{x},t)\, P(\vec{x}+\hat{i})\, U_i^\dagger(\vec{x},t)\,, \qquad \forall\vec{x}\,,\ i\,. \tag{6.10}$$

This equation can be read as a constraint on the functional form of the gauge fields such that, given $P(\vec{x})$, the symmetry is realized; we will not develop here such idea, but more details on this point of view can be found in Appendix D. On the other hand Eq. (6.10) amounts to ($d = 3$)

$$P(\vec{x}) = \frac{1}{d}\sum_{i=1}^{d} \; [U_i(\vec{x},t)\; P(\vec{x}+\hat{i})\; U_i^\dagger(\vec{x},t) \\ + U_i^\dagger(\vec{x}-\hat{i},t)\; P(\vec{x}-\hat{i})\; U_i(\vec{x}-\hat{i},t)]\,, \qquad \forall \vec{x} \tag{6.11}$$

which is a solution of the generalized maximally Abelian gauge (GMAG) condition in 3 dimensions [143, 144]

$$\begin{aligned} &\sum_{\vec{x}} \mathrm{Tr}_R \left(P(\vec{x}) \sum_i \left[U_i(\vec{x},t)\; P(\vec{x}+\hat{i})\; U_i^\dagger(\vec{x},t) + U_i^\dagger(\vec{x}-\hat{i},t)\; P(\vec{x}-\hat{i})\; U_i(\vec{x}-\hat{i},t) \right] \right) \\ &\equiv \sum_{\vec{x}} \mathrm{Tr}_R \left(P(\vec{x}) \sum_{\pm i} \left[U_i(\vec{x},t)\; P(\vec{x}+\hat{i})\; U_i^\dagger(\vec{x},t) \right] \right) \\ &= \text{Extremum}\,. \end{aligned} \tag{6.12}$$

But this gauge fixing condition is equivalent, up to gauge transformations (see Eq. (6.7)), to the standard 3d MAG

$$\sum_{\vec{x}} \mathrm{Tr}_R \left(J_3 \sum_{\pm i} \left[U_i(\vec{x},t)\; J_3\; U_i^\dagger(\vec{x},t) \right] \right) = \text{Extremum}\,.$$

where J_3 is just $(\mathbb{I}_3 + 2T_3^2)$ for $SO(3)$ and $i\sigma_3$ in $SU(2)$. The operator J_3 is then used to transform all temporal links at a fixed time-slice t_1 as

$$\widetilde{U}_4(\vec{x},t_1) \equiv J_3 U_4(\vec{x},t_1)\,, \qquad \forall \vec{x} \tag{6.13}$$

mapping the action value S into $\widetilde{S}$,

$$\begin{aligned} \widetilde{S} \;&=\; \sum_{P'} \left(1 - \frac{1}{d_R} \mathrm{Tr}_R \left[U_i(\vec{x},t_1) \widetilde{U}_4(\vec{x}+\hat{i},t_1) U_i^\dagger(\vec{x}+\hat{4},t_2) \widetilde{U}_4^\dagger(\vec{x},t_1) \right] \right) \\ &+\; \sum_{P} \left(1 - \frac{1}{d_R} \mathrm{Tr}_R \left[U_\mu(x) U_\nu(x+\hat{\mu}) U_\mu^\dagger(x+\hat{\nu}) U_\nu^\dagger(x) \right] \right)\,, \end{aligned}$$

where P' are the temporal plaquettes living at $t = t_1$, P are all the other plaquettes and d_R indicates the dimensionality of the representation. If all the links were pure Abelian fields, then one expects that $S = \widetilde{S}$ and the symmetry to be exact; in practice, after 3d MAG, the links are not exactly Abelian and the symmetry is expected to be realized only approximately. In Section 6.4 we will check how well is this symmetry realized in the $SO(3)$ theory with $\mathbb{Z}_2$ monopole suppression. The same operation generates a transformed Polyakov loop variable $\widetilde{L}$ (always intended after 3d MAG)

$$\widetilde{L} = \frac{1}{N_s^3} \left| \sum_{\vec{x}} \frac{1}{d_R} \mathrm{Tr}_R \left[\widetilde{U}_4(\vec{x},t_1) \dots U_4(\vec{x},t_{N_\tau}) \right] \right|\,.$$

The Polyakov loop, instead, is expected not to be invariant under the transformation by J_3, but L_A^+ should be mapped into L_A^- and vice versa. In this way an order parameter can be defined in every representation

$$\Delta = \frac{d_R}{d_R + |\mathrm{Tr} J_3|} \left| L - \widetilde{L} \right| , \tag{6.14}$$

and it interpolates between 0 ($\beta_A = 0$) and 1 ($\beta_A \to \infty$). As a first test of our ideas, we will check the order parameter defined above in the fundamental representation of $SU(2)$, for which the critical coupling of the finite temperature phase transition and its order are well known.

6.3 $SU(2)$ theory in the fundamental representation

As previously stated, the prescription to define the order parameter is representation independent and the easiest task is to apply our ideas to the fundamental representation in order to reproduce the known results. In this case $P(\vec{x}) = i\hat{n}(\vec{x}) \cdot \vec{\sigma}$ and the operator $J_3 = i\sigma_3$ is used to transform the Polyakov loop in the fundamental representation. The definition of the order parameter reads as

$$\Delta = |L_F - \widetilde{L}_F| . \tag{6.15}$$

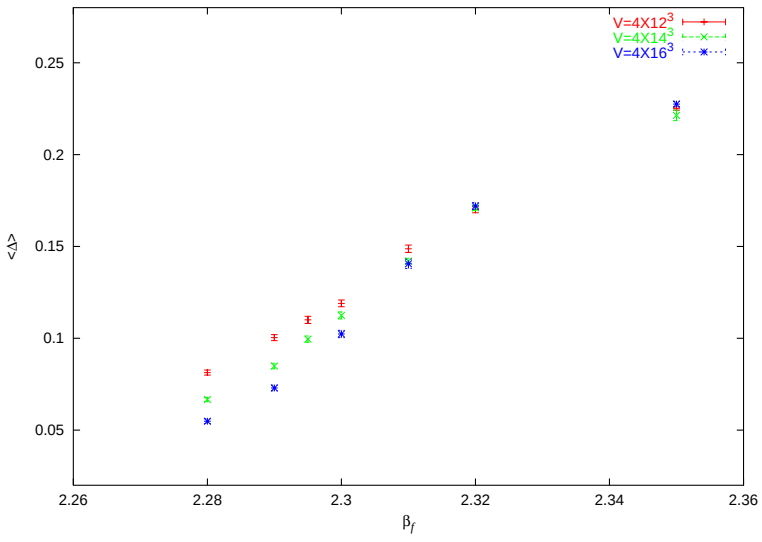

Figure 6.1: Order parameter as a function of β_F for different spatial volumes at $N_T = 4$

As can be seen from Fig. 6.1, the order parameter, computed in 3d MAG, increases for larger β_F and becomes steeper for $\beta_F \lesssim 2.32$ as the spatial volume is increased. In order to check whether it reproduces the known results, we measured also its susceptibility χ and the Binder cumulant b, defined as

$$\chi \;=\; N_S^3 \cdot (\langle \Delta^2 \rangle - \langle \Delta \rangle^2) \tag{6.16}$$

$$b = 1 - \frac{\langle \Delta^4 \rangle}{3 + \langle \Delta^2 \rangle^2} \tag{6.17}$$

The susceptibility (Fig. 6.2) shows a peak which becomes higher and narrower by increasing the spatial volume.

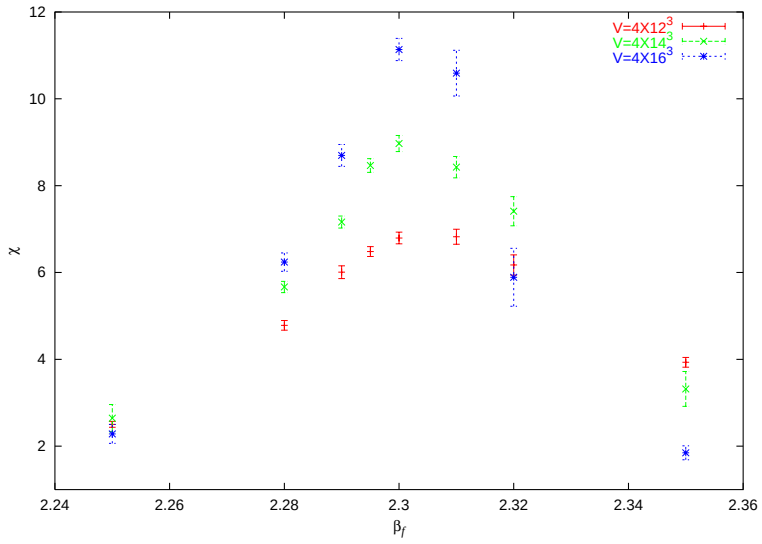

Figure 6.2: Susceptibility of the order parameter as a function of β_F for different spatial volumes at $N_T = 4$

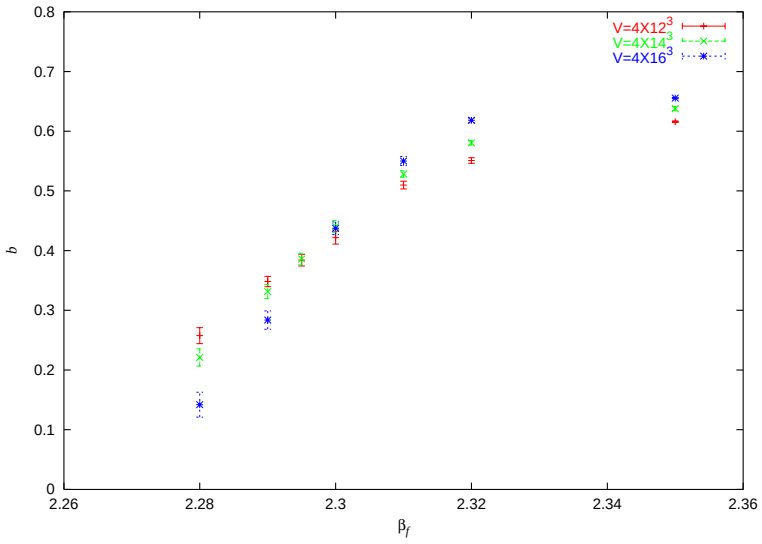

Figure 6.3: Binder cumulant of the order parameter as a function of β_F for different spatial volumes at $N_T = 4$

The Binder cumulant (Fig. 6.3) shows the typical behavior for a second order phase transition; it goes to zero below the critical coupling and approaches the value 2/3 asymptotically for large β_F. The cumulants for different volumes intersect at the

phase transition point, with the higher volume lines which become steeper as the critical coupling is reached.

The fact that this order parameter works in this case can be understood in the following way. After 3d MAG, the operator J_3 maps L_A^+ into L_A^- and in the large β_A limit $L_A^+ = 1$ and $L_A^- = -1/3$. In the large β_F limit, instead, $L_F = \pm 1$, which correspond both to $L_A^+ = 1$, while $L_A^- = -1/3$ means $L_F = 0$ (due to the well known trace properties). In conclusion the ensemble average of $\widetilde{L}_F$ is very small and in practice Δ reduces to $|L_F|$.

6.4 $SO(3)$ theory with monopole suppression term

We will now discuss the more interesting case of the adjoint Wilson action with the chemical potential which suppresses the $\mathbb{Z}_2$ monopoles. In this case $P(\vec{x}) = \mathbb{I}_3 + 2(\hat{n}(\vec{x}) \cdot \vec{T})^2$ and $J_3 = \mathbb{I}_3 + 2T_3^2$. As a preliminary test we can check whether the operator generates really a symmetry of the action. It was found indeed numerically that the symmetry, within 3d MAG, is approximately realized at the level of $1 \div 2\%$.

$$\langle (S - \widetilde{S})/S \rangle = 0.011 \quad (V = 4 \times 10^3, \beta_A = 0.9, \lambda = 1.0)\,,$$
$$\langle (S - \widetilde{S})/S \rangle = 0.018 \quad (V = 4 \times 10^3, \beta_A = 1.6, \lambda = 1.0)\,.$$

This result is of course independent from the gauge fixing algorithm; it must be anyway stressed that a better local minimum of the gauge functional ensures a better realization of the symmetry and since we used a standard gauge fixing algorithm, by refining it we expect an improvement of the numerical realization of the symmetry. One can also check whether after spatial MAG the operator J_3 flips the positive state L_A^+ into the negative one L_A^- and vice versa.

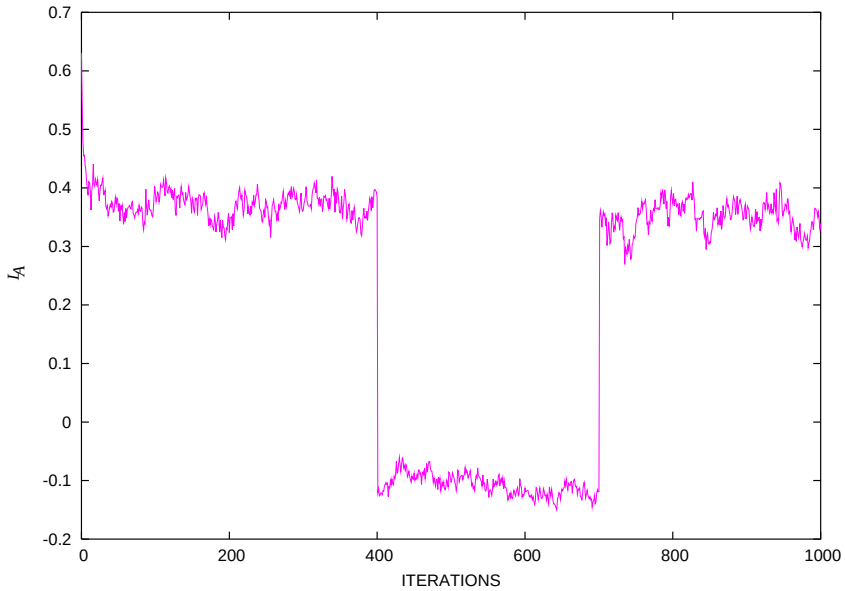

Figure 6.4: Monte Carlo history of L_A transformed by J_3 after 400 and 700 iterations ($V = 4 \times 10^3$,$\beta_A = 2.5$,$\lambda = 1.0$)

After N iterations in our Monte Carlo history, we transformed the configuration accordingly to the given recipe, substituted in the Metropolis algorithm the old configuration with the transformed one and let the system evolve for a number M of iterations, after which we applied the same procedure.

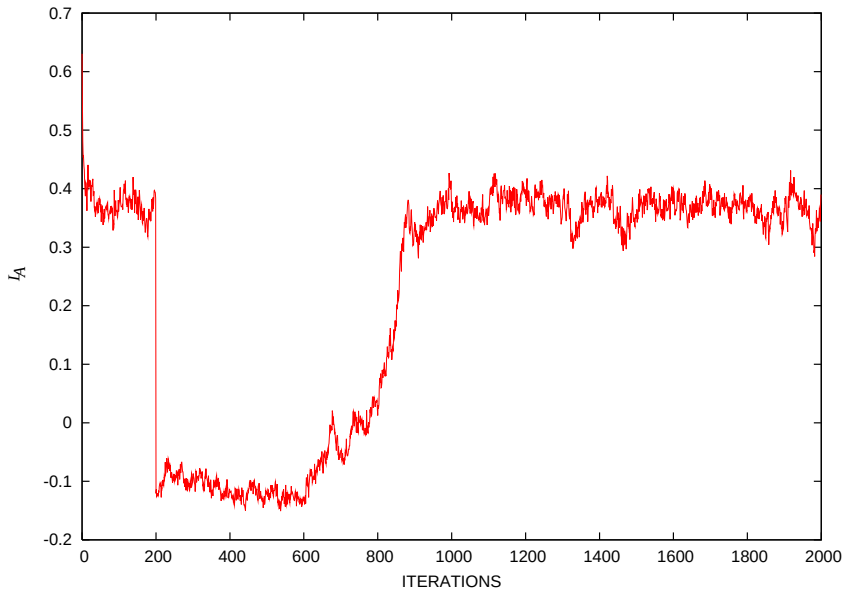

Figure 6.5: Monte Carlo history of L_A transformed by J_3 after 200 ($V = 4 \times 10^3$,$\beta_A = 2.5$,$\lambda = 1.0$)

As one can see from Fig. 6.4, L_A^+ was indeed mapped into L_A^- and vice versa. But unfortunately the "flipped" state is not stable, as Fig. 6.5 shows.

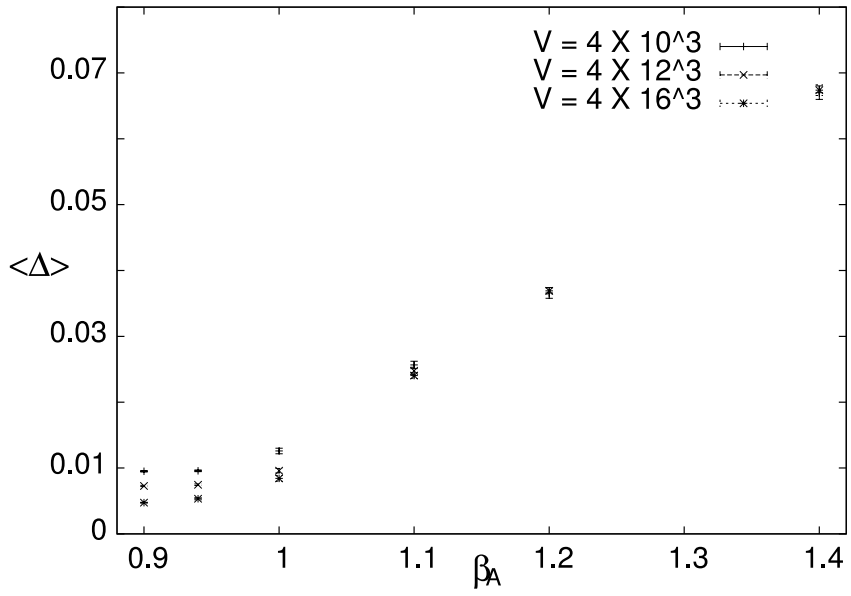

Figure 6.6: Order parameter as a function of β_A for different spatial volumes at $N_T = 4$ ($\lambda = 1.0$)

This is due to the fact that, even if we are able to reach a state (unstable) with the desired value of L_A, we cannot really change the twist sector in this way. Thus we cannot build a proper "ergodic" algorithm which tunnels between different twist sectors using this technique, but we can anyway define an order parameter. The definition of the order parameter in this representation reads as

$$\Delta = \frac{3}{4}|L_A - \widetilde{L}_A|\,, \tag{6.18}$$

As one can see from Fig. 6.6, the order parameter increases by increasing the coupling β_A and for bigger spatial volumes the raising becomes slightly steeper, as one would expect for the behavior of an order parameter and in a very similar way to the behavior of $\langle\Delta\rangle$ in the fundamental representation. Its susceptibility shows a peak around $\beta_A = 1.1$.

6.5 Abelian projected theory

As a further test of our ideas, we analyzed also the behavior of the same $SO(3)$ theory with the monopole term after MAG (in 4 dimensions) and Abelian projection [145]. This check can be understood heuristically in the following way. After MAG the links are maximally gauge transformed along $i\sigma_3$; if Abelian dominance holds, then physical quantities are quite well approximated by projecting the links along the third direction in color space. In such Abelian projected theory in the adjoint representation every link $U_\mu(x)$ can be replaced by

$$U_\mu^{AP}(x) = \mathbb{I}_3 + \sin 2\theta_\mu(x) T_3 + (1 - \cos 2\theta_\mu(x)) T_3^2\,, \tag{6.19}$$

since we have chosen T_3 as the generator of the Abelian algebra. It can be seen by inspection that an operator P exists such that it generates a symmetry for the action but not for the Polyakov loop. Also in this case $P = \mathbb{I}_3 + 2T_3^2$ and it acts at a fixed time-slice on the temporal links:

$$PU_4^{AP}(x) = \mathbb{I}_3 - \sin 2\theta_4(x) T_3 + (1 - \cos 2\theta_4(x)) T_3^2\,. \tag{6.20}$$

At the same time it is straightforward to show that

$$PU_\mu^{AP}(x) = U_\mu^{AP}(x)P \quad \text{and} \quad P^2 = \mathbb{I}_3\,. \tag{6.21}$$

As a consequence the temporal plaquettes, which are the ones involved in this transformation, are left invariant and thus the action in the Abelian projected theory. This line of reasoning is of course heuristic, because in the partition function there is not only the term representing the Abelian projected theory but also the original non Abelian action and the gauge fixing term are present. Bearing in mind this remark, it is anyway interesting to go further. The Polyakov loop, in fact, is not invariant under the action of P since it contains only one temporal link at a fixed time-slice. If we indicate the global Abelian phase of the Polyakov line as

$$\Theta_L(\vec{x}) = \sum_{n=0}^{N_T-1} \theta_4(\vec{x} + na\hat{4}) \tag{6.22}$$

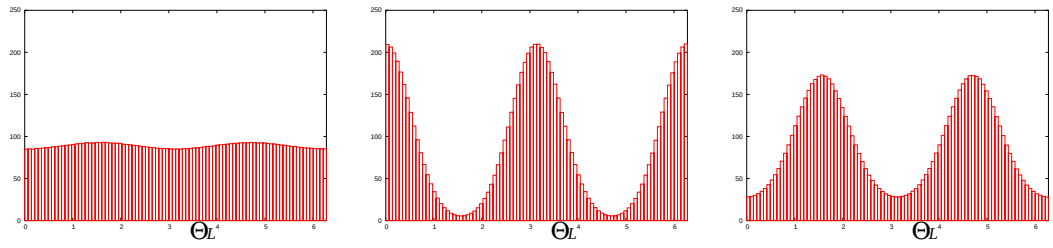

(a) $\langle \cos 2\Theta_L \rangle \simeq 0$ **(b)** $\langle \cos 2\Theta_L \rangle_+ \simeq 1$ **(c)** $\langle \cos 2\Theta_L \rangle_- \simeq -1$

Figure 6.7: Spatial $\Theta_L(\vec{x})$ distribution below ($\beta_A = 0.5$) (a) and above the transition ($\beta_A = 2.5$) (b),(c) ($\lambda = 1.0$,$V = 4 \times 10^3$).

it is again easy to show that the Abelian projected Polyakov loop

$$L_A^{AP} = (1 + 2\cos 2\Theta_L)/3 \tag{6.23}$$

is mapped by $J_3 = \mathbb{I}_3 + 2T_3^2$ into

$$\widetilde{L}_A^{AP} = (1 - 2\cos 2\Theta_L)/3\,. \tag{6.24}$$

If this symmetry is broken at the phase transition, then we expect

$$L_A^{AP} = \begin{cases} 1/3 & T < T_c \\ (1 \pm 2\Delta)/3 & T > T_c \end{cases} \tag{6.25}$$

with in the latter case $\Delta = |\overline{\cos 2\Theta_L}|$ (the bar means average over the spatial volume). Part (a) of Fig. 6.7 shows the ensemble average of the spatial distribution of the Polyakov line angle below the phase transition; above the phase transition we took the ensemble average in the trivial twist sector, indicated with $\langle\ \rangle_+$ and showed in (b), and in the non trivial twist sector, indicated in (c) with $\langle\ \rangle_-$.

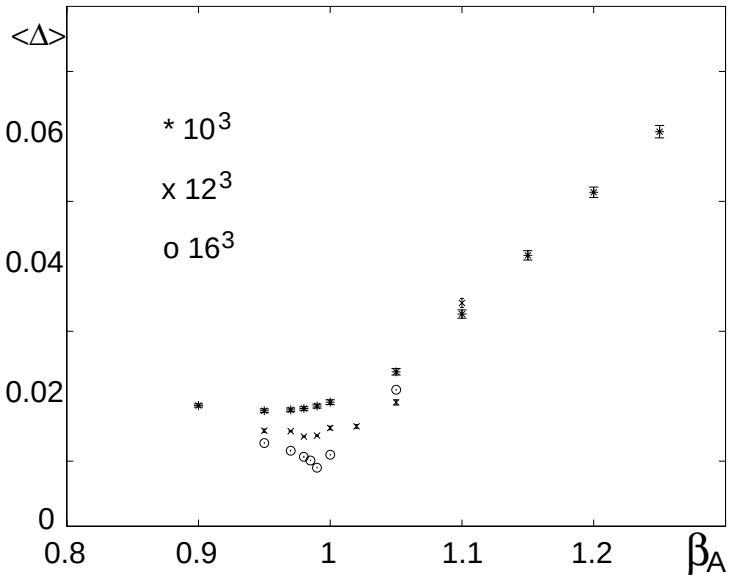

Figure 6.8: Ensemble average of Δ vs. β_A.

Although a sharp change can be observed also for the full $SU(2)$ $\mathrm{TrL}_A(\vec{x})$ distribution, in the latter case a quantitative analysis is more difficult and higher statistics is required. In the Abelian projected case, after MAG, $\Theta_L(\vec{x})$ is clearly flat below the phase transition, peaking around $0(\pi)$ and $\frac{\pi}{2}$ above. In Fig. 6.8 the proposed order parameter is plotted as a function of β_A for $\lambda = 1$ and $N_\tau = 4$. A singular behavior around $\beta_A \simeq 1$ is starting to show at $N_s = 16$. At $N_\tau = 6$ the critical β_A increases by roughly 25%.

In the next chapter we will try to detect the finite temperature phase transition in the $SO(3)$ theory with the monopole suppression term by using another tool, the Pisa disorder operator.

Chapter 7

The Pisa disorder operator

The dual superconductor scenario is, as we have already stressed, one of the most popular and studied models of QCD vacuum. There are many hints, both in the continuum and in the lattice formulation of Yang-Mills theories, that it could be a good candidate for the mechanism of confinement, through the condensation of magnetic charges.

In Chapter 2 it has been showed how a suitable defined order parameter, called disorder operator in analogy with statistical mechanics, could distinguish between the confined and deconfined phase. In particular it was studied in the fundamental representation of $SU(2)$ and $SU(3)$ groups. It turned out that it describes with very good accuracy the critical region, giving results in agreement with the known critical couplings and critical exponents.

It is then natural trying to extend this definition to the adjoint representation and to the action with the monopole suppression term. The original ideas of 't Hooft, which constitute the basis for the dual superconductor model and the associated order parameter, are in fact proper of the continuum formulation and thus independent of the representation chosen in the lattice discretization.

We extended the definition of the disorder operator to the adjoint theory with the monopole suppression term and tried a preliminary study of the phase diagram of this center-blind theory. We investigated first the bulk phase transition, i.e. the case with $\lambda = 0.0$. Then we increased the chemical potential to see how the negative peak of ρ, which signals the bulk phase transition varies; eventually the negative peak due to the lattice artifacts should disappear, for large enough λ, and the true physical finite temperature phase transition should occur. This study is anyway preliminary because we used not too large volumes; moreover, for $\lambda \geq 1$, i.e. when tunneling between different twist sectors is frozen, we performed the simulations only in the trivial twist sector, without any attempt to test the non-trivial twist sectors.

7.1 Adjoint action

The construction of a gauge invariant and magnetically charged operator μ, which can distinguish between the confined phase, characterized by a condensation of magnetic charges, from the deconfined phase, will be similar to what was done in the fundamental case. This is due to the fact that $SO(3)$ possesses also, obviously, a

Cartan subalgebra; moreover, as we have explained at the beginning, even if everything can be exactly translated for matrices in the adjoint representation, we use links in the fundamental representation to speed up our simulations.

A time-independent external field, like in Eq. (3.11), is again introduced. The next step is to modify the Wilson space-time plaquettes $U_{i4}(\vec{n},0)$ at a fixed time-slice $t=0$ introducing a shift given by the insertion of the external field, similar to Eq. (3.12). It must be stressed that only the adjoint Wilson action is modified with the insertion of the external field and not the chemical potential. The disorder operator is then defined as

$$\langle\mu(0)\rangle = \frac{\int(DU)e^{-S_M(0)}}{\int(DU)e^{-S}}\,, \tag{7.1}$$

$$S_M(0) = \beta\sum_{\mu,\nu,x}\left(1-\frac{1}{N}\left(\tilde{U}_{\mu\nu}(x)+(\tilde{U}_{\mu\nu}(x))^\dagger\right)\right)\,. \tag{7.2}$$

At finite temperature the functional integral of e^{-S} is taken with periodic boundary conditions and the integral of e^{-S_M} with C^*-periodic boundary conditions

$$U_i(\vec{n},t=N_T) = U_i^*(\vec{n},t=0)\,, \tag{7.3}$$

where U_i^* means complex conjugate of U_i. This is exactly the condition that we implemented for the fields. Since in the adjoint representation the matrices are real, one would naively say that the adjoint links are not affected by this boundary condition. This is obviously not true, because

$$U_i^C = U_i^* = i\sigma_2 U_i(-i\sigma_2)\,, \tag{7.4}$$

which translated in the language of $SO(3)$ matrices means

$$U_i^C = (\mathbb{I}_3+2T_2^2)U_i(\mathbb{I}_3+2T_2^2)\,. \tag{7.5}$$

Charge conjugation is thus realized in both the representations through rotations of a π angle around the y-axis, expressed in the fundamental representation by $i\sigma_2$ and in the fundamental by $\mathbb{I}_3+2T_2^2$. What is measured in lattice simulations is again the derivative of the logarithm of $\langle\mu\rangle$ with respect to the coupling β

$$\rho = \frac{d}{d\beta}\log\langle\mu\rangle = \langle S\rangle_S - \langle S_M\rangle_{S_M}\,, \tag{7.6}$$

which yields all the relevant informations on μ.

7.2 $SO(3)$ case

First we investigated the adjoint Wilson action without chemical potential with three different volumes, $V = 12^4, 16^4, 20^4$. The lattices were chosen symmetric because with $\lambda=0$ we expect to observe only the bulk phase transition, the finite temperature one being overshadowed. We will study asymmetric lattices, i.e. the finite temperature case, when $\lambda\neq 0$. In the zero temperature case, of course, the

transition is not of the confinement-deconfinement type. As we have seen by the analysis of various observables, the presence of the bulk transition is signalled by a jump of these observables, and in particular of the plaquette, at β_A^c; the effect of the external field is the shift of this jump along β_A and so a peak in ρ is expected.

At low β_A the derivative of the disorder operator, ρ, begins to decrease towards its minimum and we checked in particular that at $\beta_A = 0$ it is consistent with zero independently from the volume size:

$$\begin{aligned} \rho &= 0.12(46) \quad V = 12^4 \\ \rho &= 0.16(75) \quad V = 16^4 \\ \rho &= -0.79(1.00) \quad V = 20^4 \end{aligned}$$

(The jackknife error analysis is our method for estimating statistical errors). By increasing β_A the bulk phase transition occurs and it is signalled by a deep negative peak at the expected value $\beta_A \sim 2.5$.

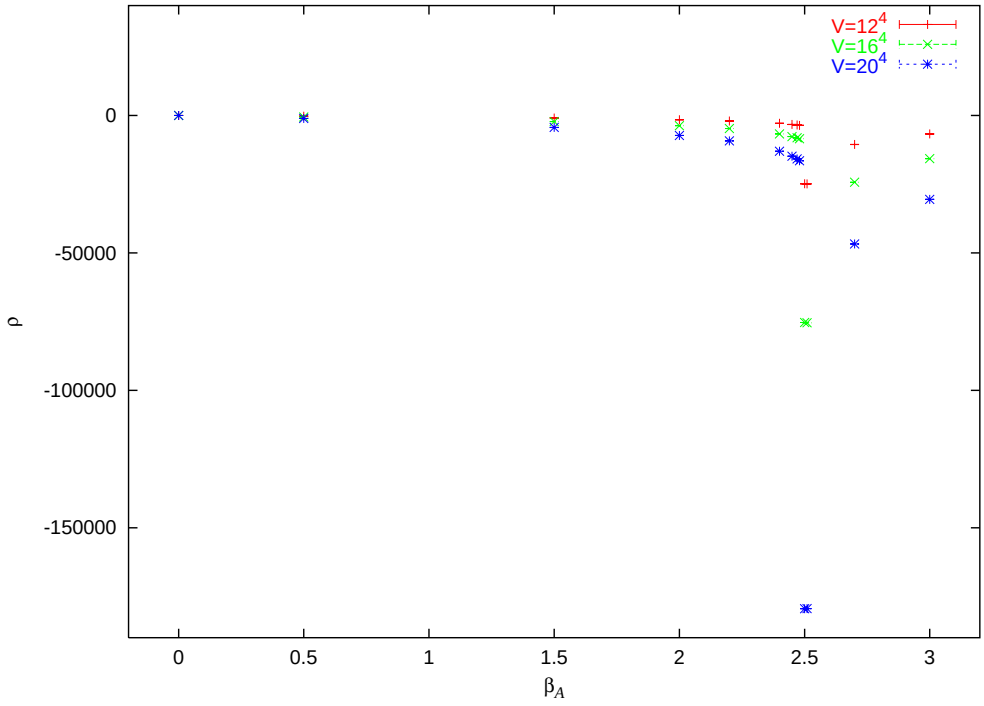

Figure 7.1: ρ as a function of β_A for different volumes at $T = 0$ and $\lambda = 0.0$

We checked also, with the aid of a finite size scaling analysis, if the bulk phase transition is really first order like the literature states and in particular we investigated whether the negative peak scales accordingly to the critical exponent $\nu = 1/d = 0.25$. For values below $\beta_A^c = 2.5$, we plotted the rescaled value of ρ, i.e. ρ/N_S^4, against the shifted values of β_A, i.e. $N_S^4 \times (2.5 - \beta_A)$. As one can see the points collapse quite nicely on the same curve, even if there are some deviations away from the critical region and above all for the smallest volume, 12^4.

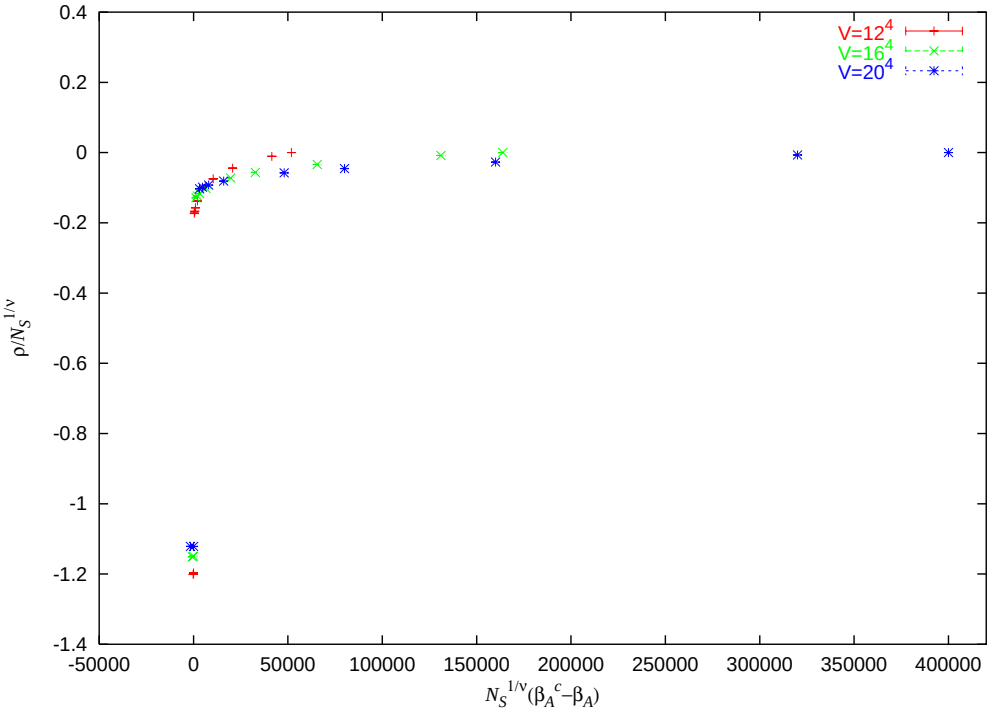

Figure 7.2: Quality of scaling of ρ for different volumes at $T = 0$ and $\lambda = 0.0$

7.3 $SO(3)$ with chemical potential

We studied also the case with non-zero chemical potential, which is the most interesting for us. We used always asymmetric lattices, in order to detect the finite temperature phase transition. The lattice used, since it is a preliminary study, was only $V = 4 \times 12^3$.

For small λ the dip of ρ due to the lattice artifacts is expected to be present in the phase diagram, but by increasing λ it should soften and move to smaller β_A. For a certain range in the chemical potential, it is likely that two peaks, one for the bulk and the other for the finite temperature phase transition, occur. For large λ, with the lattice artifacts suppressed, only one peak, the physical one, is expected.

As one can see from Fig. 7.3, 7.4, 7.5, as the chemical potential is increased from $\lambda = 0.0$ to $\lambda = 0.7$, the negative peak decreases and moves to smaller β_A; the negative peak is evident and above the critical coupling ρ reaches a plateau which is approximately the same for the 3 values of λ quoted, i.e $\rho \simeq -153 \pm 1$. For $\lambda > 0.7$ the situation changes. In Fig. 7.6, at $\lambda = 0.8$, still one negative peak is present, but it is no more so huge and, above all, it reaches a relative minimum, since the absolute minimum is obtained only for larger β_A. The negative peak is a remnant of the bulk phase transition and it occurs where the $\mathbb{Z}_2$ monopoles, still present even if suppressed, suddenly decrease and where the twist shows tunneling. The fact that at the plateau ρ has approximately the same value it had for smaller λ ensures us about the validity of the simulation; for large β_A, in fact, all the plaquettes are constrained to be 1 and for this reason also the 3-dimensional cubes will be all 1;

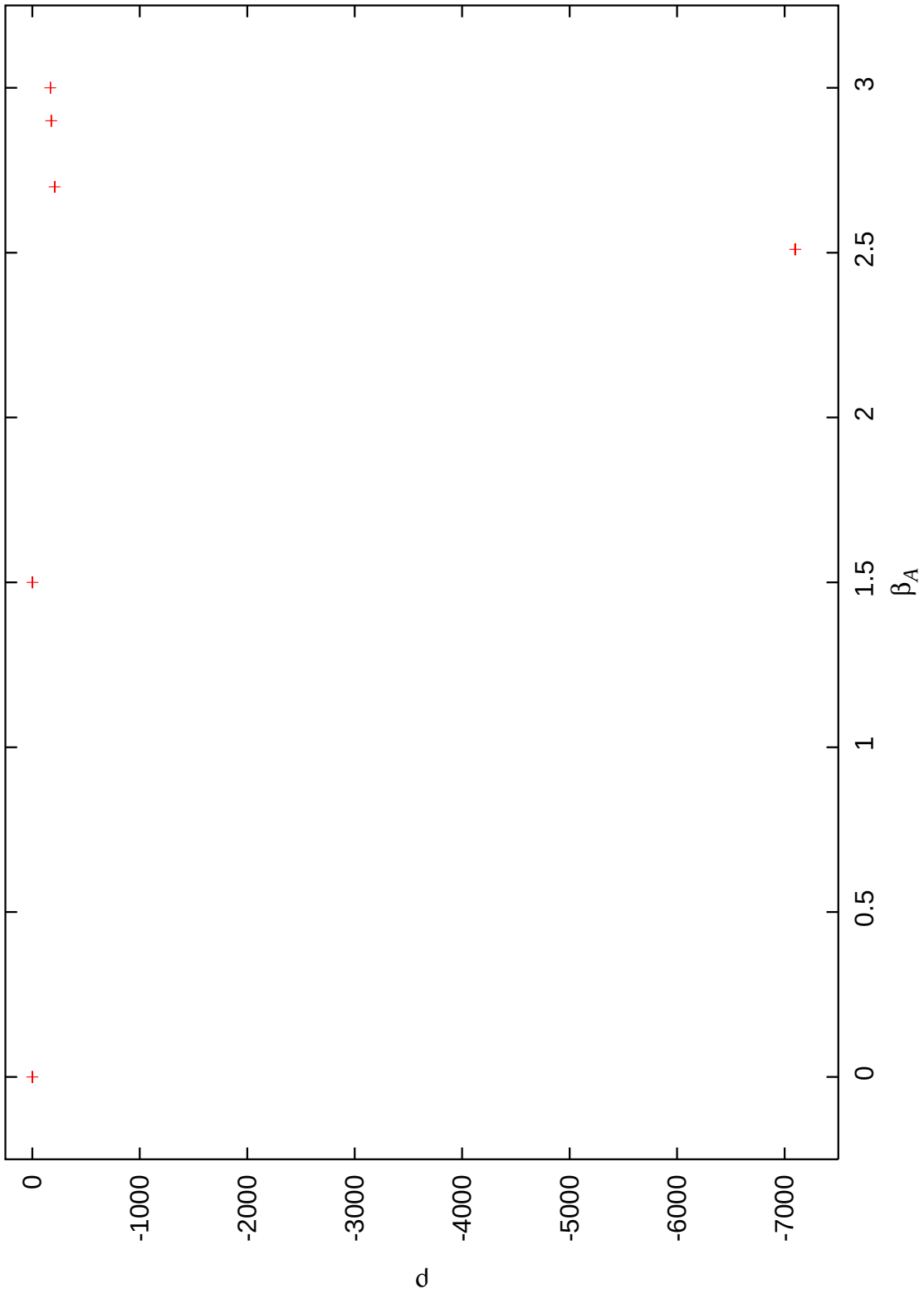

Figure 7.3: ρ as a function of β_A at $\lambda = 0.0$ and for a volume $V = 4 \times 12^3$.

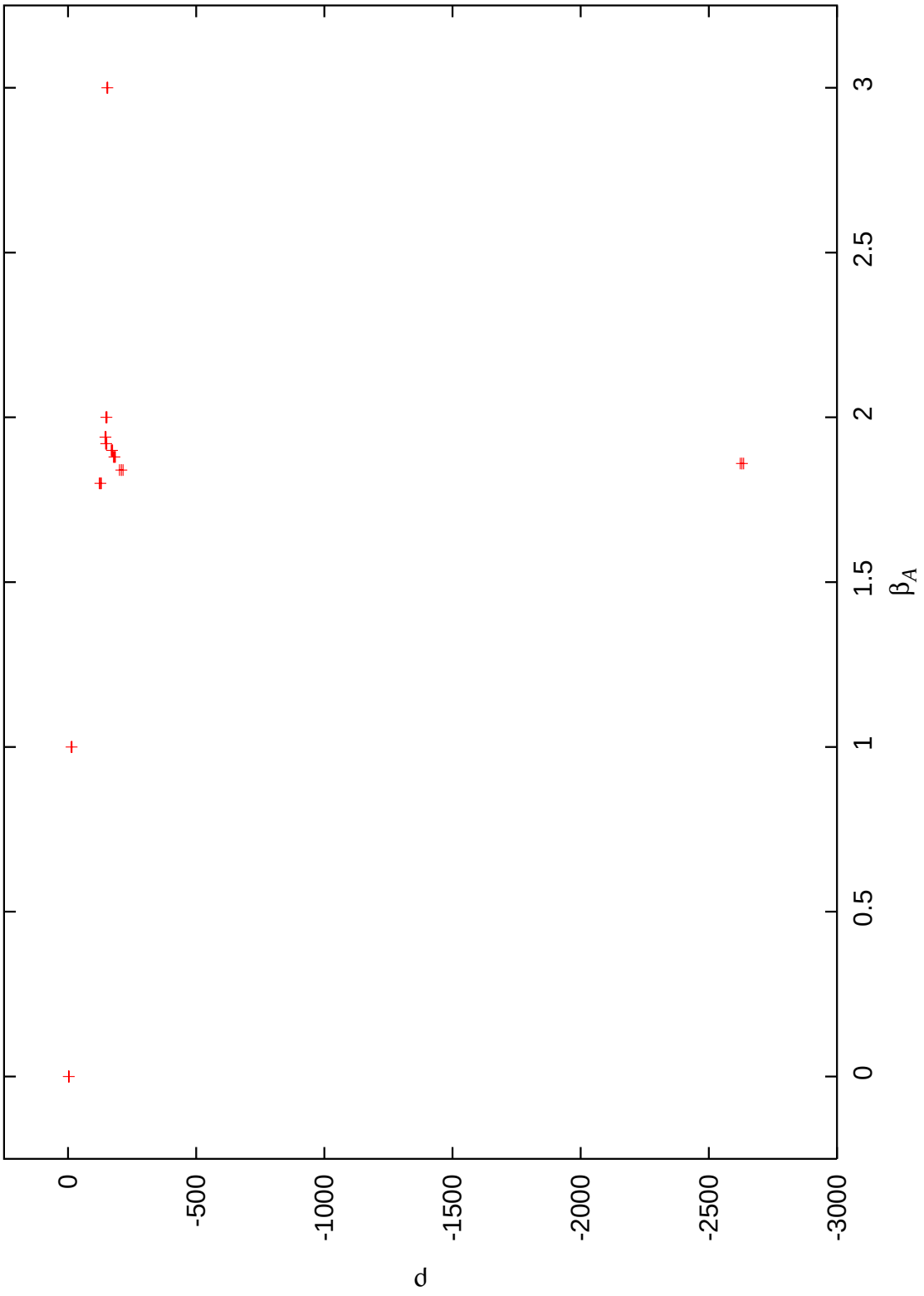

Figure 7.4: ρ as a function of β_A at $\lambda = 0.4$ and for a volume $V = 4 \times 12^3$.

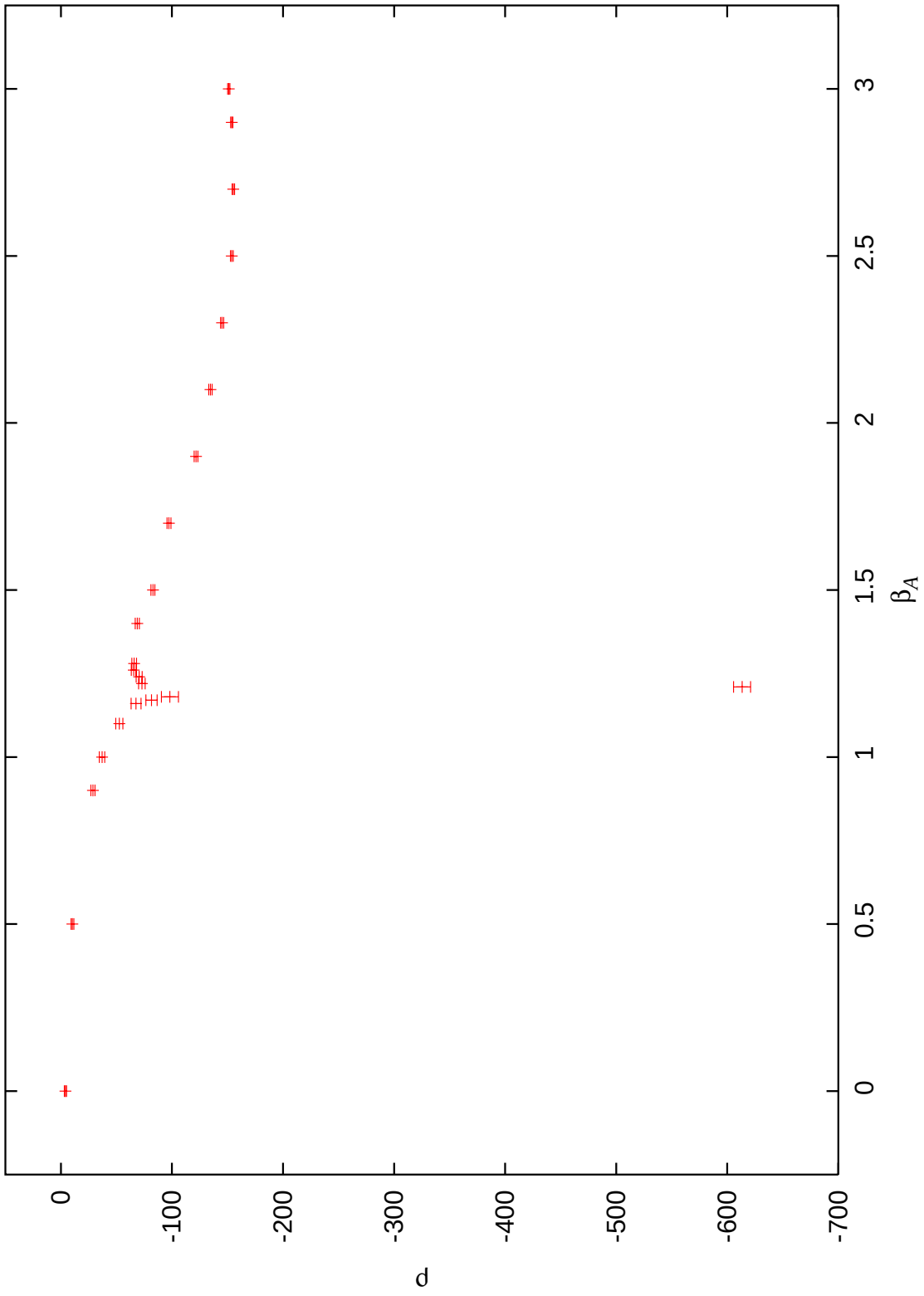

Figure 7.5: ρ as a function of β_A at $\lambda = 0.7$ and for a volume $V = 4 \times 12^3$.

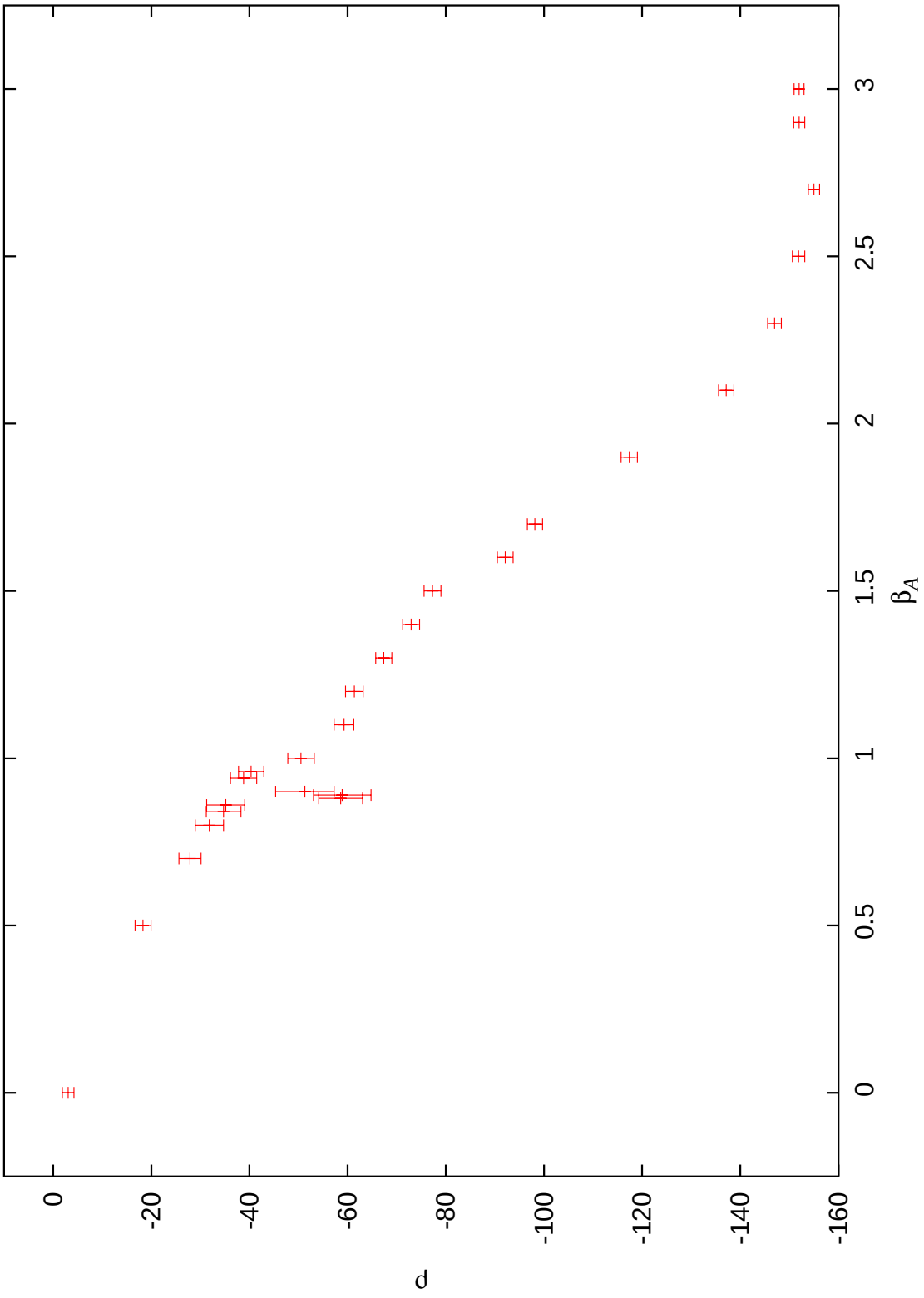

Figure 7.6: ρ as a function of β_A at $\lambda = 0.8$ and for a volume $V = 4 \times 12^3$.

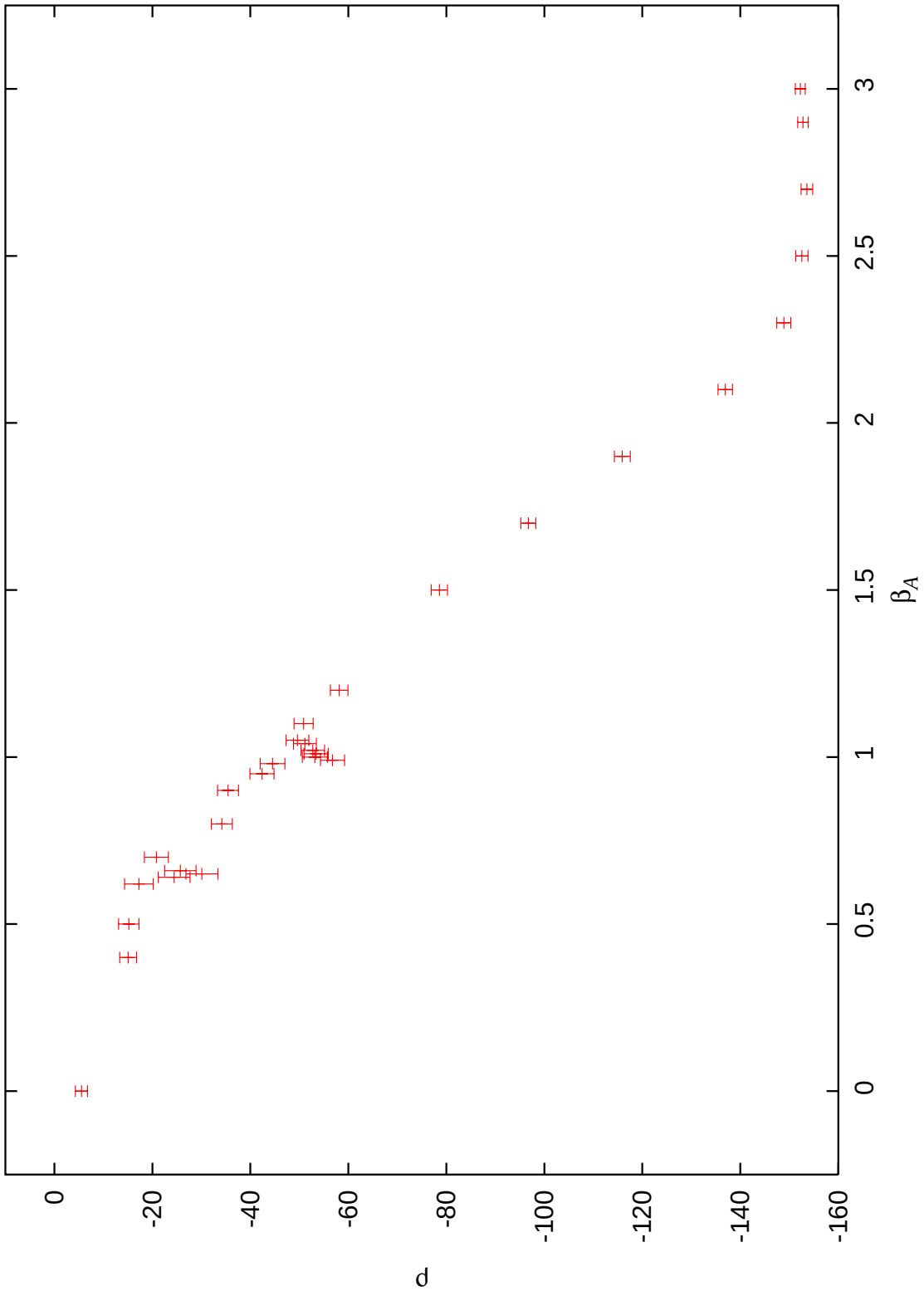

Figure 7.7: ρ as a function of β_A at $\lambda = 0.85$ and for a volume $V = 4 \times 12^3$.

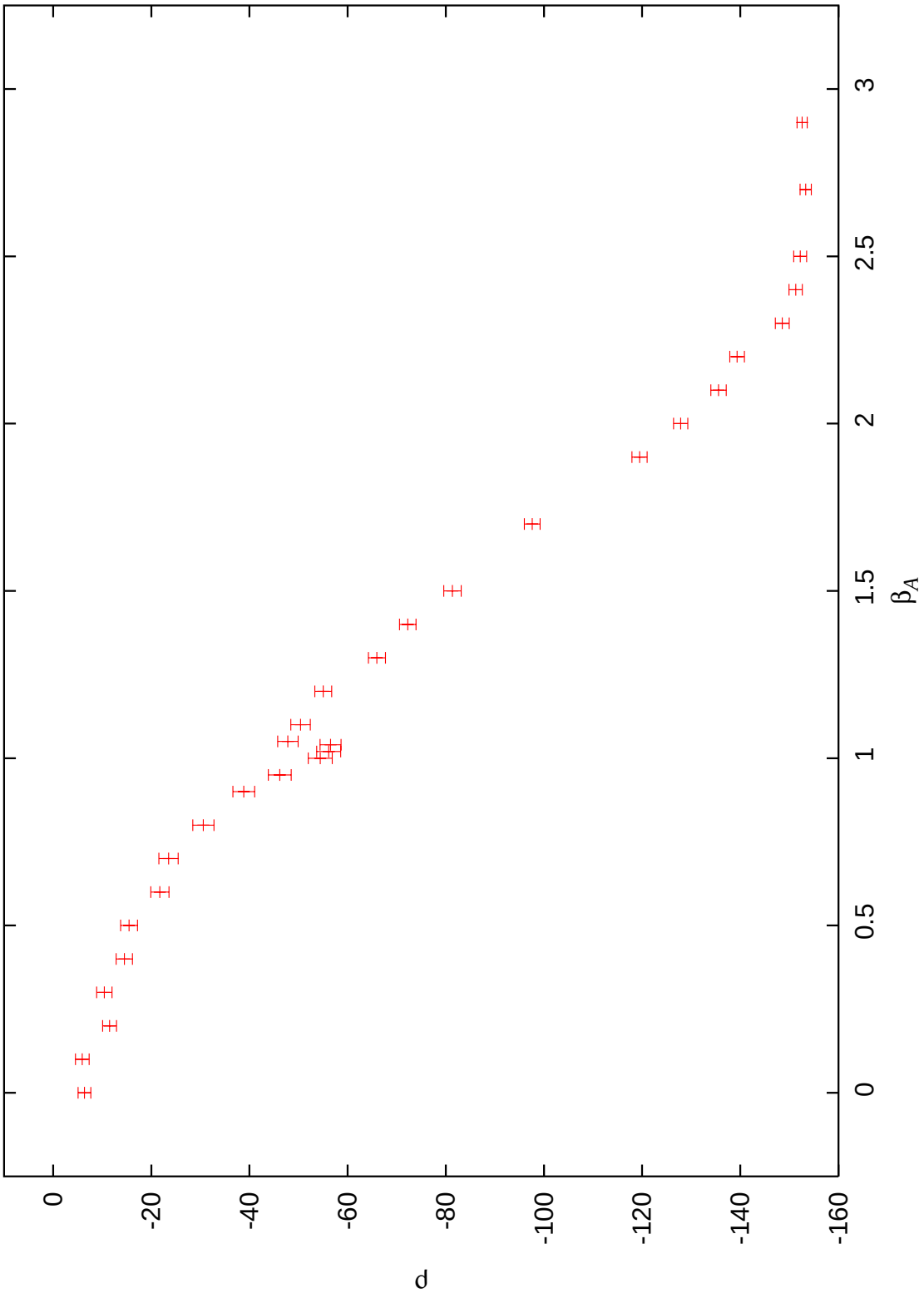

Figure 7.8: ρ as a function of β_A at $\lambda = 1.0$ and for a volume $V = 4 \times 12^3$.

the $\mathbb{Z}_2$ monopoles are naturally suppressed in this regime and every observable, included ρ, should assume roughly the same value independently of the value of λ. At $\lambda = 0.85$ two small peaks appears, one approximately around $\beta_A = 0.65$ and the other around $\beta_A = 1.0$. The one which occurs for smaller β_A is in agreement with the results obtained for the density of magnetic monopoles and for the twist observable. The negative peak at $\beta_A = 1.0$, even if very noisy, is in roughly agreement with the data about the Polyakov loop in the fundamental representation and with the spatial distribution of the fundamental Polyakov loop. Finally at $\lambda = 1.0$ only one small and noisy peak occurs, always approximately at $\beta_A = 1.0$. The remnant of the bulk phase transition is disappeared, as one expects from the behavior of the magnetic monopoles and of the other observables. As one can see from Fig. 7.7 and 7.8, also in this case for large β_A the value of ρ is always roughly the same, independently from λ.

This investigation is of course only preliminary. In fact larger spatial volumes should be studied and observe the scaling of the negative peak with the volume size. With our study we selected the interesting areas in the $\beta_A - \lambda$ plane which deserve further study.

Chapter 8

Conclusions and outlook

The aim of this thesis was the investigation of the role of the center of the gauge group in the non-perturbative regime of Yang-Mills theories and in particular for confinement.

We restricted ourselves to the simplest non Abelian group, $SU(2)$, and we employed the lattice discretization. We studied the adjoint representation, which has a trivial center. Since both the fundamental and the adjoint representations share the same perturbative continuum limit, they are believed to behave universal. However, the corresponding quantized theories undergo (bulk) phase transitions making the proof (or disproof) of universality highly non-trivial.

Here, we have presented a detailed investigation of the phase diagram of a lattice $SO(3)$ theory with Wilson action and center-blind $\mathbb{Z}_2$ monopole suppression term for $T = 0$ and for $T \neq 0$ using various methods.

On one hand, these methods rely partly on the $U(1)$ dominance observation within the maximally Abelian gauge and partly on the Pisa Abelian monopole order parameter. In the first case we have introduced a new order parameter based on a (weakly broken) global symmetry replacing the global and spontaneously broken center symmetry in $SU(N)$. Our observations underline the role of $U(1)$ degrees of freedom and/or monopole condensation in the center blind theory.

On the other hand we confirm the observation of de Forcrand and Jahn that twist variables play an important role, pointing to the importance of center vortices also in a theory with a trivial center.

We have investigated the well-known bulk transition. We showed that it weakens from first to probably second order and that tunnelling between different twist sectors is enhanced along it, by increasing the strength of the $\mathbb{Z}_2$ monopole suppression. Whether the phase transition line ends could not been answered. If the answer were positive, then the different phases would be smoothly connected, and the confinement phenomenon should be universal.

Our main observation is that we have found some evidence for the existence of a finite temperature transition. We take this as an indication for universality between the $SU(2)$ and $SO(3)$ lattice theories. However, more evidence is necessary in order to draw final conclusions. In particular more simulations at larger lattice volumes are required to prove whether there is a continuum limit, i.e. whether the critical temperature scales according to the renormalization group and the critical

exponents allow the identification of the universality class of the 3d Ising model. In any case the occurence of a finite temperature transition shows that in our lattice model with sufficiently strong monopole suppression the lattice spacing becomes reasonably small for physical investigations. This differs drastically from the Villain model at the bulk phase transition; in that case the presence of the lattice artifacts caused the lattice spacing to be extremely fine, such that only temperatures above the deconfinement transition could be investigated.

Assuming that there is really universality, it is still not clear how to prove that fermions (i.e. quarks), which couple to the gauge fields within the fundamental representation, are confined. In fact in a center-blind theory all the observables in the fundamental representation are trivially zero. As a consequence the string tension between two fundamental static charges, usually extracted from large Wilson loops in the fundamental representation, cannot be measured. Another way of measuring the string tension or another criterion for confinement should be considered.

Most of our investigations have been done within fixed twist sectors because of strongly suppressed tunneling above the bulk phase transition. A final answer requires the use of an algorithm allowing to tunnel between these sectors. A multicanonical algorithm could be useful but it turned out to give satisfactory results only for rather small volumes. The implementation of such an algorithm was a task going beyond the scope of this work.

Appendix A

Monte Carlo method and updating algorithm

In this appendix we will briefly review some basic aspects about Monte Carlo techniques and we will also explain the algorithm used in this work. In order to calculate the expectation value of a gauge field observable, the functional integral

$$\langle O \rangle = \frac{1}{Z} \int (dU) O \exp(-S(U_\mu)) \tag{A.1}$$

has to be computed. On the lattice it reduces to a multiple integral, but the number of integration variables is normally so large that only statistical methods can be used. In fact the high number of variables involved forbids a direct numerical evaluation of the integral but, at the same time, the majority of the field configurations give a large contribution to the action; in this way, thanks to the weight factor $\exp(-S(U_\mu))$, the integral receives a contribution only from a limited number of configurations and importance sampling allows to apply Monte Carlo techniques.

A.1 Monte Carlo method

According to this method a set of N configurations $\{U_i\}$ is generated in such a way that they are representative of the configuration space, i.e. distributed with the weight e^{-S} and an estimator for the expectation value of the observable becomes

$$\langle O \rangle = \frac{1}{N} \sum O[U_i] \,. \tag{A.2}$$

The statistical ensemble is generated through a Markov chain of configurations $U_0, U_1, \ldots U_i$, where U_i is obtained from U_{i-1} through an update algorithm characterized by the transition probability $P(U_{i-1} \to U_i)$. P has to be chosen such that the distribution for the $\{U_i\}$ always converges to the equilibrium distribution. A necessary condition to fulfill this requirement is

$$\int dU W_{eq}[U] P(U \to U') = W_{eq}[U'] \,, \tag{A.3}$$

with $W_{eq}[U] \propto e^{-S[U]}$. By using the normalization condition $\int dU' P(U \to U') = 1$, it can be easily proven that a sufficient condition for (A.3) is

$$W_{eq}[U]P(U \to U') = W_{eq}[U']P(U' \to U)\,, \tag{A.4}$$

which is known as the detailed balance principle. The configurations generated in this way are of course correlated to each other. The necessary iterations to obtain independent configurations depend very much on the algorithm used and on the observable computed. It is useful then to make the measurements every a certain number of Monte Carlo steps, in order to obtain decorrelated configurations. Statistical methods in data analysis which permit to take properly into account the autocorrelations will be explained in detail in Appendix B.

A.2 Algorithm

We will now describe the algorithm used for the Monte Carlo simulation of the mixed fundamental-adjoint Wilson action with chemical potential for the suppression of the $\mathbb{Z}_2$ monopoles. The action is given by

$$S = \sum_P \left[\beta_A \left(1 - \frac{\mathrm{Tr}_A U_P}{3}\right) + \beta_F \left(1 - \frac{\mathrm{Tr}_F U_P}{2}\right)\right] + \sum_c \lambda(1 - \sigma_c)\,, \tag{A.5}$$

which, due to the well-known trace property

$$\mathrm{Tr}_A = \mathrm{Tr}_F^2 - 1\,, \tag{A.6}$$

can be rewritten as

$$S = \sum_P \left[\frac{4}{3}\beta_A \left(1 - \frac{\mathrm{Tr}_F^2 U_P}{4}\right) + \beta_F \left(1 - \frac{\mathrm{Tr}_F U_P}{2}\right)\right] + \sum_c \lambda(1 - \sigma_c)\,, \tag{A.7}$$

where

$$\begin{aligned} \sigma_c &= \prod_{P \epsilon \partial c} \eta_P\,, & \text{(A.8)}\\ \eta_P &= \mathrm{sign}\mathrm{Tr}_F U_P\,, & \text{(A.9)}\\ U_P &= U_\mu(x) U_\nu(x+\hat{\mu}) U_\mu^\dagger(x+\hat{\nu}) U_\nu^\dagger(x)\,. & \text{(A.10)} \end{aligned}$$

In other words we used always links in the fundamental representation, i.e. 2×2 matrices, which require a smaller computational effort compared with the 3×3 adjoint matrices, and to compute the adjoint observables we always used the property (A.6).

For the updating of a given link variable $U_\mu(x)$ the action can be rewritten in the following way:

$$\begin{aligned} S[U_\mu(x)] = &- \frac{\beta_A}{3}\mathrm{Tr}_F^2[U_\mu(x)V_\mu(x)] - \frac{\beta_F}{2}\mathrm{Tr}_F[U_\mu(x)V_\mu(x)] - \\ &- \lambda\, \mathrm{sign}\{\mathrm{Tr}_F[U_\mu(x)V_\mu(x)]\}\, \mathrm{sign}\{\mathrm{Tr}_F[U_\mu(x)V'_\mu(x)]\}\, W\,, \end{aligned} \tag{A.11}$$

where $V_\mu(x)$ and $V'_\mu(x)$ are the sum of the products of the links over the six staples around the link $U_\mu(x)$ in the ν and α directions respectively

$$\begin{aligned} V_\mu(x) &= \sum_\nu \{\, U_\nu\,(x+\hat{\mu})U^\dagger_\mu(x+\hat{\nu})U^\dagger_\nu(x) + \\ &\qquad U^\dagger_\nu\,(x+\hat{\mu}-\hat{\nu})U^\dagger_\mu(x-\hat{\nu})U_\nu(x-\hat{\nu}) \;\;,\;\; \nu \neq \mu\,, \\ V'_\mu(x) &= \sum_\alpha \{\, U_\alpha\,(x+\hat{\mu})U^\dagger_\mu(x+\hat{\alpha})U^\dagger_\alpha(x) + \\ &\qquad U^\dagger_\alpha\,(x+\hat{\mu}-\hat{\alpha})U^\dagger_\mu(x-\hat{\alpha})U_\alpha(x-\hat{\alpha}) \;\;,\;\; \alpha \neq \nu \neq \mu\,, \end{aligned} \tag{A.12}$$

and W is the products of the signs of the plaquette in the fundamental representation of the four remaining faces of the 3-dimensional cube c.

Since the action is quadratic in the link $U_\mu(x)$, we used a Metropolis algorithm [146] to update the gauge field. The procedure can be summarized in the following steps:

- generate a random $SU(2)$ matrix close to the identity, where closeness is controlled by a parameter ϵ;
- obtain a trial link $U^{trial}_\mu(x)$ by multiplying the old link with the previously generated random matrix;
- compute the new action with the trial link and then the difference $\Delta S = S[U^{trial}_\mu(x)] - S[U_\mu(x)]$;
- if $\Delta S < 0$ then accept always the change;
- if $\Delta S > 0$ accept the change with probability $\exp(-\Delta S)$.

The parameter ϵ was tuned in such a way to have always an acceptance rate greater than 60%.

Appendix B

Statistical error analysis

An essential part of the Monte Carlo simulations is the analysis of the errors of the observables computed. In this short review we will closely follow [147].

The observables measured in a Monte Carlo simulation are usually distinguished into primary and secondary quantities, which are functions of primary quantities. Besides the naive statistical error, associated with the finite number of measurements N and proportional to $1/\sqrt{N}$, there are other fundamental sources of errors:

- Initialization bias. The algorithm needs a number of thermalization steps before it "forgets" the arbitrary initial configuration and reaches the thermal equilibrium where the field configurations are distributed according to the Boltzmann factor $\exp(-S)$.

- Autocorrelation in equilibrium. When thermal equilibrium is reached, the field configurations generated by the updating algorithm are correlated. This causes the statistical error of $\langle O \rangle$ to be a factor $2\tau_{\rm int}(O)$ larger than in an ensemble of independent configurations. The quantity $\tau_{\rm int}(O)$ is called the integrated autocorrelation time for the observable O.

The dependency on the initial (arbitrary) configuration can be avoided by waiting a large enough number of updating steps before starting the measurements. By measurements we mean the evaluation of the observables on the field configurations generated by the algorithm. What is large enough can be estimated from the integrated autocorrelation times of the observables. They can be very different for different observables. In practice, the observed autocorrelation times have almost the same order of magnitude and a number of thermalization steps equal 20 to 100 times the maximum observed autocorrelation time $\tau_{int,max}$ is a sensible choice.

The central role in the determination of the statistical errors is played by the integrated autocorrelation times. How to estimate them is the subject of this appendix.

B.1 Primary quantities

We consider a sequence of measurements $O_i \equiv O[U_i],\ i = 1, ..., N$ of the observable $O \equiv O[U]$ performed on a large ensemble of field configurations $\{[U_i],\ i = 1, ..., N\}$

already in the equilibrium distribution. We denote by

$$\langle O \rangle = \frac{1}{N} \sum_{i=1}^{N} O_i \tag{B.1}$$

the ensemble average of O. The exact path integral expectation value of O is denoted by $\langle O \rangle_E$. If the measurements are statistically independent the value of $\langle O \rangle$ is normally distributed around the expectation value $\langle O \rangle_E$ with variance

$$var(\langle O \rangle) = \langle O^2 \rangle - \langle O \rangle^2 \; = \; \langle (O - \langle O \rangle)^2 \rangle \, . \tag{B.2}$$

The (naive) statistical error is then given by

$$(\Delta_{\text{naive}}(\langle O \rangle))^2 = \frac{var(O)}{N-1} \, . \tag{B.3}$$

In general, there are correlations in the sequence of generated field configurations (and hence in the measurements), called autocorrelations and (B.3) underestimates the statistical error.

The (unnormalized) autocorrelation function is defined as

$$\Gamma_O(i-j) = \langle (O_i - \langle O \rangle_E)(O_j - \langle O \rangle_E) \rangle_{\text{MC}} \; = \; \Gamma_O(j-i) \, , \tag{B.4}$$

where $\langle \cdots \rangle_{\text{MC}}$ denotes the average over infinitely many independent ensembles of configurations in thermal equilibrium. The autocorrelation function Γ_O depends only on the distance between the measurements $|t| = i - j$. Typically, it decays exponentially

$$\Gamma_O(t) \sim \exp(-|t|/\tau) \qquad \text{for large } t \, . \tag{B.5}$$

The integrated autocorrelation time is defined as

$$\tau_{\text{int}}(O) = \frac{1}{2} \sum_{t=-\infty}^{\infty} \frac{\Gamma_O(t)}{\Gamma_O(0)} \, , \tag{B.6}$$

where $\Gamma_O(0) = \langle (O - \langle O \rangle_E)^2 \rangle_E = var(O)$ is the variance[1] of the observable O. Here, time refers to the Monte Carlo time of the simulation and labels the measurements.

The goal is to estimate the effects of the autocorrelations based on a finite (but large) sequence of measurements $O_i, \; i = 1, ..., N$. The ensemble average $\langle O \rangle$ in (B.1) has statistical error, corrected for autocorrelations, given by

$$\begin{aligned} (\Delta(\langle O \rangle))^2 \; &= \; \frac{1}{N^2} \sum_{i,j=1}^{N} \Gamma_O(i-j) \\ &= \; \frac{1}{N} \sum_{t=-(N-1)}^{N-1} \left(1 - \frac{|t|}{N} \right) \Gamma_O(t) \\ &\approx \; \frac{1}{N} (2\tau_{\text{int}}(O)) \Gamma_O(0) \qquad \text{for} \quad N \gg \tau \, . \end{aligned} \tag{B.7}$$

[1] We note that $\langle O_i \rangle_{\text{MC}} = \langle O \rangle_E$.

Comparing with (B.3), we see that the statistical error is a factor $\sqrt{2\tau_{\rm int}(O)}$ larger than for independent measurements. Stated differently, the number of effectively independent measurements in a run of length N is roughly $N/(2\tau_{\rm int}(O))$. The natural estimator of $\Gamma_O(t)$ is

$$\Gamma_O(t) \approx \frac{1}{N-|t|} \sum_{i=1}^{N-|t|} (O_i - \langle O\rangle)(O_{i+|t|} - \langle O\rangle)\,. \tag{B.8}$$

In order to get a good estimator of $\tau_{\rm int}(O)$, one sums the terms in (B.6) (with Γ_O computed according to (B.8)) up to $|t| \le M$, where M is a suitably chosen cut-off. This cut-off is necessary since the signal for $\Gamma_O(t)/\Gamma_O(0)$ gets lost in the noise for $|t| \gg \tau$.

In the following subsection, we describe an alternative method for estimating the error, the binning method. Knowing $\Delta(\langle O\rangle)$ one can use (B.7) together with (B.3) to estimate the integrated autocorrelation time:

$$\tau_{\rm int}(O) = \frac{1}{2}\left(\frac{\Delta(\langle O\rangle)}{\Delta_{\rm naive}(\langle O\rangle)}\right)^2 . \tag{B.9}$$

B.2 Binning

An easy method to analyze the data of a Monte Carlo simulation is the binning method. The measurements $O_i,\ i = 1, ..., N$ are first averaged into blocks of length B called bins

$$O_{b,B} = \frac{1}{B} \sum_{i=1+(b-1)B}^{bB} O_i\,, \quad b = 1, ..., N_B = [N/B]\,. \tag{B.10}$$

If N is divisible by B, the average over the blocked measurements is the same as the average $\langle O\rangle$ in (B.1). The variance computed from the blocked measurements is

$$var(\langle O\rangle, B) = \frac{1}{N_B} \sum_{b=1}^{N_B} \left(O_{b,B} - \frac{1}{N_B}\sum_{b'=1}^{N_B} O_{b',B}\right)^2 . \tag{B.11}$$

The blocked measurements still suffer from autocorrelations. The error $\Delta(\langle O\rangle, B)$ of the average $\langle O\rangle$, estimated through the variance (B.11), is

$$(\Delta(\langle O\rangle, B))^2 = \frac{var(\langle O\rangle, B)}{N_B - 1}\,. \tag{B.12}$$

It increases with the bin length B: if the integrated autocorrelation time $\tau_{\rm int}(O)$ is small with respect to B, the systematic effect due to autocorrelations is proportional to $\tau_{\rm int}(O)/B$. The relative statistical uncertainty of the error estimate (B.12) is approximately given by $(2N_B)^{-1/2}$. Increasing the value of B the error (B.12) flattens and oscillates around its correct value $\Delta(\langle O\rangle)$, if the number of measurements is large enough to see this. The integrated autocorrelation time can then be estimated as in (B.9), with $\Delta_{\rm naive}(\langle O\rangle) \equiv \Delta(\langle O\rangle, B = 1)$. The error of this estimate is dominated by the uncertainty of $\Delta(\langle O\rangle)$ and is given by

$$\frac{\Delta(\tau_{\rm int}(O))}{\tau_{\rm int}(O)} = 2\,\frac{\Delta(\Delta(\langle O\rangle))}{\Delta(\langle O\rangle)}\,. \tag{B.13}$$

B.3 Secondary quantities: jackknife binning

Secondary quantities are defined as

$$y = f(O^{(1)}, O^{(2)}, \cdots) \,, \tag{B.14}$$

where f is an arbitrary function of the primary quantities $O^{(1)}$, $O^{(2)}$, $\cdots$. The best estimate of a secondary quantity is

$$\langle y \rangle = f(\langle O^{(1)} \rangle, \langle O^{(2)} \rangle, \cdots) \,. \tag{B.15}$$

To estimate the statistical error of $\langle y \rangle$ one can in principle use the binning method described in B.2: the quantities $y_{b,B} = f(O^{(1)}_{b,B}, O^{(2)}_{b,B}, \cdots)$ are inserted in (B.11) and (B.12) at the place of $O_{b,B}$. The problem in practice, is often that the bins are too small (because of the time costs of the measurements) and they fluctuate too much around $\langle y \rangle$. This problem can be overcome with the method of jackknife binning.

For the primary quantities, we consider the bins $O_{b,B}$, $b = 1, ..., N_B$ and build the jackknife averages

$$O_{b,\bar{B}} = \frac{1}{N_B - 1} \sum_{b' \neq b} O_{b',B} \,, \quad b = 1, ..., N_B \,, \tag{B.16}$$

obtained by omitting a single bin in all possible ways. The index $\bar{B}$ means that $O_{b,\bar{B}}$ is the complement of the bin $O_{b,B}$. Evaluating the secondary quantity y with the jackknife averages (B.16) we obtain the jackknife estimators

$$y_{b,\bar{B}} = f(O^{(1)}_{b,\bar{B}}, O^{(2)}_{b,\bar{B}}, \cdots) \,, \tag{B.17}$$

with an average

$$\langle y_{\bar{B}} \rangle = \frac{1}{N_B} \sum_b y_{b,\bar{B}} \,. \tag{B.18}$$

The error estimate for $\langle y \rangle$ can be obtained from

$$(\Delta(\langle y \rangle, B))^2 = (N_B - 1) \left(\frac{1}{N_B} \sum_b y^2_{b,\bar{B}} - \langle y_{\bar{B}} \rangle^2 \right) \,. \tag{B.19}$$

For a primary quantity $y \equiv O$, (B.19) reproduces (B.12). The error estimate (B.19) can be studied under variation of the bin length B. Increasing B, the error estimate flattens and oscillates around the correct error. The integrated autocorrelation time for the secondary quantity y can then be estimated as in (B.9), the naive error being the error (B.19) for $B = 1$.

The jackknife error analysis is our standard method for estimating statistical errors.

Appendix C

Procedure of Maximally Abelian Gauge Fixing

The maximally Abelian gauge (MAG) [83] is the special Abelian gauge exhibiting infrared Abelian dominance in the lattice QCD. In this appendix we will review this procedure following [148].

In the SU(2) lattice formalism, the MAG is defined so as to maximize

$$\begin{aligned} R_{\mathrm{MAG}}[U_\mu] &\equiv \sum_x R(x) \\ &\equiv \frac{1}{2}\sum_{x,\mu} \mathrm{Tr}\{U_\mu(x)\sigma_3 U_\mu^\dagger(x)\sigma_3\} \\ &= \sum_{x,\mu}\{U_\mu^0(x)^2 + U_\mu^3(x)^2 - U_\mu^1(x)^2 - U_\mu^2(x)^2\} \\ &= \sum_{x,\mu}\left[1 - 2\{U_\mu^1(x)^2 + U_\mu^2(x)^2\}\right] \end{aligned} \tag{C.1}$$

with respect to the gauge transformation. Here, $R(x)$ is a local scalar variable defined as

$$R(x) \equiv \frac{1}{2}\sum_{\pm\mu} \mathrm{Tr}\{U_\mu(x)\sigma_3 U_\mu^\dagger(x)\sigma_3\} \qquad \text{with} \qquad U_{-\mu}(x) = U_\mu^\dagger(x-\hat{\mu}). \tag{C.2}$$

Here, $R(x)$ is manifestly invariant under the lattice rotation and the reflection. In the MAG , the operator

$$\Phi(x) \equiv \sum_{\pm\mu} U_\mu(x)\sigma_3 U_\mu^\dagger(x) \tag{C.3}$$

is diagonalized. In this appendix, we show the procedure of the MAG fixing on the lattice.

To begin with, we introduce a local gauge transformation, whose gauge function $\Omega_{x_0}(x)$ is not unity at the site x_0 only,

$$\begin{cases} \Omega_{x_0}(x) = \Omega(x_0) & \text{for } x = x_0 \\ \Omega_{x_0}(x) = 1 & \text{for } x \neq x_0. \end{cases} \tag{C.4}$$

In order to maximize the value $R_{\rm MAG}[U_\mu]$, one may consider to maximize the local variables $R(x)$ at each site x by the local gauge transformation Ω_x. However, since $R(x_0)$ at the site x_0 is changed not only by the gauge transformation $\Omega_{x_0}(x)$ but also by the gauge transformation $\Omega_{x_0-\hat{\mu}}(x)$ with neighboring sites $x_0-\hat{\mu}$, one cannot obtain the MAG gauge configuration $U_\mu(x_0)^{\rm MAG}$ only by simple local gauge transformation $\Omega_{x_0}(x)$. After the local gauge transformation at all sites on the whole lattice, one has to repeat this procedure until $R_{\rm MAG}$ is maximized.

Now, let us derive the gauge transformation $\Omega_{x_0}(x)$ to maximize $R(x_0)$. After the gauge transformation by $\Omega_{x_0}(x)$, $R(x_0)$ is changed as

$$\begin{aligned} R^\Omega(x_0) &= \sum_\mu {\rm Tr}\{\Omega(x_0)U_\mu(x_0)\sigma_3 U_\mu^\dagger(x_0)\Omega^\dagger(x_0)\sigma_3 \\ &\quad +U_\mu(x_0-\hat{\mu})\Omega^\dagger(x_0)\sigma_3\Omega(x_0)U^\dagger(x_0-\hat{\mu})\sigma_3\} \\ &= {\rm Tr}[\sum_\mu\{U_\mu(x_0)\sigma_3U^\dagger(x_0)+U_\mu^\dagger(x_0-\hat{\mu})\sigma_3U_\mu(x_0-\hat{\mu})\}\cdot\Omega^\dagger(x_0)\sigma_3\Omega(x_0)] \\ &\equiv {\rm Tr}[\Phi(x_0)S(x_0)]. \end{aligned} \tag{C.5}$$

Here, we define

$$S(x)\equiv S^a(x)\sigma^a\equiv\vec{S}\cdot\vec{\sigma}\equiv\Omega^\dagger(x)\sigma_3\Omega(x) \qquad \in {\rm su(2)}, \tag{C.6}$$

$$\Phi(x)\equiv\Phi^a(x)\sigma^a\equiv\vec{\Phi}\cdot\vec{\sigma}\equiv\sum_{\pm\mu}U_\mu(x)\sigma_3U_\mu^\dagger(x) \qquad \in {\rm su(2)}, \tag{C.7}$$

which are both elements of Lie algebra and satisfy relations ${\rm Tr}(\Phi)={\rm Tr}(S)=0$ and $S^2=1$. To maximize $R(x_0)$ by this gauge transformation, $\vec{S}(x_0)$ is taken to be the same direction as $\vec{\Phi}(x_0)$ in the ${\rm SU(2)}\simeq{\rm O(3)}$ parameter space, $\vec{S}//\vec{\Phi}$. After this gauge transformation, $\Phi(x_0)$ is diagonalized as $\Phi^\Omega(x_0)=\Omega(x_0)\Phi(x_0)\Omega^\dagger(x_0)=\Phi_3^\Omega(x_0)\sigma_3$, and $S(x_0)$ becomes σ_3. Here, Φ plays a similar role as the Higgs field in the 't Hooft-Polyakov monopole.

In the Abelian gauge, the gauge function $\Omega(x)$ is an element of the coset space ${\rm SU(2)/U(1)_3}$ using the residual ${\rm U(1)_3}$ degrees of freedom. We take the representative element of $\Omega(x)$ so as to satisfy $\Omega^3(x)=0$, or

$$\Omega(x)=\Omega^0(x)+i\{\Omega^1(x)\sigma^1+\Omega^2(x)\sigma^2\}. \tag{C.8}$$

Because of $(\Omega^1)^2+(\Omega^2)^2+(\Omega^3)^2=1$, we can parameterize $\Omega(x)$ as

$$\left\{\begin{array}{lcl}\Omega^0(x) &=& \cos\theta(x) \\ \Omega^1(x) &=& \sin\theta(x)\cos\phi(x) \\ \Omega^2(x) &=& \sin\theta(x)\sin\phi(x),\end{array}\right. \tag{C.9}$$

and then $S(x)$ is expressed as

$$S\equiv S^a\sigma^a\equiv\Omega^\dagger\sigma_3\Omega=\sin2\theta\cos\phi\sigma_1+\sin2\theta\sin\phi\sigma_2+\cos2\theta\sigma_3. \tag{C.10}$$

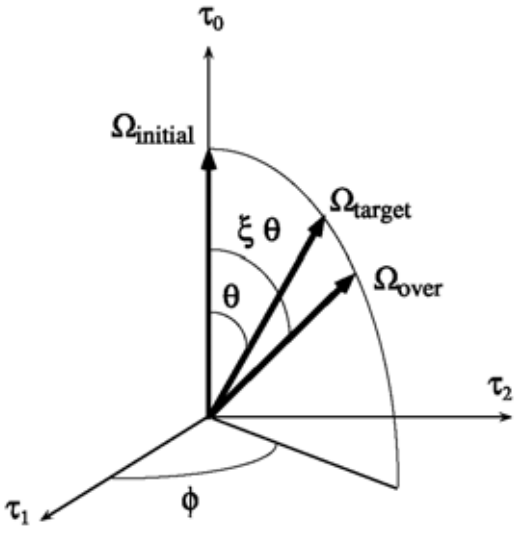

Figure C.1: The gauge function $\vec{\Omega}_{\rm over}$ used in the over-relaxation method. The vector $\vec{\Omega}_{\rm target}$ corresponds to the gauge function which maximizes $R(x_0)$.

Since $\Phi(x_0) \equiv \Phi^a(x_0)\sigma^a$ is obtained from the original gauge configuration $U_\mu(x)$, we get $\Omega_{x_0}(x_0)$ as

$$\left\{ \begin{array}{lcl} \tan^2 2\theta(x_0) & = & \frac{(S^1)^2+(S^2)^2}{(S^3)^2} = \frac{(\Phi^1)^2+(\Phi^2)^2}{(\Phi^3)^2} \\ \tan\phi(x_0) & = & \frac{S^2}{S^1} = \frac{\Phi^2}{\Phi^1}. \end{array} \right. \tag{C.11}$$

Thus, the gauge function $\Omega(x)$ which maximizes $R(x_0)$ is obtained so as to obey $\vec{S}(x_0)//\vec{\Phi}(x_0)$. This procedure makes $R(x_0)$ defined in (C.5) maximum by $\Omega_{x_0}(x)$. This gauge transformation, however, influences $R(x)$ of the neighboring sites, $x = x_0 \pm \hat{\mu}$, and in fact does not make them maximum. Therefore, we have to perform this procedure to the neighboring sites. By doing this, however, the original $R(x_0)$ gets some change and hence $R(x_0)$ is no more in its maximum. This fact forces us to repeat the local-gauge transformation many times.

To optimize the convergence, in the practical simulation, we take an over-relaxation method. We show the vector $(\cos\theta, \sin\theta\cos\phi, \sin\theta\sin\phi)$ in Fig.C.1, corresponding to the gauge function $\Omega(x_0)$ in Eq.(C.9). In the over-relaxation method, we take the angle value $\xi\theta$ instead of θ obtained in Eq.(C.9),

$$\left\{ \begin{array}{lcl} \Omega^0_{\rm over}(x_0) & = & \cos(\xi\theta) \\ \Omega^1_{\rm over}(x_0) & = & \sin(\xi\theta)\cos\phi \\ \Omega^2_{\rm over}(x_0) & = & \sin(\xi\theta)\sin\phi. \end{array} \right. \tag{C.12}$$

This overrelaxation parameter ξ is taken as $1 \sim 2$.

Appendix D

Symmetry and restricted connection

In Chapter 6 we exposed our ideas to define a new order parameter and we showed the results obtained. We can summarize our strategy as follows; given a thermalized lattice configuration, we want to find a symmetry operator P such that it generates a symmetry for the action and it maps L_A^+ into L_A^-. We have already shown that a sufficient condition is given by

$$\sum_{\vec{x}} \mathrm{Tr}_R \left(J_3 \sum_{\pm i} \left[U_i(\vec{x},t)\ J_3\ U_i^\dagger(\vec{x},t) \right] \right) = \text{Extremum}\ , \tag{D.1}$$

with $P = J_3$, i.e. 3d MAG. But this condition is gauge equivalent to

$$\sum_{\vec{x}} \mathrm{Tr}_R \left(P(\vec{x}) \sum_{\pm i} \left[U_i(\vec{x},t)\ P(\vec{x}+\hat{i})\ U_i^\dagger(\vec{x},t) \right] \right) = \text{Extremum}\ , \tag{D.2}$$

which at fixed $\vec{x}$ and i reduces to

$$P^\dagger(\vec{x}) U_i(\vec{x},t) P(\vec{x}+\hat{i}) = U_i(\vec{x},t)\,. \tag{D.3}$$

This equation can be read as a constraint on the functional form of the gauge fields such that, given $P(\vec{x})$, the symmetry is realized. This condition can be solved in A_μ by using the form of the links $U_\mu = e^{iag\vec{A}_\mu(\vec{x})\cdot\frac{\vec{\sigma}}{2}}$. In the following we will show some analytical computations done in the fundamental representation for simplicity, but they can be easily generalized to the adjoint representation. By defining

$$P(\vec{x}) = i\hat{n}(\vec{x}), P(\vec{x}+\hat{i}) = \frac{i\hat{n}(\vec{x}+\hat{i})}{\sqrt{1+(a\partial_i\hat{n})^2}} \tag{D.4}$$

at first order in a it is straightforward to show that (D.3) is equivalent to

$$e^{i\frac{\pi}{2}\hat{n}(\vec{x})\cdot\vec{\sigma}}(\vec{A}_i(\vec{x})\cdot\frac{\vec{\sigma}}{2})e^{-i\frac{\pi}{2}\hat{n}(\vec{x})\cdot\vec{\sigma}} - \frac{i}{g}e^{i\frac{\pi}{2}\hat{n}(\vec{x})\cdot\vec{\sigma}}\partial_i e^{-i\frac{\pi}{2}\hat{n}(\vec{x})\cdot\vec{\sigma}} = (\vec{A}_i(\vec{x})\cdot\frac{\vec{\sigma}}{2}) \tag{D.5}$$

The last equation shows explicitly that the sufficient condition (D.3) at first order in a is equivalent to the requirement that the gauge connection is invariant

under particular gauge transformations, i.e. under rotations of $\frac{\pi}{2}$ around $\hat{n}(\vec{x})$. A step forward shows that it gives a restriction to the functional form of the gauge connection

$$\vec{A}_i(\vec{x}) \cdot \vec{\sigma} = C_i \hat{n}(\vec{x}) \cdot \vec{\sigma} + \frac{1}{g}(\hat{n}(\vec{x}) \times \partial_i \hat{n}(\vec{x})) \cdot \vec{\sigma} \tag{D.6}$$

with $\hat{n}(\vec{x}) \cdot \vec{A}_i(\vec{x}) = C_i$. This decomposition can be generalized to all orders in a. Defining

$$\begin{aligned} \hat{\partial}_i \hat{n}(\vec{x}) \cdot \vec{\sigma} &= \frac{1}{a}(\hat{n}(\vec{x} + \hat{\imath}) \cdot \vec{\sigma} - \hat{n}(\vec{x}) \cdot \vec{\sigma}) \,, \\ v &= \|\hat{\partial}_i \hat{n}(\vec{x})\| = \frac{2}{a} \sin\theta \,, \\ \hat{n}(\vec{x}) \cdot \hat{\partial}_i \hat{n}(\vec{x}) &= -v \sin\theta \,, \end{aligned}$$

one obtains

$$\vec{A}_i \cdot \vec{\sigma} = \frac{1}{\cos\theta} C_i \hat{n}(\vec{x}) \cdot \vec{\sigma} + \frac{\tan\theta}{v} C_i \hat{\partial}_i \hat{n}(\vec{x}) \cdot \vec{\sigma} + B(\hat{n}(\vec{x}) \times \hat{\partial}_i \hat{n}(\vec{x})) \cdot \vec{\sigma} \tag{D.7}$$

with $\|\vec{A}_i\| = \sqrt{C_i^2 + B^2 v^2 \cos^2\theta}$, or

$$\vec{A}_i \cdot \vec{\sigma} = C_i \hat{n}(\vec{x}) \cdot \vec{\sigma} + \frac{\sin\theta}{v} C_i \hat{\partial}_i \hat{n}(\vec{x}) \cdot \vec{\sigma} + B(\hat{n}(\vec{x}) \times \hat{\partial}_i \hat{n}(\vec{x})) \cdot \vec{\sigma} \tag{D.8}$$

with $\|\vec{A}_i\| = |\cos\theta| \sqrt{C_i^2 + B^2 v^2}$. The field B is found by solving the following equation

$$\frac{2B\cos^2\theta}{a\sqrt{C_i^2 + B^2 v^2 \cos^2\theta}} \tan\left(\frac{ag}{2}\sqrt{C_i^2 + B^2 v^2 \cos^2\theta}\right) = 1 \tag{D.9}$$

or

$$\frac{2B\cos\theta}{a\sqrt{C_i^2 + B^2 v^2}} \tan\left(\frac{ag}{2}|\cos\theta|\sqrt{C_i^2 + B^2 v^2}\right) = 1 \tag{D.10}$$

The decomposition of the connection that we obtained is similar to the decomposition given by Cho [149,150], Faddeev-Niemi [151] and Shabanov [152], but in our case it was motivated by the request for a symmetry which is broken at the deconfinement phase transition and we solved the constraint (D.3) not only in the continuum limit $a \to 0$, but at finite lattice spacing a.

Bibliography

[1] C. N. Yang and R. L. Mills. *Conservation of isotopic spin and isotopic gauge invariance*. Phys. Rev. 96, 191–195 (1954).

[2] C. N. Yang. *Selected papers 1945 - 1980. With commentary*. San Francisco, Usa: W.H. Freeman (1983) 596p.

[3] P. W. Higgs. *Broken symmetries, massless particles and gauge fields*. Phys. Lett. 12, 132–133 (1964).

[4] S. L. Glashow. *Partial symmetries of weak interactions*. Nucl. Phys. 22, 579–588 (1961).

[5] J. Goldstone, A. Salam, and S. Weinberg. *Broken symmetries*. Phys. Rev. 127, 965–970 (1962).

[6] S. Weinberg. *A model of leptons*. Phys. Rev. Lett. 19, 1264–1266 (1967).

[7] M. Gell-Mann. *A Schematic model of baryons and mesons*. Phys. Lett. 8, 214–215 (1964).

[8] G. Zweig. *An SU(3) model for strong interaction symmetry and its breaking. 2*. CERN-TH-412.

[9] J. D. Bjorken. *Asymptotic sum rules at infinite momentum*. Phys. Rev. 179, 1547–1553 (1969).

[10] J. D. Bjorken and E. A. Paschos. *Inelastic electron proton and gamma proton scattering, and the structure of the nucleon*. Phys. Rev. 185, 1975–1982 (1969).

[11] R. P. Feynman. *Very high-energy collisions of hadrons*. Phys. Rev. Lett. 23, 1415–1417 (1969).

[12] H. Fritzsch, M. Gell-Mann, and H. Leutwyler. *Advantages of the color octet gluon picture*. Phys. Lett. B47, 365–368 (1973).

[13] G. 't Hooft. *Unpublished remarks at the 1972 Marseille Conference on Yang-Mills Fields*. Quoted, for example, in Politzer, Phys. Rep. 14C, p. 132 .

[14] D. J. Gross and F. Wilczek. *Ultraviolet behavior of non-abelian gauge theories*. Phys. Rev. Lett. 30, 1343–1346 (1973).

[15] H. D. Politzer. *Reliable perturbative results for strong interactions?* Phys. Rev. Lett. 30, 1346–1349 (1973).

[16] T. Matsui and H. Satz. *J / psi suppression by quark - gluon plasma formation.* Phys. Lett. B178, 416 (1986).

[17] G. 't Hooft. *On the phase transition towards permanent quark confinement.* Nucl. Phys. B138, 1 (1978).

[18] G. 't Hooft. *Topology of the gauge condition and new confinement phases in nonabelian gauge theories.* Nucl. Phys. B190, 455 (1981).

[19] A. M. Polyakov. *Quark confinement and topology of gauge groups.* Nucl. Phys. B120, 429–458 (1977).

[20] A. A. Belavin, A. M. Polyakov, A. S. Shvarts, and Yu. S. Tyupkin. *Pseudoparticle solutions of the Yang-Mills equations.* Phys. Lett. B59, 85–87 (1975).

[21] G. 't Hooft. *Symmetry breaking through Bell-Jackiw anomalies.* Phys. Rev. Lett. 37, 8–11 (1976).

[22] G. 't Hooft. *Computation of the quantum effects due to a four- dimensional pseudoparticle.* Phys. Rev. D14, 3432–3450 (1976).

[23] E. M. Ilgenfritz and M. Mueller-Preussker. *Interacting instantons, 1/N expansion and the gluon condensate.* Phys. Lett. B99, 128 (1981).

[24] E. M. Ilgenfritz and M. Mueller-Preussker. *Statistical mechanics of the interacting Yang-Mills instanton gas.* Nucl. Phys. B184, 443 (1981).

[25] D. Diakonov and V. Yu. Petrov. *Instanton based vacuum from Feynman variational principle.* Nucl. Phys. B245, 259 (1984).

[26] D. Diakonov and V. Yu. Petrov. *A theory of light quarks in the instanton vacuum.* Nucl. Phys. B272, 457 (1986).

[27] Y. Nambu. *Strings, monopoles, and gauge fields.* Phys. Rev. D10, 4262 (1974).

[28] S. Mandelstam. *Vortices and quark confinement in nonabelian gauge theories.* Phys. Lett. B53, 476–478 (1975).

[29] S. Mandelstam. *Vortices and quark confinement in nonabelian gauge theories.* Phys. Rept. 23, 245–249 (1976).

[30] G. 't Hooft. *Gauge fields with unified weak, electromagnetic, and strong interactions.* Rapporteur's talk given at Int. Conf. on High Energy Physics, Palermo, Italy, Jun 23-28, 1975.

[31] G. 't Hooft. *A property of electric and magnetic flux in nonabelian gauge theories.* Nucl. Phys. B153, 141 (1979).

[32] G. Mack. *Properties of lattice gauge theory models at low temperatures*. DESY 80/03.

[33] H. B. Nielsen and P. Olesen. *A quantum liquid model for the QCD vacuum: gauge and rotational invariance of domained and quantized homogeneous color fields*. Nucl. Phys. B160, 380 (1979).

[34] N. Seiberg and E. Witten. *Electric - magnetic duality, monopole condensation, and confinement in N=2 supersymmetric Yang-Mills theory*. Nucl. Phys. B426, 19–52 (1994), `hep-th/9407087`.

[35] N. Seiberg and E. Witten. *Monopoles, duality and chiral symmetry breaking in N=2 supersymmetric QCD*. Nucl. Phys. B431, 484–550 (1994), `hep-th/9408099`.

[36] K. G. Wilson. *Confinement of quarks*. Phys. Rev. D10, 2445–2459 (1974).

[37] M. Creutz. *Monte Carlo study of quantized SU(2) gauge theory*. Phys. Rev. D21, 2308–2315 (1980).

[38] M. Creutz and K. J. M. Moriarty. *Numerical studies of Wilson loops in SU(3) gauge theory in four-dimensions*. Phys. Rev. D26, 2166 (1982).

[39] B. Svetitsky and L. G. Yaffe. *Critical behavior at finite temperature confinement transitions*. Nucl. Phys. B210, 423 (1982).

[40] L. G. Yaffe and B. Svetitsky. *First order phase transition in the SU(3) gauge theory at finite temperature*. Phys. Rev. D26, 963 (1982).

[41] R. D. Pisarski and F. Wilczek. *Remarks on the chiral phase transition in chromodynamics*. Phys. Rev. D29, 338–341 (1984).

[42] F. Karsch, E. Laermann, and A. Peikert. *Quark mass and flavor dependence of the QCD phase transition*. Nucl. Phys. B605, 579–599 (2001), `hep-lat/0012023`.

[43] T. Suzuki and I. Yotsuyanagi. *A possible evidence for Abelian dominance in quark confinement*. Phys. Rev. D42, 4257–4260 (1990).

[44] S. Hioki et al. *Abelian dominance in SU(2) color confinement*. Phys. Lett. B272, 326–332 (1991).

[45] L. Del Debbio, M. Faber, J. Greensite, and S. Olejnik. *Center dominance and Z(2) vortices in SU(2) lattice gauge theory*. Phys. Rev. D55, 2298–2306 (1997), `hep-lat/9610005`.

[46] A. V. Smilga. *Are Z(N) bubbles really there?* Ann. Phys. 234, 1–59 (1994).

[47] K. Langfeld and H. Reinhardt. *The Stefan-Boltzmann law: SU(2) versus SO(3) lattice gauge theory*. (2000), `hep-lat/0001009`.

[48] Ph. de Forcrand and O. Jahn. *SO(3) versus SU(2) lattice gauge theory.* (2002), `hep-lat/0205026`.

[49] Ph. de Forcrand and O. Jahn. *Vortex free energies in SO(3) and SU(2) lattice gauge theory.* (2002), `hep-lat/0209060`.

[50] Ph. de Forcrand and O. Jahn. *Comparison of SO(3) and SU(2) lattice gauge theory.* Nucl. Phys. B651, 125–142 (2003), `hep-lat/0211004`.

[51] K. Holland, P. Minkowski, M. Pepe, and U. J. Wiese. *Confinement without a center: The exceptional group G(2).* (2002), `hep-lat/0209093`.

[52] K. Holland, P. Minkowski, M. Pepe, and U. J. Wiese. *Exceptional Confinement in G(2) Gauge Theory.* (2003), `hep-lat/0302023`.

[53] S. Datta and R. V. Gavai. *Phase transitions in SO(3) lattice gauge theory.* Phys. Rev. D57, 6618–6624 (1998), `hep-lat/9708026`.

[54] I. Montvay and G. Muenster. *Quantum fields on a lattice.* Cambridge, UK: Univ. Pr. (1994) 491 p. (Cambridge monographs on mathematical physics).

[55] W. Celmaster. *Gauge theories on the body - centered hypercubic lattice.* Phys. Rev. D26, 2955 (1982).

[56] N. H. Christ, R. Friedberg, and T. D. Lee. *Random lattice field theory: general formulation.* Nucl. Phys. B202, 89 (1982).

[57] N. H. Christ, R. Friedberg, and T. D. Lee. *Gauge theory on a random lattice.* Nucl. Phys. B210, 310 (1982).

[58] H. B. Nielsen and M. Ninomiya. *Absence of neutrinos on a lattice. 1. proof by homotopy theory.* Nucl. Phys. B185, 20 (1981).

[59] P. Hasenfratz. *Lattice QCD without tuning, mixing and current renormalization.* Nucl. Phys. B525, 401–409 (1998), `hep-lat/9802007`.

[60] P. H. Ginsparg and K. G. Wilson. *A remnant of chiral symmetry on the lattice.* Phys. Rev. D25, 2649 (1982).

[61] H. Neuberger. *Exactly massless quarks on the lattice.* Phys. Lett. B417, 141–144 (1998), `hep-lat/9707022`.

[62] M. Luescher. *Exact chiral symmetry on the lattice and the Ginsparg- Wilson relation.* Phys. Lett. B428, 342–345 (1998), `hep-lat/9802011`.

[63] J. Kapusta. *Finite temperature field theory.* Cambridge, UK: Univ. Pr. (1989) (Cambridge monographs on mathematical physics).

[64] L. D. McLerran and B. Svetitsky. *A Monte Carlo study of SU(2) Yang-Mills theory at finite temperature.* Phys. Lett. B98, 195 (1981).

[65] J. Kuti, J. Polonyi, and K. Szlachanyi. *Monte Carlo study of SU(2) gauge theory at finite temperature*. Phys. Lett. B98, 199 (1981).

[66] A. M. Polyakov. *Thermal properties of gauge fields and quark liberation*. Phys. Lett. B72, 477–480 (1978).

[67] L. Susskind. *Lattice models of quark confinement at high temperature*. Phys. Rev. D20, 2610–2618 (1979).

[68] Y. Iwasaki, K. Kanaya, S. Sakai, and T. Yoshie. *Finite temperature transition in two flavor QCD with renormalization group improved action*. Nucl. Phys. Proc. Suppl. 42, 502–504 (1995), `hep-lat/9412054`.

[69] G. Boyd et al. *Thermodynamics of SU(3) Lattice Gauge Theory*. Nucl. Phys. B469, 419–444 (1996), `hep-lat/9602007`.

[70] A. D. Linde. *Infrared problem in thermodynamics of the Yang-Mills gas*. Phys. Lett. B96, 289 (1980).

[71] J. P. Blaizot, E. Iancu, and A. Rebhan. *Approximately self-consistent resummations for the thermodynamics of the quark-gluon plasma. I: Entropy and density*. Phys. Rev. D63, 065003 (2001), `hep-ph/0005003`.

[72] M. Luescher, K. Symanzik, and P. Weisz. *Anomalies of the free loop wave equation in the WKB approximation*. Nucl. Phys. B173, 365 (1980).

[73] E. Seiler. *Upper bound on the color confining potential*. Phys. Rev. D18, 482–483 (1978).

[74] C. Borgs and E. Seiler. *Lattice Yang-Mills theory at nonzero temperature and the confinement problem*. Commun. Math. Phys. 91, 329 (1983).

[75] G. Muenster. *High temperature expansions for the free energy of vortices, respectively the string tension in lattice gauge theories*. Nucl. Phys. B180, 23 (1981).

[76] S. Deser. *Absence of static solutions in source - free Yang-Mills theory*. Phys. Lett. B64, 463 (1976).

[77] R. Bott. *An Application of Morse theory to the topology of Lie groups*. Bull. Soc. Math. Fr. 84, 251–281 (1956).

[78] G. 't Hooft. *Magnetic monopoles in unified gauge theories*. Nucl. Phys. B79, 276–284 (1974).

[79] A. M. Polyakov. *Particle spectrum in quantum field theory*. JETP Lett. 20, 194–195 (1974).

[80] R. Savit. *Duality in field theory and statistical systems*. Rev. Mod. Phys. 52, 453 (1980).

[81] H. B. Nielsen and P. Olesen. *Vortex-line models for dual strings*. Nucl. Phys. B61, 45–61 (1973).

[82] T. T. Wu and C. N. Yang. *Properties of matter under unusual conditions*. page 349 (1969). Edited by Mark, H. and Fernbach, S.

[83] A. S. Kronfeld, M. L. Laursen, G. Schierholz, and U. J. Wiese. *Monopole condensation and color confinement*. Phys. Lett. B198, 516 (1987).

[84] A. Di Giacomo, B. Lucini, L. Montesi, and G. Paffuti. *Colour confinement and dual superconductivity of the vacuum. I*. Phys. Rev. D61, 034503 (2000), `hep-lat/9906024`.

[85] A. Di Giacomo, B. Lucini, L. Montesi, and G. Paffuti. *Colour confinement and dual superconductivity of the vacuum. II*. Phys. Rev. D61, 034504 (2000), `hep-lat/9906025`.

[86] J. M. Carmona, M. D'Elia, A. Di Giacomo, B. Lucini, and G. Paffuti. *Color confinement and dual superconductivity of the vacuum. III*. Phys. Rev. D64, 114507 (2001), `hep-lat/0103005`.

[87] A. S. Kronfeld and U. J. Wiese. *SU(N) gauge theories with C periodic boundary conditions. 1. Topological structure*. Nucl. Phys. B357, 521–533 (1991).

[88] A. S. Kronfeld and U. J. Wiese. *SU(N) gauge theories with C periodic boundary conditions. 2. Small volume dynamics*. Nucl. Phys. B401, 190–205 (1993), `hep-lat/9210008`.

[89] J. Cardy. *Scaling and renormalization in statistical physics*. Cambridge, UK: Univ. Pr. (1996) 238 p. (Cambridge lecture notes in physics: 3).

[90] P. van Baal. *Some results for SU(N) gauge fields on the hypertorus*. Commun. Math. Phys. 85, 529 (1982).

[91] J. Ambjorn and H. Flyvbjerg. *'t Hooft's nonabelian magnetic flux has zero classical energy*. Phys. Lett. B97, 241 (1980).

[92] J. Groeneveld, J. Jurkiewicz, and C. P. Korthals Altes. *Twist as a probe for phase structure*. Phys. Scripta 23, 1022 (1981).

[93] J. C. Vink and U. J. Wiese. *Gauge fixing on the lattice without ambiguity*. Phys. Lett. B289, 122–126 (1992), `hep-lat/9206006`.

[94] A. J. van der Sijs. *Laplacian Abelian projection*. Nucl. Phys. Proc. Suppl. 53, 535–537 (1997), `hep-lat/9608041`.

[95] Ph. de Forcrand and M. Pepe. *Laplacian center vortices*. Published in *Osaka 2000, Quantum chromodynamics and color confinement* 141-149 (2000), `hep-lat/0008013`.

[96] T. G. Kovacs and E. T. Tomboulis. *Computation of the vortex free energy in SU(2) gauge theory*. Phys. Rev. Lett. 85, 704–707 (2000), `hep-lat/0002004`.

[97] C. Hoelbling, C. Rebbi, and V. A. Rubakov. *Free energy of an SU(2) monopole-antimonopole pair*. Nucl. Phys. Proc. Suppl. 73, 527–529 (1999), `hep-lat/9809113`.

[98] L. Del Debbio, A. Di Giacomo, and B. Lucini. *Vortices, monopoles and confinement*. Nucl. Phys. B594, 287–300 (2001), `hep-lat/0006028`.

[99] Ph. de Forcrand, M. D'Elia, and M. Pepe. *A study of the 't Hooft loop in SU(2) Yang-Mills theory*. Phys. Rev. Lett. 86, 1438 (2001), `hep-lat/0007034`.

[100] Ph. De Forcrand and L. Von Smekal. *'t Hooft loops and consistent order parameters for confinement*. Nucl. Phys. Proc. Suppl. 106, 619–621 (2002), `hep-lat/0110135`.

[101] A. Ukawa, P. Windey, and A. H. Guth. *Dual variables for lattice gauge theories and the phase structure of Z(N) systems*. Phys. Rev. D21, 1013 (1980).

[102] M. Srednicki and L. Susskind. *SU(5) monopoles on the lattice*. Nucl. Phys. B179, 239 (1981).

[103] G. Bhanot and M. Creutz. *Variant actions and phase structure in lattice gauge theory*. Phys. Rev. D24, 3212 (1981).

[104] J. Greensite and B. Lautrup. *First order phase transition in four-dimensional SO(3) lattice gauge theory*. Phys. Rev. Lett. 47, 9–11 (1981).

[105] I. G. Halliday and A. Schwimmer. *The phase structure of SU(N) / Z(N) lattice gauge theories*. Phys. Lett. B101, 327 (1981).

[106] L. Caneschi, I. G. Halliday, and A. Schwimmer. *The phase structure of mixed lattice gauge theories*. Nucl. Phys. B200, 409 (1982).

[107] F. J. Wegner. J. Math. Phys. 12, 2259 (1971).

[108] R. V. Gavai. *A study of the bulk phase transitions of the SU(2) lattice gauge theory with mixed action*. Nucl. Phys. B474, 446–460 (1996), `hep-lat/9603003`.

[109] A. Gonzalez-Arroyo and C. P. Korthals-Altes. *Asymptotic freedom scales for any lattice action*. Nucl. Phys. B205, 46–76 (1982).

[110] S. Cheluvaraja and H. S. Sharathchandra. *Finite temperature properties of mixed action lattice gauge theory*. (1996), `hep-lat/9611001`.

[111] R. V. Gavai, M. Grady, and M. Mathur. *Finite temperature phase transition in SU(2) lattice gauge theory with extended action*. Nucl. Phys. B423, 123–136 (1994), `hep-lat/9403001`.

[112] P. W. Stephenson. *Physical and unphysical effects in the mixed SU(2)/SO(3) gauge theory.* (1996), `hep-lat/9604008`.

[113] K. M. Bitar, S. Gottlieb, and C. K. Zachos. *Phase structure and renormalization trajectories of lattice SU(2) gauge theory.* Phys. Rev. D26, 2853 (1982).

[114] K. Ghoroku, Y. Myozyo, and H. Nagai. *Phase diagram of the SU(2) lattice gauge theory with a mixed action.* Prog. Theor. Phys. 69, 1823 (1983).

[115] M. Baig. *Monte Carlo analysis of the lambda parameter in an SU(2) lattice gauge theory with a mixed action.* Phys. Lett. B149, 387 (1984).

[116] J. W. Dash. *Universality for a three parameter mixed action.* Nucl. Phys. B251, 414 (1985).

[117] M. Creutz and K. J. M. Moriarty. *Monte Carlo studies of SU(N) / Z(N) lattice gauge theories in four-dimensions.* Nucl. Phys. B210, 50 (1982).

[118] M. Creutz. *Phase transition in SU(5) lattice gauge theory.* Phys. Rev. Lett. 46, 1441 (1981).

[119] K. J. M. Moriarty. *A phase transition in SU(4) four-dimensional lattice gauge theory.* Phys. Lett. B106, 130 (1981).

[120] H. Bohr and K. J. M. Moriarty. *A phase transition in SU(5) lattice gauge theory in four- dimensions.* Phys. Lett. B104, 217 (1981).

[121] M. Creutz and K. J. M. Moriarty. *Phase transition in SU(6) lattice gauge theory.* Phys. Rev. D25, 1724–1726 (1982).

[122] L. Del Debbio, H. Panagopoulos, P. Rossi, and E. Vicari. *k-string tensions in SU(N) gauge theories.* Phys. Rev. D65, 021501 (2002), `hep-th/0106185`.

[123] U. M. Heller. *SU(3) lattice gauge theory in the fundamental adjoint plane and scaling along the Wilson axis.* Phys. Lett. B362, 123–127 (1995), `hep-lat/9508009`.

[124] G. G. Batrouni and B. Svetitsky. *The order of the finite temperature phase transition in the SU(4) gauge theory.* Phys. Rev. Lett. 52, 2205 (1984).

[125] Yu. M. Makeenko and M. I. Polikarpov. *Phase diagram of mixed lattice gauge theory from viewpoint of large N.* Nucl. Phys. B205, 386 (1982).

[126] I. G. Halliday and A. Schwimmer. *Z(2) monopoles in lattice gauge theories.* Phys. Lett. B102, 337 (1981).

[127] R. Savit. *Duality in field theory and statistical systems.* Rev. Mod. Phys. 52, 453 (1980).

[128] M. Kalb and P. Ramond. *Classical direct interstring action.* Phys. Rev. D9, 2273 (1974).

[129] R. V. Gavai and M. Mathur. *Z(2) monopoles, vortices and the universality of the SU(2) deconfinement transition*. Phys. Lett. B458, 331–337 (1999), hep-lat/9905030.

[130] E. Tomboulis. *The 't Hooft loop in SU(2) lattice gauge theories*. Phys. Rev. D23, 2371 (1981).

[131] T. G. Kovacs and E. T. Tomboulis. *Vortices and confinement at weak coupling*. Phys. Rev. D57, 4054–4062 (1998), hep-lat/9711009.

[132] G. Mack and V. B. Petkova. *Z2 monopoles in the standard SU(2) lattice gauge theory model*. Zeit. Phys. C12, 177 (1982).

[133] A. Alexandru and R. W. Haymaker. *Vortices in SO(3) x Z(2) simulations*. Phys. Rev. D62, 074509 (2000), hep-lat/0002031.

[134] B. A. Berg and T. Neuhaus. *Multicanonical algorithms for first order phase transitions*. Phys. Lett. B267, 249–253 (1991).

[135] S. Datta and R. V. Gavai. *Impact of Z(2) monopoles and vortices on the deconfinement transition*. Nucl. Phys. Proc. Suppl. 83, 366–368 (2000), hep-lat/9908040.

[136] S. Datta and R. V. Gavai. *The deconfinement transition in SO(3) gauge theory*. Phys. Rev. D60, 034505 (1999), hep-lat/9901006.

[137] C. Michael. *Adjoint sources in lattice gauge theory*. Nucl. Phys. B259, 58 (1985).

[138] Ph. de Forcrand and O. Philipsen. *Adjoint string breaking in 4d SU(2) Yang-Mills theory*. Phys. Lett. B475, 280–288 (2000), hep-lat/9912050.

[139] E. M. Ilgenfritz, W. Kerler, M. Mueller-Preussker, and H. Stuben. *Parallel tempering and decorrelation of topological charge in full QCD*. (2000), hep-lat/0007039.

[140] A. Barresi, G. Burgio, and M. Mueller-Preussker. *SO(3) Yang-Mills theory on the lattice*. (2002), hep-lat/0209011.

[141] G. S. Bali, V. Bornyakov, M. Mueller-Preussker, and K. Schilling. *Dual Superconductor Scenario of Confinement: A Systematic Study of Gribov Copy Effects*. Phys. Rev. D54, 2863–2875 (1996), hep-lat/9603012.

[142] V. Bornyakov and M. Mueller-Preussker. *Continuum limit in abelian projected SU(2) lattice gauge theory*. Nucl. Phys. Proc. Suppl. 106, 646–648 (2002), hep-lat/0110209.

[143] M. N. Chernodub, M. I. Polikarpov, and A. I. Veselov. *Effective monopole potential for SU(2) lattice gluodynamics in spatial maximal Abelian gauge*. JETP Lett. 69, 174–179 (1999), hep-lat/9812012.

[144] H. Ichie and H. Suganuma. *Monopoles and gluon fields in QCD in the maximally Abelian gauge*. Nucl. Phys. B574, 70–106 (2000), `hep-lat/9808054`.

[145] A. Barresi, G. Burgio, and M. Mueller-Preussker. *Finite temperature phase transition, adjoint Polyakov loop and topology in SU(2) LGT*. Nucl. Phys. Proc. Suppl. 106, 495–497 (2002), `hep-lat/0110139`.

[146] N. Metropolis, A. W. Rosenbluth, M. N. Rosenbluth, A. H. Teller, and E. Teller. *Equation of state calculations by fast computing machines*. J. Chem. Phys. 21, 1087–1092 (1953).

[147] F. Knechtli. *The static potential in the SU(2) Higgs model*. Ph.D. thesis (1999), `hep-lat/9910044`.

[148] H. Ichie and H. Suganuma. *Dual Higgs theory for color confinement in quantum chromodynamics*. Paper based on Ichie's Ph.D. thesis (1999), `hep-lat/9906005`.

[149] Y. M. Cho. *A restricted gauge theory*. Phys. Rev. D21, 1080 (1980).

[150] Y. M. Cho. *Extended gauge theory and its mass spectrum*. Phys. Rev. D23, 2415 (1981).

[151] L. D. Faddeev and Antti J. Niemi. *Partially dual variables in SU(2) Yang-Mills theory*. Phys. Rev. Lett. 82, 1624–1627 (1999), `hep-th/9807069`.

[152] S. V. Shabanov. *An effective action for monopoles and knot solitons in Yang-Mills theory*. Phys. Lett. B458, 322–330 (1999), `hep-th/9903223`.

Acknowledgements

During my staying in Berlin for my PhD thesis I met a lot of people and many of them contributed to my scientific and human growth. Among them I'd like to thank first of all Prof. Ebert, who gave the opportunity to begin this experience and helped me throughout with many discussions, Prof. Müller-Preussker, who initiated me to numerical simulations and was always rich in suggestions and explanations, and Prof. Lüst, who accepted my application for the Graduate College "The Standard Model of Particle Physics - structure, precision tests and extensions".

Some special words are for Giuseppe, Silvia and Thomas, who shared with me not only scientific work, lectures and seminars, but also parties and dinners, and upon whom I could rely during my life in Berlin. I'd like to remind also the other members of my group and in particular Frank, with whom I enjoyed discussions, coffee breaks (indeed in the last period only the breaks) and beers, Hiro (and his family), who helped me several times inside and outside physics, Nikolai, a singularity in space-time, Stanislav and Andre. I cannot of course forget the secretaries of our group and in particular Frau Preisser, who helped me so much with bureaucracy.

It is also a pleasure to acknowledge discussions with Andrei Smilga and Tamás Kovács in the early stages of this work and with Oliver Jahn and Philippe de Forcrand, who shared with me their point of view during the last part of my thesis. I'd like also to thank the Pisa group, where I could finish this thesis in a nice atmosphere, and in particular Prof. Adriano Di Giacomo, Massimo D'Elia and Luigi Del Debbio, with whom I had frequent discussions.

Finally a special thank to my parents, Francesco and Sandra, who always supported and encouraged me during these three difficult years away from home, and to Franziska, who could understand me and help me in the last period of my staying in Berlin.

Lebenslauf

Name:	Andrea Barresi
geboren am:	02.09.1975 in Genova
Nationalität:	Italienisch

09/1989 - 06/1994	Besuch des Liceo Scientifico “G.D. Cassini”
07/1994	Abitur mit der Abschlußnote 60/60
10/1994 - 06/1999	Studium an der Universität in Genova in der Fachrichtung Physik
10/1999	Laurea in Physik mit der Note 110/110
01/2000 - 10/2002	Mitglied des Graduiertenkollegs “ Strukturuntersuchungen, Präzisionstests und Erweiterungen des Standardmodells der der Elementarteilchenphysik ” an der Humboldt Universität zu Berlin bei Prof. Dr. M. Müller–Preußker

Publikationen

[*a*] Andrea Barresi, Giuseppe Burgio and Michael Müller-Preussker, *Finite temperature phase transition, adjoint polyakov loop and topology in SU(2) LGT*, Nucl. Phys. Proc. Suppl. 106:495-497,2002.
[*b*] Andrea Barresi, Giuseppe Burgio and Michael Müller-Preussker, *SO(3) Yang-Mills theory on the lattice*, hep-lat/0209011, to appear in Nucl. Phys. Proc. Suppl.
.

Selbständigkeitserklärung

Hiermit erkläre ich, die vorliegende Arbeit selbständig ohne fremde Hilfe verfasst zu haben und nur die angegebene Literatur und Hilfsmittel verwendet zu haben.

Andrea Barresi